This is to certify that the
dissertation entitled

Signaling Pathways Involved in Zinc-induced Apoptosis

presented by

James J. Mann, Jr

has been accepted towards fulfillment
of the requirements for the

Doctoral degree in Cell and Molecular Biology

Pamela J. Fraker
Major Professor's Signature

April 28, 2005
Date

DATE DUE	DATE DUE	DATE DUE

SIGNALING PATHWAYS INVOLVED IN ZINC-INDUCED APOPTOSIS

By

James J. Mann, Jr

A DISSERTATION

Submitted to
Michigan State University
in partial fulfillment of the requirements
for the degree of

DOCTOR OF PHILOSOPHY

Program in Cell and Molecular Biology

2005

ABSTRACT

SIGNALING PATHWAYS INVOLVED IN ZINC-INDUCED APOPTOSIS

By

James J. Mann, Jr

Although the traditional role of zinc is as an essential biological trace metal, a non-traditional role has emerged that includes its ability to induce apoptosis. The mechanisms whereby zinc induces apoptosis remained uncertain. Zinc pyrithione, a potent inducer of apoptosis at nanomolar concentrations (400nM), induced 40-60% apoptosis in various cells of the immune system. These cells included: mouse thymocytes, splenic lymphocytes, S49 T cells as well as human Ramos B and Jurkat T cell lines. Thymocytes were protected from zinc pyrithione induced apoptosis by TPEN, a zinc specific chelator. Zinc-induced apoptosis was dependent upon transcription and translation. SQ22536, an inhibitor of adenylate cyclase, reduced zinc-pyrithione mediated apoptosis in thymocytes from 52% to 29%. This result indicated a potential role for the cAMP signaling pathway during zinc-induced apoptosis. The wild type S49 T cell line and two variants that were deficient in the ability to activate adenylate cyclase (S49 Cyc^-) or deficient in protein kinase A activity (S49 Kin^-) were used to determine the role of the cAMP-PKA pathway in response to zinc treatment. Zinc pyrithione (400nM) induced 51% apoptosis in S49 WT cells. A prolonged 2 fold increase in cAMP was observed in S49 WT cells in response to zinc. Activation of PKA resulted in the strong and sustained phosphorylation of the cAMP response element binding protein (CREB) in both S49 WT cells and thymocytes but not in S49 Kin^- and Cyc^- cells. Increased binding of a ^{32}P-labeled DNA

probe containing a cAMP response element (CRE) was observed in S49 WT cells. The BH3-only proapoptotic protein Bim was strongly up-regulated in response to zinc treatment in both S49 WT cells and thymocytes. Additionally, treatment of thymocytes with actinomycin D, an inhibitor of transcription, blocked the up-regulation of Bim and apoptosis in response to zinc. This is the first time that zinc has been shown to promote the up-regulation of Bim. Chromatin immunoprecipitation (ChIP) analysis demonstrated a 2 fold increase in CREB occupancy at the Bim promoter in S49 WT cells in response to zinc. Additionally, no change in the expression levels of Bcl-2 was observed in either thymocytes or S49 WT cells. Thus the increase in Bim expression would shift the cells fate toward death. However, overexpression of either Bcl-2 or Bcl-xL provided substantial protection of Ramos B and Jurkat T cells against zinc-induced apoptosis. Furthermore, another transcription factor cascade, the NF-κB pathway, was activated in response to zinc. IκBα was degraded in response to zinc treatment in both thymocytes and S49 WT cells. Increased binding of a ^{32}P-labled DNA probe containing a NF-κB site was observed presenting a potential second link to the transcriptional regulation of Bim. The data presented herein adds to the increasing evidence that free zinc could be harmful to cells of the immune system and foremost defines the mechanisms by which zinc induces apoptosis.

AKNOWLEDGMENTS

I would like to thank Dr. Pamela J. Fraker for her mentorship and guidance. I wish to thank my guidance committee: Dr. Walter J. Esselman, Dr. Shelagh M. Ferguson-Miller, Dr. R. William Henry, Dr. Mark S. Kaminski, and Dr. Bruce D. Uhal. I would also like to thank past and present members of the Fraker laboratory, especially Dr. Louis King for imparting upon me his wisdom and the art of Flow Cytometry as well as Joseph Frentzel for the many hours of scientific discussions and all of his help over the years - I owe you many more than 'one'. I would also like to thank other friends and collogues including Dr. Craig Hinkley, Dr. Paolo Struffi, Dr. Fransisco Herrera, and Gauri Jawdekar. I would also like to thank my family including those no longer here to see this day. Finally, I would especially like to thank my wife, Dr. Heather Anne Hirsch-Mann, for her support, her wisdom and her love without which I would not be here today.

TABLE OF CONTENTS

LIST OF TABLES

LIST OF FIGURES

KEY TO ABBREVIATIONS

Act. D	Actinomycin D
AICD	Activation-induced cell death
AIF	Apoptosis-inducing factor
AMP	Adenosine 5'-monophosphate
ANT	Adenine nucleotide translocator
Apaf-1	Apoptotic protease activating factor-1
ATP	Adenosine 5'-triphosphate
Bad	Bcl-2 antagonist of cell death
Bag1	Bcl-2 associated athanogene
Bak	Bcl-2 antagonist/killer
Bax	Bcl-2 associated X protein
Bcl-2	B-cell lymphoma 2
Bcl-w	Bcl-2 like 2
Bcl-xL	B-cell leukemia/lymphoma x-long
Bfl1	Bcl-2 related protein A1
BH	Bcl-2 homology domains
BIR	Baculoviral IAP Repeat domains
Bid	BH3 interacting domain death agonist
Bik	Bcl-2 interacting killer
Bim	Bcl-2 interacting mediator of cell death
Bok	Bcl-2 related ovarian killer
CAD	Caspase activated DNase

cAMP	Cyclic adenosine 5'-monophosphate
CARD	Caspase recruitment domain
Caspase	Cysteine aspartic acid protease
CBP	CREB binding protein
CDF-1	Cation diffusion facilitator protein
C.elegans	Caenorhabditis elegans
ChIP	Chromatin Immunoprecipitation
CHX	Cycloheximide
CREB	cAMP response element binding protein
Diablo	Direct IAP-binding and low pI
DNA	Deoxyribonucleic acid
EDTA	Ethylenediaminetetraacetic acid
EndoG	Endonuclease G
EMSA	Electrophoretic mobility shift assay
ER	Endoplasmic reticulum
ERK	Extracellular signal regulated kinases
DAPI	4',6-Diamidno-2-phenylindole
DED	Death effector domain
FACS	Fluorescence-activated cell sorter
FADD	Fas associated via death domain
FasL	Fas ligand
FasR	Fas receptor
FITC	Fluorescein isothiocyanate

FLICE	Fas ligand interacting cell effector
FLIP	FLICE inhibitory protein
FOXO3a	Forkhead box class O 3a transcription factor
G-protein	GTP binding protein
GSH	Reduced Glutathione
GSSG	Oxidized Glutathione
HtrA	High temperature requirement A
Hrk	Hara-kiri, Bcl-2 family
H_2O_2	Hydrogen peroxide
IAP	Inhibitor of Apoptosis
IBMX	3-isobutyl-1-methylxanthine
ICAD	Inhibitor of CAD
ICP-AES	Inductively Coupled Plasma-Atomic Emission Spectrometry
IκBα	Inhibitor of NF-κB
IKK	Inhibitor of NF-κB kinase
IL-3	Interleukin 3
IP	Immunoprecipitation
JNK	c-Jun NH_2 terminal kinase
KGDHC	α-ketoglutarate dehydrogenase complex
LC8	Light chain 8 (dynein motor complex)
LDH	Lactate dehydrogenase
MC540	Merocyanine 540
Mcl-1	Myeloid cell leukemia sequence 1

MEK	ERK kinase
mRNA	Messenger ribonucleic acid
NAC	N-acetylcysteine
NADH	Nicotinamide adenine dinucleotide
NaPy	Sodium pyrithione
NF-κB	Nuclear Factor κ B
NGF	Nerve Growth Factor
NLS	Nuclear localization sequence
Noxa	induced by noxious stresses
O_2^-	Superoxide
PAGE	Ployacrylamide gel electrophoresis
PBS	Phosphate-buffered saline
PCR	Polymerase chain reaction
PE	Phycoerythrin
PI	Propidium Iodide
PI3K	Phosphoinositide-3 kinase
PKC	Protein kinase C
PVDF	Polyvinylidene difluoride
Puma	p53 up-regulated modulator of apoptosis
RNA	Ribonucleic acid
ROS	Reactive oxygen species
SDS	Sodium dodecyl sulphate
Smac	Second mitochondrial derived activator of caspases

TBS	Tris buffered saline
TCA Cycle	Tricarboxylic Acid Cycle
TNF-α	Tumor necrosis factor
TNFR	Tumor necrosis factor receptor
TPEN	N,N,N',N'-tetrakis (2-pyridinylmethyl) ethanediamine
TRAIL	TNF-related apoptosis inducing ligand
UV	Ultraviolet
VDAC	Voltage-dependent anion channel
XIAP	X-linked inhibitor of apoptosis
ZnPy	Zinc pyrithione
$ZnSO_4$	Zinc sulfate
Z-DEVD-fmk	Benzyloxycarbonyl-Asp-Glu-Val-Asp-fluoromethylketone
Z-LEHD-fmk	Benzyloxycarbonyl-Leu-Glu-His-Asp-fluoromethylketone
Z-VAD-fmk	Benzyloxycarbonyl-Val-Ala-Asp-fluoromethylketone
$\Delta\Psi_m$	Mitochondrial transmembrane potential
8-CPT-cAMP	8-(4-chlorophenylthio)-cAMP

Chapter 1

Introduction

Zinc: Traditional roles

Zinc is an essential trace element critically involved in growth and development where the sufficient availability of zinc is required for every highly proliferating cell system (13, 197). This requirement for zinc has been established through numerous studies where deficiencies in zinc results in dysfunction during embryogenesis as well as in other highly proliferating systems such as the immune system (54, 58, 101). Zinc has further been established as an integral cofactor for more than 300 enzymes and numerous proteins where it is required for either structural integrity or enzymatic activity (7, 197). Furthermore, zinc is involved in gene expression through numerous zinc-finger containing transcription factors (129, 156).

Zinc: Non-Traditional roles

Zinc has been shown to be a potent inducer of apoptosis in various cell types including cells of the immune and nervous systems which are particularly influenced by increased levels of zinc (33, 63, 87, 128, 156, 182, 190, 191, 213). Excess zinc may result from a variety of factors including environmental exposure from pollution or industrial accidents to over-supplementation or in the case of small children the ingestion of pennies (12, 86, 188, 204). Additionally, the increased use of intranasal sprays containing zinc results, in

some cases, in the temporary or permanent loss of smell (90). Furthermore, zinc has been shown to be released by certain neurons in response to neurotrauma or excitotoxicity resulting in cell death (33). Overall, the phenomenon of zinc-induced cell death has been illustrated in numerous cell types over more than ten years; however, it is only recently that the underlying mechanisms by which zinc induces apoptosis have been documented. Additional information on the proapoptotic role of zinc will be discussed herein.

Zinc and Alzheimer's disease:

The hallmarks of Alzheimer's disease (AD) are the insoluble deposits of amyloid plaques and neuronal degradation (40, 84, 132). The normally soluble amyloid β-protein (Aβ), the main constituent of these amyloid plaques, is a metalloprotein that binds Zn^{2+}, Cu^{2+} and Fe^{3+} *in vitro* (41, 42). Zinc causes aggregation of Aβ *in vitro* and is greatly enriched in Aβ plaque cores (84, 108). Additionally, H_2O_2 is generated when Cu^{2+} is bound to Aβ. It was speculated that Aβ may bind zinc as a protective mechanism against this oxidative insult initiated by Cu^{2+} bound Aβ (41). However, this protective role zinc plays may ultimately represent a deleterious role in AD through the production of these Aβ plaques (84). Whether plaque deposition is the critical pathogenic entity in AD still remains to be determined (70).

One therapeutic approach currently under investigation in the treatment of AD is the chelation of metals in Aβ plaques (40). Clioquinol (CQ), an antibiotic with zinc/copper chelating properties, is one promising candidate (79). CQ has been shown to solubilize Aβ deposits that are enriched for zinc and copper *in vitro* and in postmortem brain tissue

from patients with AD (79). In a pilot study 12-month old APP2576 mice (a transgenic mouse model of AD) were treated with CQ (20mg/kg/d) for 12-weeks (31). A significant 65% decrease in the levels of sedimentable Aβ was reported. A larger study conducted on 21-month old APP2576 mice treated with CQ (30mg/kg/d) for 9 weeks showed a significant decrease in amyloid plaque surface area as detected by immunohistochemistry (31). Accompanying this was a 49% decrease in levels of insoluble Aβ. A rating scale based on motor activity, alertness, and general health indicated improvement in CQ treated mice (31). A phase II clinical trial that assessed the therapeutic value of this zinc/copper chelator in the treatment of patients with AD has shown promising efficacy (31, 157). Additionally, the transgenic mouse model (APP2576) that normally develops amyloid plaques *in vivo* was crossed with mice lacking zinc transporter 3 (ZnT-3) in order to further study the role of zinc in plaque accumulation during AD (112). ZnT-3 is required for zinc transport into synaptic vesicles. Interestingly, ZnT-3 deficient APP2576 mice develop essentially no plaques compared to mice with ZnT-3 (66). Therefore, synaptic zinc contributes to amyloid deposition in this transgenic mouse model of Alzheimer's disease and further demonstrates a role for zinc in neuronal degeneration (112). Additionally, as will be discussed below synaptically released zinc has also been shown to induce cell death in surrounding neurons in response to excitotoxic stimuli.

Zinc and neuronal injury:

Certain neurons contain large amounts (300μM) of releasable free zinc at their synaptic terminals (61). Synaptically released zinc normally functions as a conventional neurotransmitter that modulates glutamate receptors. However, in response to global

ischemic insults, head trauma, or seizures, synaptically released zinc was shown to translocate to postsynaptic neurons which contributed to excitotoxic brain injury (33, 61, 62). It was shown that postsynaptic neurons which developed zinc positivity were also the neurons showing signs of injury. It was thus proposed that the synaptically released zinc was responsible for this cell death (33, 61, 62). Zinc chelation was therefore predicted to protect these neurons from injury and in fact did provided significant protection against cell death thus reducing excitotoxic neuronal injury (61, 62, 78, 104). This is another example of released or free zinc playing a role in cell injury and death.

This original model of synaptically released zinc inducing neuronal cell death has been well documented (61, 62, 78, 104). Nevertheless, recent evidence has indicated that this original model may be inadequate (62). A study was undertaken utilizing ZnT-3 deficient mice which lack histochemically reactive zinc in synaptic vesicles. Interestingly, zinc still accumulated in these mice in response to excitotoxic injury as assessed by a zinc-specific fluorescent dye (111). This indicated that the zinc accumulation in these cells had to originate from other sources besides that of the synaptic vesicles. Therefore, an expanded model has been proposed that included involvement of both synaptically released zinc as well as zinc released from zinc-binding proteins such as metallothionein (MT) during the regulation of neuronal cell death (62). Additionally, the release of zinc from zinc-binding proteins may be a predominant event in regions of the brain that contain little or no synaptic zinc (62). In addition to neuronal cells, intracellular zinc fluxes, consistent with release from metalloproteins, have also been observed in cells of the immune system in response to apoptosis (221).

Zinc Toxicity:

In addition to the examples of zinc toxicity discussed earlier, a variety of different cell types are susceptible to increased levels of zinc. These cell types include: intestinal and retinal pigment epithelial (25, 213), thyroid (87), lung (205), liver (148), prostate (56), as well as cells of the immune system (128, 190, 191). Interestingly, zinc has also been implicated in the death of pancreatic islet β-cells in a streptozotocin (STZ)-induced model of diabetes (97). Zinc is stored and released with insulin from pancreatic islet β-cells (97). It was shown that zinc was functioning in a paracrine fashion to further accelerate cell death, which over time may be a factor in the development of diabetes (97). Additionally, exposure to increased levels of zinc may result from a variety of factors. In some cases this may be due to environmental exposure such as with pollution or industrial accidents (188, 204). In other cases this may be self-induced due to over-supplementation or as has recently become prevalent through the increased use of intranasal cold remedies containing zinc that are sold over the counter (86, 90). The use of intranasal sprays containing zinc can be toxic to olfactory epithelium which in some circumstances result in temporary or permanent anosmia, which is the loss of smell (90). Interestingly, a link between zinc and anosmia has been known since studies on the prevention of polio in 1934 (90, 160). At the time it was believed that the olfactory epithelium was the only route of entry of the polio virus and that nasal zinc administration would protect against the development of polio (90). However, the protective use of nasal zinc did not alter the rate of polio and in many patients resulted in anosmia (90). A number of other studies have additionally verified this toxic effect of zinc (75, 133, 165, 184). In addition to these potential routes of zinc exposure, increases

in free intracellular zinc may also occur as a result of release from metalloproteins such as metallothionein. Activation of protein kinase C by diacylglycerol or reactive oxygen species has also been shown to release labile zinc (107). Moreover, intracellular zinc fluxes have been observed in cells of the immune system undergoing apoptosis (221). Zinc's involvement in apoptosis will be further explored in the following sections.

General Role of Apoptosis:

Apoptosis is a regulated form of cell death that plays an essential role in the development and maintenance of a wide variety of tissues (37, 146). Typical features of cells undergoing apoptosis include: nuclear condensation, inter-nucleosomal cleavage of chromatin, blebbing of the plasma membrane as well as shrinkage of the cell (37). As illustrated in Figure 1-1, two primary apoptotic programs exist. The intrinsic pathway utilizes the mitochondria as a central point of regulation for many diverse signals that initiate apoptosis. This pathway is regulated by the Bcl-2 family of antiapoptotic (Bcl-2, Bcl-xL) and proapoptotic (Bax, Bak, BH3 only proteins) proteins (146). Activation of this pathway results in the release of various factors from the mitochondria including cytochrome c which activates the apoptosome (3). This in turn results in activation of caspases which are the executioners of apoptosis (44, 146). The extrinsic pathway involves stimulation of the plasma membrane bound death receptors which directly activate caspases, although in certain cases there can be cross-talk between these pathways (203). Apoptosis is a complicated but highly regulated process and its dysregulation is significant to the pathogenesis of a number of diseases (192). Where apoptosis is insufficient cancer and autoimmune disease occurs, while unwarranted

Figure 1-1: Cell Death Pathways.
General components of the Intrinsic (Mitochondrial) and Extrinsic (Death Receptor) apoptotic cascades.

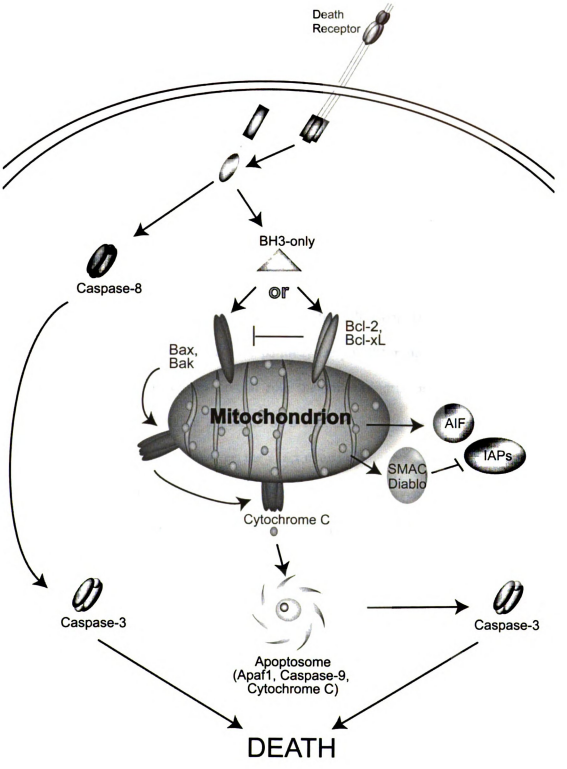
Death
Receptor
BH3-only
or
Caspase-8
Bcl-2,
Bcl-xL
Bax,
Bak
Mitochondrion
AIF
IAPs
SMAC
Diablo
Cytochrome C
Caspase-3
Caspase-3
Apoptosome
(Apaf1, Caspase-9,
Cytochrome C)
DEATH

apoptosis is apparent in diseases such as diabetes and AIDS as well as in neurodegenerative disorders (192). A variety of therapeutic approaches are aimed at resolving these imbalances (9, 143). As a result, the factors that regulate the induction of apoptosis, such as zinc, are being intensively studied. An understanding of these factors as well as the signaling pathways employed is crucial to the pursuit of medical advances designed to combat such disorders. Therefore, apoptosis, and the apoptotic signaling cascade utilized during zinc-induced apoptosis will be discussed herein.

Mitochondria:

Mitochondria are the complex power generators of the cell which have long been know to accommodate many critical biosynthetic pathways required for survival. Over the past decade the previously unknown pivotal role the mitochondria play in apoptosis has become evident. Mitochondria appear to be a central focusing point for many diverse signals initiating apoptosis. However, the exact nature of the mitochondrial contribution to cell death still remain controversial (142). Several key events may occur during apoptosis involving the mitochondria including changes in electron transport, loss of mitochondrial transmembrane potential, altered oxidation-reduction reactions, the release of factors such as cytochrome c, AIF (Apoptosis-inducing factor) and Smac/Diablo, as well as the interaction with pro and antiapoptotic Bcl-2 family members (71). Whether these events occur individually or in parallel may depend on the inducer of cell death and remain under continued investigation. As will be discussed, there is a role for zinc in mitochondrial mediated apoptosis.

Disruption of electron transport:

As illustrated in Figure 1-2, electron transport is carried out in the mitochondrial inner membrane by complex I- complex IV, ATP synthase and water soluble cytochrome c. The outer mitochondrial membrane is permeable to small charged molecules due to VDAC (voltage-dependent anion channel), though it is impermeable to proteins such as cytochrome c in the intermembrane space (142). However, during apoptosis cytochrome c can be released from the intermembrane space and this loss of cytochrome c may result in a disruption of electron transport (142).

Inner mitochondrial transmembrane potential:

The inner mitochondrial transmembrane potential ($\Delta\Psi_m$) is derived from the H^+ ion gradient created by electron transport and used by ATP synthase to produce ATP. During apoptosis the release of cytochrome c is independent of and in many cases precedes a loss of $\Delta\Psi_m$(16). The loss of $\Delta\Psi_m$ reflects a block in electron transport. This is not simply due to the reduced concentration of cytochrome c, which is present in functional excess, and may be able to maintain respiration even after release into the cell (208). There is evidence that membrane potential loss may be due to disruption of complex I and complex II by activated caspases (155).

While disruption of electron transport may occur as a general factor during apoptosis due to caspase activity it can be directly modulated by intracellular free or labile zinc. Intracellular zinc accumulation has been shown to contribute to neuronal damage initiated during ischemia or epilepsy as discussed (33, 62, 167). Mobilization of zinc

Figure 1-2: Components of the mitochondria that may play a role in apoptosis.

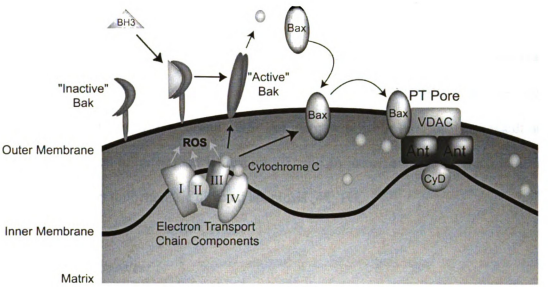
BH3
Bax
"Inactive"
Bak
"Active"
Bak
Bax
PT Pore
Bax
VDAC
Ant
Ant
CyD
ROS
Cytochrome C
Outer Membrane
I
II
III
IV
Inner Membrane
Electron Transport
Chain Components
Matrix

between the cytosolic and mitochondrial pools may contribute to this damage by inducing a loss of $\Delta\Psi_m$ thus disrupting the normal function of the mitochondria (167, 169). Metallothionine, the small zinc binding protein, has been shown to transport zinc into liver mitochondria and inhibit respiration in a zinc dependent manner (219). Several locations where zinc may function to inhibit respiration were identified. Zinc has been shown to inhibit electron transport at complex III (cytochrome bc_1) in bovine heart mitochondria (121). Investigation into the role of zinc inhibition during earlier stages of mitochondrial energy metabolism upstream of complex III revealed a point of regulation in the TCA Cycle. Zinc strongly inhibited the α-ketoglutarate dehydrogenase complex (KGDHC) (22). The lipoamide dehydrogenase subunit of KGDHC catalyzes the oxidation of NADH by O_2 generating ROS. An increase in labile zinc may thus result in an overall reduction of mitochondrial respiration with an increase in ROS, which in turn may be involved in mitochondria directed apoptosis (49, 169, 172).

Reactive Oxygen Species:

Reactive oxygen species are thought to be an important participant in the aging process and neuronal degeneration (91, 220). During normal function of the mitochondria a small portion of electrons leak out of the electron transport chain and react with molecular oxygen to form superoxide (O_2^-) (71). Superoxide in turn is quickly converted to H_2O_2 by superoxide dismutase. Generally complex I – complex III are thought to be involved in the production of these ROS (142). However, more specifically the flavin mononucleotide group of complex I was identified as an important source for ROS generation through reverse electron transfer (123). Glutathione and thioredoxin are two

important protection mechanisms for cellular defense against this ROS production (48, 150, 176). Glutathione peroxidase catalyzes the reduction of H_2O_2 and GSH into water and GSSG thus rendering the damaging ROS harmless (48). Replenishment of GSH occurs through the reduction of GSSG and *de novo* synthesis in order for GSH to remain at millimolar levels in the cell.

GSH depletion was previously shown to be an early event in thymocyte apoptosis for a variety of inducers (124). ROS may be one of several mechanisms through which zinc participates in cell death in a number of cell types. Synaptically released zinc was able to enter into some neurons through the calcium permeable AMPA/kainate channels and trigger superoxide production (168, 169). ROS also modulates zinc-induced apoptosis in the human mammary adenocarcinoma cell line TS/A (152). Exposure of rat primary astrocytes or C6 glioma cell line to zinc resulted in the depletion of GSH within 2 hours and with a 250% increase in ROS (161). Zinc toxicity appears to be mediated by GSH and GSSG reductase activity in various pulmonary cell lines (206). An increase in ROS would initially reduce available GSH levels and a concurrent decrease in GSSG reductase activity would result in an overall lower amount of GSH available for protection (205, 206). Treatment with antioxidants such as GSH, N-acetylcysteine (NAC) and ascorbic acid substantially reduced the cell death stimulated by zinc indicating a role for ROS in zinc mediated apoptosis in these cells (205).

Accompanying the loss of $\Delta\Psi_{m,}$ an increase in ROS production occurs in the presence of zinc (22). As a consequence of the induction of ROS by zinc, depletion of the cellular

protection provided by GSH can result in the activation of signaling pathways which may be associated with cell death such as ERK, JNK (170), and p53 (152) while superoxide itself may activate and stimulate zinc release from PKC (103, 107). These signaling pathways are involved in everything from proliferation and differentiation to stress and immune responses. It appears that the Ras/Raf/MEK/ERK signaling pathway may be important for ROS in NGF differentiated PC12 cells since a dominant negative Ras blocked ERK activation and zinc-induced cell death (170). Treatment with antioxidants also blocked activation of ERK by zinc. Activation of Ras may therefore be ROS or cell type specific since in *C.elegans* zinc accumulation inhibited Ras. CDF-1 (cation diffusion facilitator protein), which is similar to the zinc transporter ZnT-1, functions as a positive regulator of Ras by reducing cytosolic zinc (23, 74). Zinc regulation is therefore important for maintaining the Ras pathway in an inactive state in *C.elegans* (23). JNK, another signaling molecule which can be activated by various inducers of apoptosis, was activated by zinc in differentiated PC12 cells (170). However, in this case inhibition with a dominant negative failed to block cell death. This result indicated that in these cells this pathway was not significant in zinc induced apoptosis (170).

ROS are also capable of causing DNA strand breaks which can lead to the stabilization and accumulation of p53. In the proper redox environment p53 can switch between the wild-type and mutant form (136). Cadmium inhibits DNA binding and has been shown to suppress the wild type p53 response to DNA damage (135) while the addition of zinc was reported to mediate the renaturation of wild-type p53 exposed to metal chelators (136). Consequently zinc binding is crucial for the stabilization of p53 in wild type formation

and for DNA binding (32). Low intracellular zinc induced ROS in a rat glioma cell line (C6) resulting in increased p53 expression but with greatly reduced DNA binding ability (82). The addition of zinc to TS/A mammary cancer cells resulted in the accumulation of p53 in a ROS dependent manner since antioxidant NAC blocked the increase in p53 and apoptosis (152). Prostate epithelial cells in contrast showed a loss of $\Delta\Psi_m$ but no sign of p53 activation to high levels of zinc (196). While zinc induced ROS can in some cases activate signaling pathways such as ERK and p53, ROS itself can activate preparations of PKC with a concomitant release of zinc (103). Similar results were obtained with a zinc chelator indicating that zinc release is required for superoxide-induced activation of PKC. Under certain conditions this released zinc could possible result in a feedback regulation of ROS production by the mitochondria. Overall, zinc-induced cell death in some types of cells may therefore be mediated by a loss of $\Delta\Psi_m$, GSH depletion and ROS.

Permeability Transition Pore (PTP):

A variety of proapoptotic factors such as cytochrome c and Smac/Diablo can be released from the intermembrane space of the mitochondria during apoptosis. Understanding how this occurs is still controversial. One model implicates a sustained opening of the permeability transition pore (PTP) (222). This pore is thought to be composed of the outer mitochondrial membrane (OMM) proteins VDAC, peripheral benzodiazepine receptor, the inter membrane space protein creatine kinase (CK), and the inner mitochondrial membrane (IMM) protein adenine nucleotide translocator (ANT), as well as the mitochondrial matrix protein cyclophilin D and Bcl-2 family members (222). In this model a large pore forms between the OMM and IMM which allows an influx of

water and solutes from the cytoplasm into the mitochondrial matrix resulting in a loss of $\Delta\Psi_m$, osmotic swelling and rupture of the OMM (131). While this model can account for some forms of cell death, it does not account for the majority of apoptosis that is observed in which the mitochondria do not swell and rupture but instead remain intact with the release of proapoptotic factors (142). Another model that may better account for the lack of morphological changes associated with PTP opening in the mitochondria entails a channel formation in only the OMM large enough to allow the release of proapoptotic factors. Proteins that may be involved in this model include the proapoptotic Bcl-2 family members Bax and Bak which can interact and stimulate VDAC opening through which cytochrome c could leak out of the intermembrane space (131, 174, 198)). (see below).

Release of cytochrome c from the mitochondria:

One of the first mitochondrial components identified in the involvement of the intrinsic apoptotic pathway was the release of cytochrome c from the intermembrane space. Cytochrome c activates the intrinsic pathway through the assembly of the apoptosome which promotes the proficient cleavage and activation of caspase 3 as seen in Figure 1-1 (71, 80). The apoptosome is a large wheel like structure (~1MDa) composed of seven arms that radiate from the center. It is composed of apoptotic protease activating factor-1 (Apaf-1), procaspase 9, and cytochrome c (2). Apoptosome assembly results when cytosolic cytochrome c binds the WD40 repeats of monomeric Apaf-1 which alters its conformation allowing the binding of ATP to the N-terminal caspase recruitment domain (CARD) and subsequent heptameric multimerization and association of procaspase 9 to

the exposed C-terminal CARD (3, 119). The apoptosome initially binds seven monomers of inactive procaspase 9; this locally high concentration of procaspase 9 drives the recruitment of more inactive procaspase 9 which results in activation of only one active caspase 9 in the dimer (2, 154). Caspase 9 has much greater proteolytic activity when bound to the apoptosome than when free in solution so it has been suggested that the apoptosome functions as a holoenzyme in which Apaf-1 is the regulatory subunit and caspase 9 is the catalytic subunit (2, 158). However, in order to maintain procaspase 9 in an inactive state in the absence of apoptotic signals the procaspase 9 CARD will not bind to full length Apaf-1 in the absence of cytochrome c. It is thought that in the absence of cytochrome c the WD40 repeats of Apaf-1 may inhibit apoptosome formation by blocking access to its CARD thus keeping Apaf-1 and procaspase 9 in a monomeric state (2).

During zinc-induced apoptosis cytochrome c was shown to be released from mitochondria in prostate cells (55, 56). Additionally we have demonstrated a requirement for caspase 9 and caspase 3 activity in response to zinc treatment in mouse thymocytes undergoing apoptosis (128). Others have also similarly demonstrated activation of caspase 9 and/or caspase 3 in response to zinc treatment in other cell types (105, 166, 213).

The Bcl-2 family of proteins has long been thought to modulate apoptosis through the release of proapoptotic factors from the mitochondria such as cytochrome c. The apoptosome is very important in many instances of cell death since knockout mice

deficient in Apaf-1 or caspase 9 generally die before birth due to defects in the central nervous system. However, it appears that the apoptosome may not be necessary for all apoptosis regulated by the Bcl-2 family (46, 130). Donor derived B-cells and T-cells deficient in either apaf-1 or caspase 9 from reconstituted mice showed little protection against a variety of treatments while noticeable protection was observed with overexpression of Bcl-2 (130). Activation of the extrinsic apoptotic pathway by TRAIL (TNF-related apoptosis inducing ligand) in some cancer cells also requires the proapoptotic Bcl-2 family mediated release of factors other than cytochrome c from the mitochondria for apoptosis to occur (46). It has been proposed that the apoptosome is therefore not an essential trigger in certain cell types but is instead involved in the amplification of apoptotic signals mediated by the Bcl-2 family (130).

Release of Smac/Diablo and Omi/HtrA2 from the mitochondria:

Two other proteins known as the second mitochondrial derived activator of caspases or direct IAP-binding and low pI (Smac/Diablo) and Omi/HtrA2 are also released with cytochrome c from the mitochondria during apoptosis (50, 53, 199). While cytochrome c directly activates apoptosome formation and caspase activation, Smac/Diablo and Omi/HtrA2 instead neutralizes various IAP (Inhibitor of Apoptosis) family members inhibition of caspase activation as illustrated in Figure 1-1 (173). IAPs were first identified in baculovirus in which they were able to block apoptosis in mammalian cells (47). IAPs contain the unique Baculoviral IAP Repeat (BIR) domains which may have a novel zinc-binding fold. Eight mammalian IAPs have been identified including XIAP, c-IAP1 and c-IAP2 which contain 3 BIR domains with different functions. A linker region

between BIR1 and BIR2 is required for caspase 3 and 7 interaction in XIAP, but BIR3 is required for caspase 9 interaction. XIAP does not interact with unprocessed procaspase 9. The BIR3 domain of XIAP interacts with the exposed N-terminus tetrapeptide of the small subunit of processed caspase 9 resulting in inhibition of its catalytic activity (177). XIAP also has E3-ubiquitin ligase activity which marks active but not procaspases for proteasomal degradation (187, 218). This E3 activity also regulates autoubiquitination of XIAP (218).

Smac/Diablo and Omi/HtrA2 are initially produced as precursor proteins that are targeted to intermembrane space of the mitochondria. Processing of this precursor protein results in the exposure of an N-terminal tetrapeptide sequence that is required for interaction with IAPs. Smac/Diablo, which functions as a dimer, antagonizes the role of IAPs by binding their BIR3 domain with the N-terminal peptide (AVPI) (214). The Smac/Diablo peptide can remove the inhibition of caspase 9 by IAPs. This allows the processed caspase 9 to remain active and cleave downstream targets such as caspase 3. Positive feedback occurs when caspase 3 cleaves a 15-residue peptide from caspase 9 thus removing the ability of IAPs to interact and block the catalytic activity of caspase 9. This released peptide can then bind IAPs which along with Smac/Diablo reversibly removes IAP inhibition of caspase activity and allows fully activated caspases to cleave downstream targets (173). Omi/HtrA2 is the mammalian homologue of the bacterial HtrA (high temperature requirement A) protein. In bacteria damaged and denatured proteins resulting from exposure to high temperatures are removed by the protease activity of HtrA while at normal temperatures HtrA functions as a chaperone (53).

Omi/HtrA2 operates as a homotrimer which binds and antagonizes IAP function in a similar manner as Smac/Diablo (53, 186, 217). However, in contrast to Smac/Diablo, Omi/HtrA2 has serine protease activity that is indispensable for its proapoptotic function. Cleavage of c-IAP1 by Omi//HtrA2 significantly reduces its E3 ligase activity on caspase substrates (217).

Nucleases released by the mitochondria

A third type of factor released from the mitochondria during apoptosis includes the nucleases AIF and EndoG. When liberated during apoptosis AIF translocates to the nucleus and induces large scale (~50Kbp) DNA fragmentation and chromatin condensation (43). Like AIF, EndoG also translocates to the nucleus where it causes high molecular weight fragmentation as well as nucleosomal DNA fragmentation similar to the caspase activated DNase (CAD) (5, 212). However, unlike the CAD which is activated when caspase 3 removes repression by the inhibitor of CAD (ICAD), nuclear DNA fragmentation by AIF or EndoG require release from the mitochondria (118, 122). Interestingly permeabilization of the mitochondria by the proapoptotic Bcl-2 family members Bax/Bak results in the release of cytochrome c, Smac/Diablo and Omi/HtrA2 although AIF and EndoG are still retained in the mitochondria (5). Release of EndoG and AIF occurs downstream of caspase activation in this case (5). Conversely, there may be a role for AIF in a caspase-independent cell death. It was shown that AIF was able to translocate to the nucleus in the presence of the caspase inhibitor Z-VAD-fmk. However, only large DNA fragments were observed with a phenotypic appearance of necrosis (43).

Overall these nucleases may have a role in both caspase-dependent and caspase-independent cell death.

Interaction with the Bcl-2 Family:

The Bcl-2 family constitutes an important checkpoint for the intracellular regulation of cell death. Bcl-2 was initially identified at the chromosomal break point t(14;18) translocation in the human follicular B-cell lymphoma (8, 34, 195). This translocation resulted in the increased expression of Bcl-2. Overexpression of Bcl-2 protected these cells from a variety of apoptotic stimuli thus resulting in lymphoma. The Bcl-2 family has since expanded to include both proapoptotic and antiapoptotic proteins as illustrated in Figure 1-3 (4). Bcl-2 family members are classified based upon four conserved α-helical segments designated Bcl-2 homology (BH) domains (BH1-BH4) (73). All family members contain at least one BH domain. The most highly conserved antiapoptotic Bcl-2 members contain all four BH domains of which BH1, BH2 and BH3 structurally form a pocket allowing interaction with the BH3 domain of other family members (146). While the highly conserved antiapoptotic family members such as Bcl-xL and Mcl-1 contain four BH domains, the proapoptotic family members can be subdivided into two general groups based upon the number of BH domains they possess. The multidomain proapoptotic family members such as Bax, Bak and Bok are similar to Bcl-2 and contain BH1, BH2 and BH3 domains. However, in contrast to these conserved family members the remaining proapoptotic members such as Bim, Bad, Noxa (100, 202), Puma (202), and Bik (39) contain only the BH3 domain and are known as the "BH3-only" family members. These members show little sequence conservation to Bcl-2 outside of the BH3

Figure 1-3: The Bcl-2 family of proteins.

Antiapoptotic

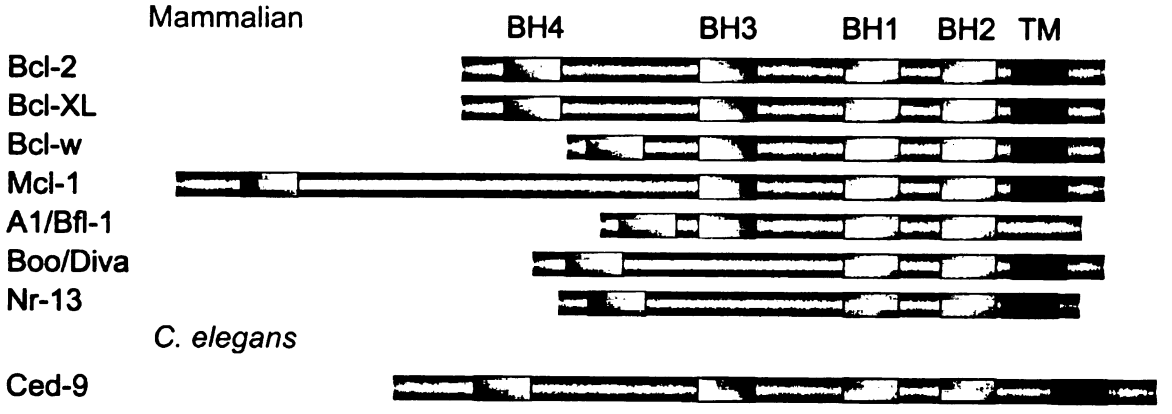

Proapoptotic

domain and are unrelated to any other known proteins. Furthermore, the BH3 domain is indispensable for their proapoptotic role as physiological antagonists to the antiapoptotic Bcl-2 family members.

The proapoptotic multidomain Bcl-2 family members:

The antiapoptotic Bcl-2 family members are integral membrane proteins generally found at the mitochondria, the endoplasmic reticulum or nuclear membrane while the BH3-only proapoptotic members localize to the cytosol or cytoskeleton prior to activation by death stimuli (73, 153). Activation of the proapoptotic members results in a conformational change which enables them to antagonize the antiapoptotic proteins located at the mitochondrial membrane (73). However, in many cases the multidomain proapoptotic proteins Bax and Bak are required and appear to be an essential gateway for mitochondrial dysfunction and apoptotic cell death (210). Cells from mice deficient for both Bax and Bak demonstrated resistance to a variety of different death stimuli: staurosporine, UV radiation, growth factor deprivation, and etoposide, all of which activate the intrinsic mitochondrial apoptotic caspase cascade (210). The lack of both of these genes in deficient mice is severe, as demonstrated by abnormalities in cellular homeostasis, and can be embryonic lethal (146). However, mice individually deficient in either Bax or Bak may show some lymphoid hyperplasia or no immunological phenotype thus demonstrating some compensation for the lack of the other multidomain proapoptotic member (120). Furthermore, the combined functions of Bax and Bak are essential for normal development of many tissues (120).

The multidomain proapoptotic protein Bax exists as inactive monomers in unstimulated viable cells and is generally located in the cytosol or loosely attached to membranes (83). The C-terminal α-helix of Bax is bound by the pocket formed by the BH1-BH3 domains in the inactive monomer thus keeping it inactive in the cytosol (185). However, in response to apoptotic signals Bax homo-oligomerizes, forming multimers, and inserts deeply into the outer mitochondrial membrane (51, 72). Bak on the other hand is an integral mitochondrial membrane protein and thus already resides in the outer mitochondrial membrane (209). In response to activation Bak also undergoes homo-oligomerization and activation resulting in the release of cytochrome c from the mitochondria and activation of the intrinsic caspase cascade (115, 209).

BH3-only proapoptotic family members are upstream activators of Bax and Bak. Compelling evidence demonstrated an essential downstream role for Bax and Bak where ectopic expression of BH3-only proteins resulted in homo-oligomerization of Bax or Bak and release of cytochrome *c* (30). This occurred whether ectopic expression involved wild-type cells or cells deficient in either Bax alone or Bak alone. However, when cells were deficient in both multidomain proteins, Bax and Bak, the BH3-only proteins failed to induce cell death further implicating these multidomain proteins as an essential gateway for mitochondrial dysfunction and cell death (30). Interestingly, the BH3-only proteins could still target the mitochondria. The BH3-only domains are the functional domain of BH3-only proteins since short peptides derived from various BH3-only proteins are able to activate Bax and Bak resulting in the release of cytochrome *c* (115, 146, 209).

While it is known that activation of Bax and Bak result in oligomerization and the release of cytochrome c it is still under debate whether additional proteins are required for permeabilization of the mitochondria outer membrane (142). Conflicting data has been reported as to the minimum requirements for permeabilization which may be due to the different experimental strategies utilized by the various laboratories (110, 174). Using cell-free systems and reconstituted vesicles from defined molecules it was shown that permeabilization of the mitochondrial outer membrane did not require the mitochondrial matrix, inner membrane or other proteins (110). However, in the absence of other proteins the BH3-only protein Bid activated monomeric Bax, required cardiolipin, and produced membrane openings that allowed the passage of very large (2 megadalton) molecules (110). Additionally, these openings were inhibited by the antiapoptotic protein Bcl-xL (110).

It has also been demonstrated that Bax and Bak interacts with and activates the permeability transition pore (PTP) members such as VDAC during pore formation and release of cytochrome *c* (174, 198). Recombinant Bax and Bak accelerate the opening of voltage dependent anion channel (VDAC) in liposomes whereas Bcl-xL closes this channel through direct interaction (174). Furthermore, VDAC1 deficient mitochondria (from yeast) did not release cytochrome *c* demonstrating a requirement for this additional mitochondrial protein (174). In contrast, embryonic stem cells deficient in VDAC1 were as similar in sensitivity as the wild type cells in response to activators of the intrinsic mitochondrial pathway indicating VDAC1 may not be as essential in the activation of

mitochondrial apoptosis (29). In some cases opening of the PTP may act as an initiating event stimulating Bax translocation to the mitochondrial outer membrane (151). Overall, the role Bax or Bak plays in connection with the PTP and release of cytochrome c is presently unclear and still controversial. However, what is clear is that activation of Bax or Bak results in the release of cytochrome c (142).

***Roles of zinc in Bcl-2 mediated apoptosis*:**

The PTP may also be a potential site of action for zinc. It was demonstrated that low concentrations of zinc (10nM) could induce the opening of the PTP in isolated mitochondria and result in the release of cytochrome *c* (92). However, since isolated mitochondria were utilized, the amount of zinc required for the effect on the PTP may be higher in intact cells. It has been proposed that zinc could directly activate the mitochondria resulting in the release of cytochrome c (166). However, in our hands, intact mouse thymocytes required transcription and translation in order to undergo apoptosis (128, 190). The inhibition of transcription would have no affect upon apoptosis if zinc were directly activating the mitochondria thus resulting in release of cytochrome *c* and activation of the caspases. However, it does not appear that the direct activation of the mitochondria occurred in our system since transcription was required (128). As will be discussed below, our laboratory was the first to demonstrate the ability of zinc to promote the transcriptionally dependent up-regulation of the BH3-only protein Bim, which is known to function through activation of the multidomain proapoptotic proteins Bax and Bak (128).

Interestingly, it has been reported that VDAC2, a VDAC isoform present in low abundance in the outer mitochondrial membrane, interacts with and maintains the integral outer mitochondrial membrane protein Bak as a monomer in an inactive state (29). Cells deficient in VDAC2 were more susceptible to apoptotic stimuli and demonstrated enhanced Bak oligomerization (29). Overexpression of VDAC2 significantly inhibited apoptosis in Bax deficient cells which still contain Bak; however, it had little effect on Bak deficient cells that contained Bax, further demonstrating the specificity of the interaction with Bak (29). BH3-only proteins can displace VDAC2 from Bak allowing oligomerization and activation of Bak resulting in apoptosis (29).

It has been reported that high concentrations of exogenous zinc could inhibit Bax or Bak oligomerization and apoptosis in response to chemical inducers (67). Since Bax and Bak are regarded as a gateway to mitochondrial induced apoptosis this could be one of the many potential sites of action for zinc. The antagonistic effects of high concentrations (mM levels) of zinc on apoptosis have been widely reported for many years (59, 194). However, most studies demonstrating the suppression of apoptosis *in vitro* have used supraphysiological levels of zinc salts (up to 10mM) (10, 67). The use of very high concentrations of zinc in the millimolar range can also non-specifically cross link proteins so caution must be taken with the interpretation of the results. While high concentrations of zinc have been shown to suppress apoptosis, it does not appear to provide long term protection from cell death for mouse thymocytes (60). In order to explore the role of zinc in apoptosis others have used the zinc ionophore, pyrithione, and more physiological (25μM) levels of zinc salts (194). Instead of suppressing cell death much lower concentrations of zinc pyrithione (400nM), in our hands, induced apoptosis

in mouse thymocytes and utilized the intrinsic mitochondrial pathway of which Bax is an essential gateway (128).

The proapoptotic BH3-only Bcl-2 family members:

While mitochondria as a whole are the central focusing point for many diverse signals that initiate apoptosis, the antiapoptotic proteins Bcl-2/Bcl-xL and the multidomain proapoptotic proteins Bax/Bak function as gatekeepers. Throughout the cell the BH3-only proteins function as sensors for a variety of cellular insults such as growth factor deprivation (Bad, Bim), T-cell receptor activation (Bim), DNA damage (Noxa, Puma), or even activation of death receptors (Bid) which in turn activate the mitochondrial gatekeepers as illustrated in Figure 1-4 (146). The antagonism between the antiapoptotic and proapoptotic gatekeepers determines the cells fate.

A variety of death stimuli activate BH3-only family members (146). However, different BH3-only family members appear to be utilized in response to various apoptotic death stimuli (146). Additionally, the utilization of particular BH3-only members may be cell type specific (146). BH3-only proteins require the multidomain proapoptotic proteins Bax or Bak in order to release cytochrome c from the mitochondria (115). BH3-only domains from BH3-only family members differ in there abilities to induce the release of cytochrome *c* (109, 115). The BH3-only proteins can either interact directly with the multidomain proapoptotic proteins resulting in oligomerization and release of cytochrome *c* or BH3-only proteins can interact directly with antiapoptotic proteins such as Bcl-xL (30, 109, 115). Bcl-2 and Bcl-xL can sequester BH3-only proteins preventing

Figure 1-4: Regulation of apoptosis by proapoptotic BH3-only family members.
Different BH3-only proapoptotic family members are utilized in response to various inducers of apoptosis and their interaction with antiapoptotic and proapoptotic Bcl-2 family members determine the cells fate.

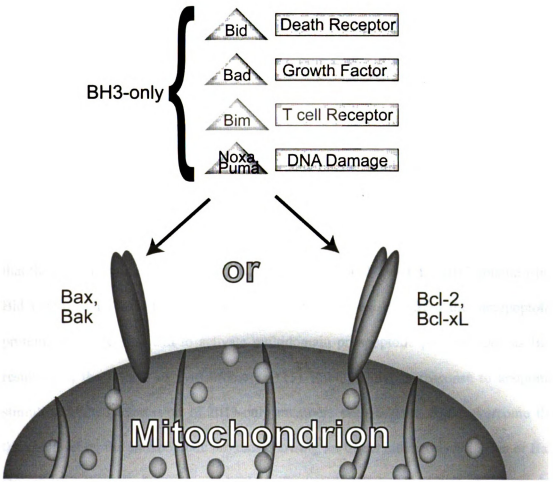
BH3-only
Bid
Death Receptor
Bad
Growth Factor
Bim
T cell Receptor
Noxa
Puma
DNA Damage
or
Bax,
Bak
Bcl-2,
Bcl-xL
Mitochondrion

the activation of Bax and Bak mediated mitochondrial apoptosis (30). However, if Bcl-2 or Bcl-xL previously sequestered Bax or Bak, a new interaction with BH3-only proteins could relieve this inhibition by displacing Bax and result in activation and permeabilization of the mitochondria (109).

Certain BH3-only proteins such as Bim or Bid are capable of directly binding and activating Bax or Bak (115, 139). In contrast, others such as Bad only interact with the antiapoptotic proteins and thus act as sensitizers that antagonize the antiapoptotic proteins. In this manner Bad functions by lowering the threshold required to induce apoptosis (115). Whereas Bim or Bid can directly interact with Bax or Bak they can also be sequestered by the antiapoptotic proteins thus preventing activation of the multidomain proapoptotic proteins (26, 76). It has been demonstrated experimentally that the BH3 domain from Bad has a higher affinity for Bcl-2 than the BH3 domain from Bid (115). This would allow Bad to efficiently displace Bid from the antiapoptotic proteins thus releasing Bid to activate multidomain proapoptotic proteins such as Bak resulting in the release of cytochrome c (115). Additionally, in response to apoptotic stimuli increased expression of BH3-only members such as Bim could overcome the threshold set by the antiapoptotic proteins allowing for direct interaction with Bax or Bak thus shifting the cells fate towards death as illustrated in Figure 1-5. Mitochondria with protective levels of the antiapoptotic protein Bcl-2 (30) or the overexpression of Bcl-2 resulted in the protection of cells from activation with BH3- only proteins (115).

Figure 1-5: Interactions between antiapoptotic and proapoptotic Bcl-2 family members regulate decisions between life and death. **A)** Antiapoptotic proteins sequester and neutralize BH3-only proteins resulting in cell survival. **B)** Increased expression of BH3-only proteins result in saturated binding of Bcl-2 and Bak resulting in cell death.

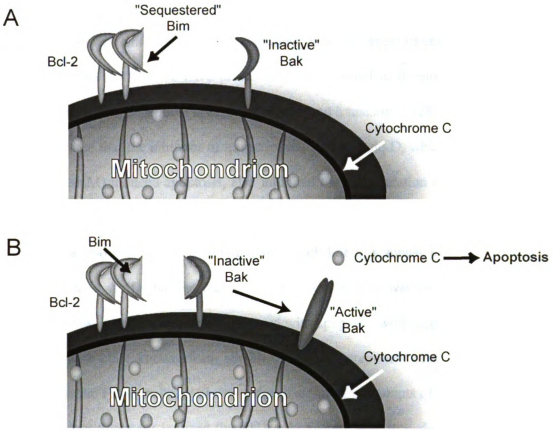
A
"Sequestered"
Bim
Bcl-2
"Inactive"
Bak
Cytochrome C
Mitochondrion
B
Bim
"Inactive"
Bak
Cytochrome C
Apoptosis
Bcl-2
"Active"
Bak
Cytochrome C
Mitochondrion

Zinc induced the up-regulation of the BH3-only family member Bim:

Over the last few years, BH3-only proteins have been established as important regulators of the intrinsic mitochondrial apoptotic signaling cascade. However, regulation of the mitochondrial pathway by zinc has remained uncertain. The question therefore arose; does a BH3-only protein regulate zinc-induced apoptosis? As will be discussed herein, our laboratory identified for the first time (to our knowledge) the strong up-regulation of the BH3-only protein Bim in response to treatment with low levels of exogenous zinc in mouse thymocytes (128). We have previously demonstrated in thymocytes that zinc-induced apoptosis was dependent upon transcription and translation (128, 190). We have also demonstrated that the inhibitor of transcription, actinomycin D, which blocked zinc-pyrithione (400nM) induced apoptosis, also inhibited the up-regulation of the BH3-only protein Bim in thymocytes (128). In addition to mouse thymocytes, an increase in Bim expression was also observed in the mouse S49 T-cell line in response to zinc treatment (126). In order to verify that the increased expression of Bim was in fact due to zinc treatment and not just a common event involved with apoptosis wild-type (WT) S49 cells were treated with other known death stimuli. Etoposide treatment or activation of the extrinsic apoptotic Fas signaling pathway induced significant amounts of apoptosis (126). However, neither treatment induced the BH3-only protein Bim thus demonstrating that the increase in Bim expression observed in response to zinc treatment was due to zinc (128).

Antiapoptotic proteins are known to sequester BH3-only proteins such as Bim (30), and overexpression of the antiapoptotic proteins such as Bcl-2 or Bcl-xL have also been

shown to protect cells from BH3-only proteins (115). If the up-regulation of Bim was responsible for zinc-induced apoptosis then overexpression of the antiapoptotic proteins should therefore block zinc-induced cell death. Indeed, we have demonstrated that overexpression of Bcl-2 or Bcl-xL in the human Jurkat T-cell line or Ramos B-cell line resulted in the protection of these cells from zinc-induced apoptosis (128). Others have also established that overexpression of Bcl-2 protected Ramos B-cells from zinc-induced apoptosis (166). On the other hand, high concentrations of zinc (1mM) were shown to increase Bcl-2 levels while reducing Bax levels in the U937 cell line (64). It was suggested that this change in Bcl-2/Bax ratio induced by zinc (1mM) was responsible for the protection of the cells from hydrogen peroxide induced cell death (64). However, in our system using only 400nM zinc pyrithione, which induced apoptosis, expression of Bax and Bcl-2 did not change in response to zinc treatment (128). Since Bcl-2 levels did not change in response to zinc, the significant up-regulation of Bim would result in the neutralization of the antiapoptotic proteins and activation of the multidomain proapoptotic proteins thus shifting the cell towards death. Taken together our data is consistent with the idea that the up-regulation of the BH3-only protein Bim is involved in the regulation of zinc-induced apoptosis in cells of the immune system (128). Furthermore, Bim has been shown to be important in the development and maintenance of the immune system (17).

A possible role for Bim in neuronal cell death:

The tissue distribution of Bim includes hematopoietic, neuronal, epithelial as well as germ cells (147). In addition to inducing apoptosis in cells of the immune system, zinc

has been demonstrated to be a key modulator of neuronal cell death in response to ischemia and seizures as previously discussed (33, 62, 63, 183). Interestingly, Bim may also regulate neuronal cell death in response to seizures and in temporal lobe epilepsy (144, 162, 175). While we have demonstrated that Bim is a regulator of zinc-induced apoptosis in cells of the immune system, whether it is a regulator of zinc-induced cell death in neuronal cells currently remains unknown (128).

Bim family members:

Bim, the Bcl-2 interacting mediator of cell death, was initially identified by screening a cDNA expression library with a Bcl-2 probe (145). Three major isoforms generated by alternative splicing were identified and designated BimEL (extra long), BimL (long) and BimS (short) (19, 145). All three isoforms interact with Bcl-2, whereas BimEL and BimL are the predominant isoforms expressed in tissues, BimS was not observed unless an apoptotic stimulus was present (145, 147, 153). However, BimS is the most cytotoxic isoform (145). Bim has important physiological roles in the immune system as demonstrated by Bim-deficient mice which show an accumulation of both lymphoid and myeloid cells as well as defects in the negative selection of thymocytes (17, 18, 201). Additionally, Bim expression was shown to be essential for the death of antigen-activated T lymphocytes during the termination of an immune response (181). Lymphocytes from Bim-deficient mice have also been shown to be resistant to various death stimuli including treatment with the calcium ionophore, ionomycin as well as growth factor withdrawal (17). Additionally, Bim was induced in response to growth factor withdrawal in neurons resulting in cell death (68). Bim can be regulated in several ways, from the

point of transcription to the level of pre-mRNA splicing, as well as post-translationally through phosphorylation or through interaction with the dynein motor complex (19, 76, 145).

Bim regulation by interaction with the dynein motor complex:

BimEL and BimL have been demonstrated to interact with light chain 8 (LC8), a component of the microtubule-associated dynein motor complex, resulting in sequestration of its proapoptotic activity (153). Interestingly, the proapoptotic activity of BimL was increased in response to single amino acid substitutions that abolished interaction with LC8 thus indicating that sequestration by the dynein motor complex can regulate the apoptotic activity of Bim (153). BimEL and BimL may play a role in apoptosis that disrupts the cytoskeleton or the dynein motor complex such as that associated with anoikis, a process where adherent cells lose contact with the extracellular matrix (65, 207). Certain apoptotic stimuli, such as treatment with taxol, have been shown to dissociate Bim from the dynein motor complex thus allowing interaction with and neutralization of Bcl-2 (153). Although BimEL is a less potent killer than BimL, BimEL and BimL interact with LC8 with similar affinity, although the most cytotoxic isoform BimS did not interact with LC8 (153). Overall, interaction with the dynein motor complex in certain cell types can be a point of regulation for Bim (145). However, most of the Bim in healthy or apoptotic T cells has been shown to be associated with the mitochondria and not the microtubules, despite its ability to bind LC8 (76, 224). In these T cells it appears that Bim is regulated by interaction with Bcl-2 family members rather than by sequestration with LC8 (224).

Bim regulation by phosphorylation:

Bim has also been shown to be regulated though phosphorylation. It has been demonstrated that JNK and ERK1/2 can phosphorylate Bim both *in vitro* and *in vivo* (11, 114). In response to UV stimulation JNK has been shown to phosphorylate BimL on Thr-56, the region that interacts with LC8, as well as at Ser-44 and Ser-58 (114). It was suggested that this phosphorylation disrupted the interaction with LC8 and resulted in the release of Bim and cell death (114). In another study JNK was shown to phosphorylate BimEL on Ser-65 in primary cerebellar granule neurons resulting in cell death (11). In contrast, others have shown that survival signals resulting in the activation of ERK1/2 resulted in the phosphorylation of BimEL on Ser-65 and this lead to a substantial increase in the turnover of the BimEL via the ubiquitin-mediated proteosome pathway (116, 117). Additionally, mutation of Ser-65 to alanine blocked phosphorylation of BimEL by ERK1/2 both *in vitro* and *in vivo* and prevented its degradation (117). It was also demonstrated that ERK1/2 could physically interact with BimEL whereas JNK could not, although JNK could still phosphorylate BimEL though not to the same extent (117). Furthermore, in response to the survival factor IL-3 (interleukin 3) in hematopoietic cells, BimEL was phosphorylated by ERK1/2 on Ser-55, Ser-65, and Ser-100 which considerably reduced interaction between Bim and the multidomain proapoptotic protein Bax (76). Withdrawal of IL-3 or BimEL containing serine to alanine mutations demonstrated that only non-phosphorylated Bim interacted with Bax (76). Overall, the role phosphorylation plays in the regulation of Bim is still conflicting. What is clear is that phosphorylation can in some cases regulate the activity of Bim, though whether this

regulation is positive or negative may depend on the differences in the cell types utilized or the differences in activation pathways.

Transcriptional regulation of Bim by zinc:

As previously discussed, Bim can be regulated via several mechanisms including at the level of transcription. It appears that this is the mechanism by which zinc regulates Bim since Bim levels are strongly increased in response to zinc treatment in T cells (126, 128) and since sequestration with LC8 may not be a prominent mechanism in T cells (76, 224). The question thus arose: what signaling components or signal transduction pathways are utilized during the induction of Bim in response to zinc?

Relatively little is known about the players involved in the up-regulation of Bim. However, in response to nerve growth factor (NGF) withdrawal JNK signaling has been implicated in the induction of Bim (77) and the expression of a dominant negative *c-jun* was able to partially blocked Bim expression (211). Another group has also demonstrated that Bim was a direct target of the Forkhead box class O 3a (FOXO3a) transcription factor in response to NGF withdrawal (14, 68). Others have demonstrated involvement of these pathways in response to growth factor withdrawal; however, whether they are common to all inducers of Bim remains unknown. On the other hand we have demonstrated that zinc activated the cyclic adenosine 5'-monophosphate (cAMP) signal transduction pathway which resulted in the induction of Bim and apoptosis in T cells (126). Consistent with this observation others have demonstrated that the direct treatment of T cells with either a cAMP analog (8-CPT-cAMP) or a β-

adrenergic receptor agonist (isoproterenol) similarly lead to increased Bim expression and cell death (223).

The cAMP signal transduction pathway: Utilized during zinc-induced apoptosis:

cAMP has been established since the 1950s as an important secondary messenger which can alter the balance between cell death and cell growth (85). cAMP has also been shown to induce apoptosis in T cells as well as a variety of other cell types (102, 134, 140, 141, 163, 178, 193). As illustrated in Figure 1-6 adenylate cyclase is the enzyme responsible for the *de novo* synthesis of cAMP from ATP being activated by the Gαs subunit of the heterotrimeric G-proteins (85). Activation of G-protein coupled receptors, such as the β-adrenergic receptor, result in the dissociation and activation of the heterotrimeric G-proteins ultimately resulting in the induction of cAMP. The newly synthesized cAMP binds to the regulatory subunits of PKA. This in turn releases the active catalytic subunits that phosphorylate a variety of substrates including the cAMP response element binding protein (CREB). Using CREB phosphorylation as an indicator of PKA activation (171) we will show that zinc induced strong CREB phosphorylation in both S49 WT cells and mouse thymocytes (126). Additionally, many studies of the cAMP signaling pathway have utilized the S49 T cell line. The S49 T cell line has been historically used as a model for cAMP signaling since there are two well characterized variants deficient in the cAMP signaling pathway (21, 35, 36, 179, 180, 216). The S49 Cyc^- cell line is deficient in the Gαs subunit of the heterotrimeric G-proteins that activate adenylate cyclase (20, 21, 36, 85, 94). The S49 *Kin*$^-$ cell line is deficient in protein kinase

Figure 1-6: Components of the cAMP and NF-κB signal transduction pathways.

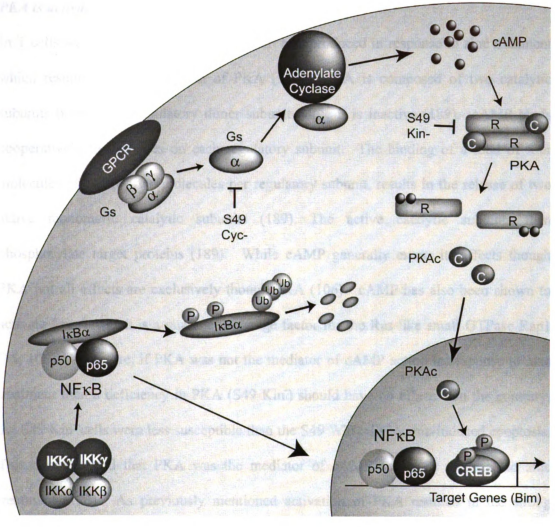
cAMP
Adenylate Cyclase
α
S49 Kin-
R
C
PKA
GPCR
β
γ
α
Gs
Gs
α
S49 Cyc-
PKAc
Ub
P
IκBα
p50
p65
NFκB
PKAc
NFκB
CREB
IKKγ
IKKα
IKKβ
Target Genes (Bim)

A (PKA) activity (113, 179, 180). We will further demonstrate utilization of the cAMP signaling pathway in response to zinc treatment with these cell lines.

PKA is activated in response to zinc treatment:

In T cells we have demonstrated that cAMP was produced in response to zinc treatment which resulted in the activation of PKA (126). PKA is composed of two catalytic subunits bound by a regulatory dimer subunit while it is inactive (189). cAMP binds cooperatively to two sites on each regulatory subunit. The binding of a total of four molecules of cAMP, two molecules per regulatory subunit, results in the release of two active monomeric catalytic subunits (189). The active catalytic subunits then phosphorylate target proteins (189). While cAMP generally exerts its effects though PKA not all effects are exclusively though PKA (106). cAMP has also been shown to activate Epac1 which is a guanine exchange factor for the Ras-like small GTPase Rap1 (15, 106). Therefore, if PKA was not the mediator of cAMP action in response to zinc treatment then a deficiency in PKA (S49 Kin$^-$) should have no effect. On the contrary, the S49 Kin$^-$ cells were less susceptible than the S49 WT cells to zinc-induced apoptosis. This demonstrated that PKA was the mediator of cAMP action in response to zinc treatment (126). As previously mentioned activation of PKA resulted in the strong phosphorylation of CREB on Ser^{133} in response to zinc treatment (126). However, CREB can be phosphorylated on Ser^{133} by a several different kinases (171). If CREB phosphorylation in the S49 WT cell line was due to these other kinases then CREB phosphorylation should also occur in the S49 Kin$^-$ cell line. No CREB phosphorylation

was observed in the PKA deficient cell line in response to zinc treatment which indicated that PKA was the responsible kinase (126).

CREB:

CREB is a 43-kDa basic leucine zipper (bZIP) transcription factor that binds to DNA as a dimer and couples the cAMP signaling pathway to gene activation (137, 171). In recent years, CREB has been shown to regulate various genes involved in neuronal function, development, signaling, and transcription (38, 52, 89, 93). However, CREB regulation may vary due to differences in cell types or variations in the activating stimulus (93). Generally prolonged phosphorylation of CREB on Ser^{133} is required for the activation of this transcription factor (69, 88, 93, 171). Prolonged phosphorylation of CREB was noted in response to zinc treatment in S49 WT cells (126). Phosphorylation at this site is required for interaction with the CREB binding protein (CBP) which acts as a transcriptional co-activator through its histone acetyltransferase activity (95, 171). Additionally, phosphorylation at Ser^{133} may increase CREB DNA binding activity though this is dependent upon the specific cAMP response element (CRE) (24, 171). The typical target sequence for CREB is the palindromic CRE first identified in the somatostatin gene (TGACGTCA) (138). We have demonstrated that treatment of S49 WT cells with zinc led to increased binding of a ^{32}P-labled probe containing the consensus CRE as analyzed by an electrophoretic mobility shift assay (EMSA) (126). Since zinc treatment led to the activation of the cAMP signaling pathway that resulted in the induction of Bim it was hypothesized that the Bim promoter was a direct transcriptional target of CREB. However, the murine Bim promoter did not contain a full consensus CRE (19). While

CREB binds the consensus CRE it can also bind variant CREs even those containing the half-site TGACG sequence (57, 137). Additionally, it was shown that the majority of CREB targets contained shorter versions or close matches to the consensus sequence in one study that mapped CREB binding sites on human chromosome 22 (52). In order to determine whether CREB was bound at the Bim promoter in S49 WT T cells we performed chromatin immunoprecipitation (ChIP) analysis (126). In response to zinc treatment we demonstrated an increase in CREB occupancy at the Bim promoter (126). Our data is consistent with a genome-wide analysis of CREB targets that combined ChIP analysis with a modified serial analysis of gene expression (SAGE) (89). This large scale analysis identified a number of novel CREB targets; however, the most interesting to us was the identification of Bim (89).

Activation of NF-κB in response to zinc:

In addition to utilizing the cAMP signal transduction pathway during apoptosis we demonstrated that zinc also activated the NF-κB signaling pathway (127). NF-κB proteins belong to a family of heterodimeric transcription factors that play essential roles in inflammatory and stress responses. The NF-κB family consists of five members: p65 (RelA), RelB, c-Rel, p50 (precursor 105), and p52 (precursor 100) (215). All five members contain a Rel-homology domain (RHD) which is required for their dimerization, nuclear translocation, and DNA binding. As illustrated in Figure 1-6 NF-κB is sequestered in the cytoplasm as an inactive complex bound by the inhibitory κB proteins (IκBα) (96). Activation of NF-κB is regulated through the phosphorylation of IκBα by the IκB kinase (IKK) complex (96). The IKK complex consists of IKKα and

IKKβ bound to a dimeric IKKγ (Nemo). Phosphorylation of IκBα at two serine residues results in its degradation via the ubiquitin-mediated proteosome pathway (96, 200). In response to IκBα degradation the nuclear localization sequence (NLS) contained in NF-κB is exposed which results in translocation to the nucleus and activation of target genes (96).

IκBα was degraded in response to zinc treatment in both mouse thymocytes and the S49 WT cell line (127). Furthermore, utilizing an electrophoretic mobility shift assay we demonstrated that treatment of S49 WT cells with zinc led to increased binding of a ^{32}P-labled probe which contained an NF-κB binding site (127). Overall, we demonstrated activation of the NF-κB signaling pathway in response to zinc treatment in T cells, similar to results seen in thyroid cells (87). While we have shown activation of the NF-κB signaling pathway in response to zinc, others have demonstrated that zinc could inhibit TNF-α induced NF-κB activation (98, 99). These discrepancies could be due to the different cell types used or the differences in the inducers of apoptosis.

While many well known targets of NF-κB include proinflammatory and antiapoptotic genes, NF-κB also has a proapoptotic role under certain conditions (45). NF-κB activity was shown to be essential for doxorubicin-induced apoptosis (6). Additionally, NF-κB has been established as a dominant transcription factor involved in apoptosis induced by the HIV-1envelope glycoprotein complex (Env) (149). In another study NF-κB was implicated in developmental cell death in an avian embryo (1). Moreover, a proapoptotic role for the activation of NF-κB was demonstrated in retinal pericytes in response to

diabetes or high glucose (159). Interestingly, another group studying T cell development *in vivo* demonstrated an essential role for NF-κB in promoting double positive T cell apoptosis in response to α-CD3 administration (81). This group utilized transgenic mice expressing a super-inhibitory IκBα that contain serine to alanine mutations which prevents phosphorylation and thus degradation, thereby retaining NF-κB in an inactive complex (81). While these double positive thymocytes were resistant to α-CD3 induced apoptosis they were still responsive to γ-irradiation further demonstrating that under certain conditions NF-κB has a proapoptotic role (81). Furthermore, the proapoptotic proteins Fas and FasL have been shown to be direct targets of NF-κB (27, 28, 125, 164). Another proapoptotic protein, Bim, may also be a potential target of NF-κB. The Bim promoter contains several candidate NF-κB binding sites and thus may be transcriptionally regulated during zinc's activation of NF-κB. However, a direct link between NF-κB and Bim has not yet been established.

Summary

Zinc has been shown to induce apoptosis in a number of cells types from neuronal to cells of the immune system. Whether increases in zinc result from potential environmental factors, released from metalloproteins within cells, or released from the cells themselves an understanding of its regulation of apoptosis is essential to combating the potential toxicity of zinc under certain circumstances. The involvement of the recently identified signaling pathways (cAMP-PKA and NF-κB) and apoptotic factors (Bim) in zinc-induced apoptosis in cells of the immune system will therefore be demonstrated in detail

in the following chapters thus considerably increasing our current knowledge of the regulation of apoptosis by zinc.

References:

1. **Abbadie, C., N. Kabrun, F. Bouali, J. Smardova, D. Stehelin, B. Vandenbunder, and P. J. Enrietto.** 1993. High levels of c-rel expression are associated with programmed cell death in the developing avian embryo and in bone marrow cells in vitro. Cell **75:**899-912.

2. **Acehan, D., X. Jiang, D. G. Morgan, J. E. Heuser, X. Wang, and C. W. Akey.** 2002. Three-dimensional structure of the apoptosome: implications for assembly, procaspase-9 binding, and activation. Mol Cell **9:**423-32.

3. **Adams, J. M., and S. Cory.** 2002. Apoptosomes: engines for caspase activation. Curr Opin Cell Biol **14:**715-20.

4. **Adams, J. M., and S. Cory.** 1998. The Bcl-2 protein family: arbiters of cell survival. Science **281:**1322-6.

5. **Arnoult, D., B. Gaume, M. Karbowski, J. C. Sharpe, F. Cecconi, and R. J. Youle.** 2003. Mitochondrial release of AIF and EndoG requires caspase activation downstream of Bax/Bak-mediated permeabilization. Embo J **22:**4385-99.

6. **Ashikawa, K., S. Shishodia, I. Fokt, W. Priebe, and B. B. Aggarwal.** 2004. Evidence that activation of nuclear factor-kappaB is essential for the cytotoxic effects of doxorubicin and its analogues. Biochem Pharmacol **67:**353-64.

7. **Auld, D. S.** 2001. Zinc coordination sphere in biochemical zinc sites. Biometals **14:**271-313.

8. **Bakhshi, A., J. P. Jensen, P. Goldman, J. J. Wright, O. W. McBride, A. L. Epstein, and S. J. Korsmeyer.** 1985. Cloning the chromosomal breakpoint of t(14;18) human lymphomas: clustering around JH on chromosome 14 and near a transcriptional unit on 18. Cell **41:**899-906.

9. **Bamford, M., G. Walkinshaw, and R. Brown.** 2000. Therapeutic applications of apoptosis research. Exp Cell Res **256:**1-11.

10. **Barbieri, D., L. Troiano, E. Grassilli, C. Agnesini, E. A. Cristofalo, D. Monti, M. Capri, A. Cossarizza, and C. Franceschi.** 1992. Inhibition of apoptosis by zinc: a reappraisal. Biochem Biophys Res Commun **187:**1256-61.

11. **Becker, E. B., J. Howell, Y. Kodama, P. A. Barker, and A. Bonni.** 2004. Characterization of the c-Jun N-terminal kinase-BimEL signaling pathway in neuronal apoptosis. J Neurosci **24:**8762-70.

12. **Beyer, W. N., J. Dalgarn, S. Dudding, J. B. French, R. Mateo, J. Miesner, L. Sileo, and J. Spann.** 2005. Zinc and lead poisoning in wild birds in the tri-state mining district (oklahoma, kansas, and missouri). Arch Environ Contam Toxicol **48:**108-17.

13. **Beyersmann, D., and H. Haase.** 2001. Functions of zinc in signaling, proliferation and differentiation of mammalian cells. Biometals **14:**331-41.

14. **Birkenkamp, K. U., and P. J. Coffer.** 2003. FOXO transcription factors as regulators of immune homeostasis: molecules to die for? J Immunol **171:**1623-9.

15. **Bos, J. L.** 2003. Epac: a new cAMP target and new avenues in cAMP research. Nat Rev Mol Cell Biol **4:**733-8.

16. **Bossy-Wetzel, E., D. D. Newmeyer, and D. R. Green.** 1998. Mitochondrial cytochrome c release in apoptosis occurs upstream of DEVD-specific caspase activation and independently of mitochondrial transmembrane depolarization. Embo J **17:**37-49.

17. **Bouillet, P., D. Metcalf, D. C. Huang, D. M. Tarlinton, T. W. Kay, F. Kontgen, J. M. Adams, and A. Strasser.** 1999. Proapoptotic Bcl-2 relative Bim required for certain apoptotic responses, leukocyte homeostasis, and to preclude autoimmunity. Science **286:**1735-8.

18. **Bouillet, P., J. F. Purton, D. I. Godfrey, L. C. Zhang, L. Coultas, H. Puthalakath, M. Pellegrini, S. Cory, J. M. Adams, and A. Strasser.** 2002. BH3-only Bcl-2 family member Bim is required for apoptosis of autoreactive thymocytes. Nature **415:**922-6.

19. **Bouillet, P., L. C. Zhang, D. C. Huang, G. C. Webb, C. D. Bottema, P. Shore, H. J. Eyre, G. R. Sutherland, and J. M. Adams.** 2001. Gene structure

alternative splicing, and chromosomal localization of pro-apoptotic Bcl-2 relative Bim. Mamm Genome **12:**163-8.

20. **Bourne, H. R., P. Coffino, and G. M. Tomkins.** 1975. Selection of a variant lymphoma cell deficient in adenylate cyclase. Science **187:**750-2.

21. **Bourne, H. R., P. Coffino, and G. M. Tomkins.** 1975. Somatic genetic analysis of cyclic AMP action: characterization of unresponsive mutants. J Cell Physiol **85:**611-20.

22. **Brown, A. M., B. S. Kristal, M. S. Effron, A. I. Shestopalov, P. A. Ullucci, K. F. Sheu, J. P. Blass, and A. J. Cooper.** 2000. Zn2+ inhibits alpha-ketoglutarate-stimulated mitochondrial respiration and the isolated alpha-ketoglutarate dehydrogenase complex. J Biol Chem **275:**13441-7.

23. **Bruinsma, J. J., T. Jirakulaporn, A. J. Muslin, and K. Kornfeld.** 2002. Zinc ions and cation diffusion facilitator proteins regulate Ras-mediated signaling. Dev Cell **2:**567-78.

24. **Bullock, B. P., and J. F. Habener.** 1998. Phosphorylation of the cAMP response element binding protein CREB by cAMP-dependent protein kinase A and glycogen synthase kinase-3 alters DNA-binding affinity, conformation, and increases net charge. Biochemistry **37:**3795-809.

25. **Cario, E., S. Jung, J. Harder D'Heureuse, C. Schulte, A. Sturm, B. Wiedenmann, H. Goebell, and A. U. Dignass.** 2000. Effects of exogenous zinc supplementation on intestinal epithelial repair in vitro. Eur J Clin Invest **30:**419-28.

26. **Cartron, P. F., T. Gallenne, G. Bougras, F. Gautier, F. Manero, P. Vusio, K. Meflah, F. M. Vallette, and P. Juin.** 2004. The first alpha helix of Bax plays a necessary role in its ligand-induced activation by the BH3-only proteins Bid and PUMA. Mol Cell **16:**807-18.

27. **Chan, H., D. P. Bartos, and L. B. Owen-Schaub.** 1999. Activation-dependent transcriptional regulation of the human Fas promoter requires NF-kappaB p50-p65 recruitment. Mol Cell Biol **19:**2098-108.

28. **Chen, X., V. Zachar, M. Zdravkovic, M. Guo, P. Ebbesen, and X. Liu.** 1997. Role of the Fas/Fas ligand pathway in apoptotic cell death induced by the human

T cell lymphotropic virus type I Tax transactivator. J Gen Virol **78 (Pt 12):**3277-85.

29. **Cheng, E. H., T. V. Sheiko, J. K. Fisher, W. J. Craigen, and S. J. Korsmeyer.** 2003. VDAC2 inhibits BAK activation and mitochondrial apoptosis. Science **301:**513-7.

30. **Cheng, E. H., M. C. Wei, S. Weiler, R. A. Flavell, T. W. Mak, T. Lindsten, and S. J. Korsmeyer.** 2001. BCL-2, BCL-X(L) sequester BH3 domain-only molecules preventing BAX- and BAK-mediated mitochondrial apoptosis. Mol Cell **8:**705-11.

31. **Cherny, R. A., C. S. Atwood, M. E. Xilinas, D. N. Gray, W. D. Jones, C. A. McLean, K. J. Barnham, I. Volitakis, F. W. Fraser, Y. Kim, X. Huang, L. E. Goldstein, R. D. Moir, J. T. Lim, K. Beyreuther, H. Zheng, R. E. Tanzi, C. L. Masters, and A. I. Bush.** 2001. Treatment with a copper-zinc chelator markedly and rapidly inhibits β-amyloid accumulation in Alzheimer's disease transgenic mice. Neuron **30:**665-76.

32. **Cho, Y., S. Gorina, P. D. Jeffrey, and N. P. Pavletich.** 1994. Crystal structure of a p53 tumor suppressor-DNA complex: understanding tumorigenic mutations. Science **265:**346-55.

33. **Choi, D. W., and J. Y. Koh.** 1998. Zinc and brain injury. Annu Rev Neurosci **21:**347-75.

34. **Cleary, M. L., and J. Sklar.** 1985. Nucleotide sequence of a t(14;18) chromosomal breakpoint in follicular lymphoma and demonstration of a breakpoint-cluster region near a transcriptionally active locus on chromosome 18. Proc Natl Acad Sci U S A **82:**7439-43.

35. **Coffino, P., H. R. Bourne, U. Friedrich, J. Hochman, P. A. Insel, I. Lemaire, K. L. Melmon, and G. M. Tomkins.** 1976. Molecular mechanisms of cyclic AMP action: a genetic approach. Recent Prog Horm Res **32:**669-84.

36. **Coffino, P., H. R. Bourne, and G. M. Tomkins.** 1975. Somatic genetic analysis of cyclic AMP action: selection of unresponsive mutants. J Cell Physiol **85:**603-10.

37. **Cohen, J. J., R. C. Duke, V. A. Fadok, and K. S. Sellins.** 1992. Apoptosis and programmed cell death in immunity. Annu Rev Immunol **10:**267-93.

38. **Conkright, M. D., E. Guzman, L. Flechner, A. I. Su, J. B. Hogenesch, and M. Montminy.** 2003. Genome-wide analysis of CREB target genes reveals a core promoter requirement for cAMP responsiveness. Mol Cell **11:**1101-8.

39. **Coultas, L., P. Bouillet, E. G. Stanley, T. C. Brodnicki, J. M. Adams, and A. Strasser.** 2004. Proapoptotic BH3-only Bcl-2 family member Bik/Blk/Nbk is expressed in hemopoietic and endothelial cells but is redundant for their programmed death. Mol Cell Biol **24:**1570-81.

40. **Cuajungco, M. P., K. Y. Faget, X. Huang, R. E. Tanzi, and A. I. Bush.** 2000. Metal chelation as a potential therapy for Alzheimer's disease. Ann N Y Acad Sci **920:**292-304.

41. **Cuajungco, M. P., L. E. Goldstein, A. Nunomura, M. A. Smith, J. T. Lim, C. S. Atwood, X. Huang, Y. W. Farrag, G. Perry, and A. I. Bush.** 2000. Evidence that the beta-amyloid plaques of Alzheimer's disease represent the redox-silencing and entombment of abeta by zinc. J Biol Chem **275:**19439-42.

42. **Curtain, C. C., F. Ali, I. Volitakis, R. A. Cherny, R. S. Norton, K. Beyreuther, C. J. Barrow, C. L. Masters, A. I. Bush, and K. J. Barnham.** 2001. Alzheimer's disease amyloid-β binds copper and zinc to generate an allosterically ordered membrane-penetrating structure containing superoxide dismutase-like subunits. J Biol Chem **276:**20466-73.

43. **Daugas, E., S. A. Susin, N. Zamzami, K. F. Ferri, T. Irinopoulou, N. Larochette, M. C. Prevost, B. Leber, D. Andrews, J. Penninger, and G. Kroemer.** 2000. Mitochondrio-nuclear translocation of AIF in apoptosis and necrosis. Faseb J **14:**729-39.

44. **Degterev, A., M. Boyce, and J. Yuan.** 2003. A decade of caspases. Oncogene **22:**8543-67.

45. **Delhalle, S., R. Blasius, M. Dicato, and M. Diederich.** 2004. A Beginner's Guide to NF-{kappa}B Signaling Pathways. Ann N Y Acad Sci **1030:**1-13.

46. **Deng, Y., Y. Lin, and X. Wu.** 2002. TRAIL-induced apoptosis requires Bax-dependent mitochondrial release of Smac/DIABLO. Genes Dev **16:**33-45.

47. **Deveraux, Q. L., and J. C. Reed.** 1999. IAP family proteins--suppressors of apoptosis. Genes Dev **13:**239-52.

48. **Dickinson, D. A., and H. J. Forman.** 2002. Glutathione in defense and signaling: lessons from a small thiol. Ann N Y Acad Sci **973:**488-504.

49. **Dineley, K. E., T. V. Votyakova, and I. J. Reynolds.** 2003. Zinc inhibition of cellular energy production: implications for mitochondria and neurodegeneration. J Neurochem **85:**563-70.

50. **Du, C., M. Fang, Y. Li, L. Li, and X. Wang.** 2000. Smac, a mitochondrial protein that promotes cytochrome c-dependent caspase activation by eliminating IAP inhibition. Cell **102:**33-42.

51. **Eskes, R., S. Desagher, B. Antonsson, and J. C. Martinou.** 2000. Bid induces the oligomerization and insertion of Bax into the outer mitochondrial membrane. Mol Cell Biol **20:**929-35.

52. **Euskirchen, G., T. E. Royce, P. Bertone, R. Martone, J. L. Rinn, F. K. Nelson, F. Sayward, N. M. Luscombe, P. Miller, M. Gerstein, S. Weissman, and M. Snyder.** 2004. CREB binds to multiple loci on human chromosome 22. Mol Cell Biol **24:**3804-14.

53. **Faccio, L., C. Fusco, A. Chen, S. Martinotti, J. V. Bonventre, and A. S. Zervos.** 2000. Characterization of a novel human serine protease that has extensive homology to bacterial heat shock endoprotease HtrA and is regulated by kidney ischemia. J Biol Chem **275:**2581-8.

54. **Falchuk, K. H., and M. Montorzi.** 2001. Zinc physiology and biochemistry in oocytes and embryos. Biometals **14:**385-95.

55. **Feng, P., T. L. Li, Z. X. Guan, R. B. Franklin, and L. C. Costello.** 2002. Direct effect of zinc on mitochondrial apoptogenesis in prostate cells. Prostate **52:**311-8.

56. **Feng, P., J. Y. Liang, T. L. Li, Z. X. Guan, J. Zou, R. Franklin, and L. C. Costello.** 2000. Zinc induces mitochondria apoptogenesis in prostate cells. Mol Urol **4:**31-6.

57. **Fink, J. S., M. Verhave, S. Kasper, T. Tsukada, G. Mandel, and R. H. Goodman.** 1988. The CGTCA sequence motif is essential for biological activity of the vasoactive intestinal peptide gene cAMP-regulated enhancer. Proc Natl Acad Sci U S A **85:**6662-6.

58. **Fraker, P. J., and L. E. King.** 2004. Reprogramming of the immune system during zinc deficiency. Annu Rev Nutr **24:**277-98.

59. **Fraker, P. J., and W. Telford.** 1996. Regulation of apoptotic events by zinc, p. 189-208. *In* C. Berdanier (ed.), Nutrition and Gene Expression. CRC Press, Boca Raton, FL.

60. **Fraker, P. J., and W. G. Telford.** 1997. A reappraisal of the role of zinc in life and death decisions of cells. Proc Soc Exp Biol Med **215:**229-36.

61. **Frederickson, C. J., and A. I. Bush.** 2001. Synaptically released zinc: physiological functions and pathological effects. Biometals **14:**353-66.

62. **Frederickson, C. J., W. Maret, and M. P. Cuajungco.** 2004. Zinc and excitotoxic brain injury: a new model. Neuroscientist **10:**18-25.

63. **Frederickson, C. J., S. W. Suh, D. Silva, and R. B. Thompson.** 2000. Importance of zinc in the central nervous system: the zinc-containing neuron. J Nutr **130:**1471S-83S.

64. **Fukamachi, Y., Y. Karasaki, T. Sugiura, H. Itoh, T. Abe, K. Yamamura, and K. Higashi.** 1998. Zinc suppresses apoptosis of U937 cells induced by hydrogen peroxide through an increase of the Bcl-2/Bax ratio. Biochem Biophys Res Commun **246:**364-9.

65. **Fukazawa, H., K. Noguchi, A. Masumi, Y. Murakami, and Y. Uehara.** 2004. BimEL is an important determinant for induction of anoikis sensitivity by mitogen-activated protein/extracellular signal-regulated kinase kinase inhibitors. Mol Cancer Ther **3:**1281-8.

66. **Gaither, L. A., and D. J. Eide.** 2001. Eukaryotic zinc transporters and their regulation. Biometals **14:**251-70.

67. **Ganju, N., and A. Eastman.** 2003. Zinc inhibits Bax and Bak activation and cytochrome c release induced by chemical inducers of apoptosis but not by death-receptor-initiated pathways. Cell Death Differ **10:**652-61.

68. **Gilley, J., P. J. Coffer, and J. Ham.** 2003. FOXO transcription factors directly activate bim gene expression and promote apoptosis in sympathetic neurons. J Cell Biol **162:**613-22.

69. **Gonzalez, G. A., and M. R. Montminy.** 1989. Cyclic AMP stimulates somatostatin gene transcription by phosphorylation of CREB at serine 133. Cell **59:**675-80.

70. **Gouras, G. K., and M. F. Beal.** 2001. Metal chelator decreases Alzheimer beta-amyloid plaques. Neuron **30:**641-2.

71. **Green, D. R., and J. C. Reed.** 1998. Mitochondria and apoptosis. Science **281:**1309-12.

72. **Gross, A., J. Jockel, M. C. Wei, and S. J. Korsmeyer.** 1998. Enforced dimerization of BAX results in its translocation, mitochondrial dysfunction and apoptosis. Embo J **17:**3878-85.

73. **Gross, A., J. M. McDonnell, and S. J. Korsmeyer.** 1999. BCL-2 family members and the mitochondria in apoptosis. Genes Dev **13:**1899-911.

74. **Hajnal, A.** 2002. Fine-tuning the RAS signaling pathway: Zn(2+) makes the difference. Mol Cell **9:**927-8.

75. **Hansen, L. F., M. Hammer, S. H. Petersen, and G. D. Nielsen.** 1994. Effects of intranasal ZnSO4 irrigation on olfactory and trigeminal cues. Physiol Behav **55:**699-704.

76. **Harada, H., B. Quearry, A. Ruiz-Vela, and S. J. Korsmeyer.** 2004. Survival factor-induced extracellular signal-regulated kinase phosphorylates BIM, inhibiting its association with BAX and proapoptotic activity. Proc Natl Acad Sci U S A **101:**15313-7.

77. **Harris, C. A., and E. M. Johnson, Jr.** 2001. BH3-only Bcl-2 family members are coordinately regulated by the JNK pathway and require Bax to induce apoptosis in neurons. J Biol Chem **276:**37754-60.

78. **Hellmich, H. L., C. J. Frederickson, D. S. DeWitt, R. Saban, M. O. Parsley, R. Stephenson, M. Velasco, T. Uchida, M. Shimamura, and D. S. Prough.** 2004. Protective effects of zinc chelation in traumatic brain injury correlate with upregulation of neuroprotective genes in rat brain. Neurosci Lett **355:**221-5.

79. **Helmuth, L.** 2000. Neuroscience. An antibiotic to treat Alzheimer's? Science **290:**1273-4.

80. **Hengartner, M. O.** 2000. The biochemistry of apoptosis. Nature **407:**770-6.

81. **Hettmann, T., J. DiDonato, M. Karin, and J. M. Leiden.** 1999. An essential role for nuclear factor kappaB in promoting double positive thymocyte apoptosis. J Exp Med **189:**145-58.

82. **Ho, E., and B. N. Ames.** 2002. Low intracellular zinc induces oxidative DNA damage, disrupts p53, NFkappa B, and AP1 DNA binding, and affects DNA repair in a rat glioma cell line. Proc Natl Acad Sci U S A **99:**16770-5.

83. **Hsu, Y. T., K. G. Wolter, and R. J. Youle.** 1997. Cytosol-to-membrane redistribution of Bax and Bcl-X(L) during apoptosis. Proc Natl Acad Sci U S A **94:**3668-72.

84. **Huang, X., M. P. Cuajungco, C. S. Atwood, R. D. Moir, R. E. Tanzi, and A. I. Bush.** 2000. Alzheimer's disease, beta-amyloid protein and zinc. J Nutr **130:**1488S-92S.

85. **Hurley, J. H.** 1999. Structure, mechanism, and regulation of mammalian adenylyl cyclase. J Biol Chem **274:**7599-602.

86. **Igic, P. G., E. Lee, W. Harper, and K. W. Roach.** 2002. Toxic effects associated with consumption of zinc. Mayo Clin Proc **77:**713-6.

87. **Iitaka, M., S. Kakinuma, S. Fujimaki, I. Oosuga, T. Fujita, K. Yamanaka, S. Wada, and S. Katayama.** 2001. Induction of apoptosis and necrosis by zinc in human thyroid cancer cell lines. J Endocrinol **169:**417-24.

88. **Impey, S., and R. H. Goodman.** 2001. CREB signaling--timing is everything. Sci STKE **2001:**PE1.

89. **Impey, S., S. R. McCorkle, H. Cha-Molstad, J. M. Dwyer, G. S. Yochum, J. M. Boss, S. McWeeney, J. J. Dunn, G. Mandel, and R. H. Goodman.** 2004. Defining the CREB regulon: a genome-wide analysis of transcription factor regulatory regions. Cell **119:**1041-54.

90. **Jafek, B. W., M. R. Linschoten, and B. W. Murrow.** 2004. Anosmia after intranasal zinc gluconate use. Am J Rhinol **18:**137-41.

91. **Jenner, P.** 2003. Oxidative stress in Parkinson's disease. Ann Neurol **53 Suppl 3:**S26-36; discussion S36-8.

92. **Jiang, D., P. G. Sullivan, S. L. Sensi, O. Steward, and J. H. Weiss.** 2001. Zn(2+) induces permeability transition pore opening and release of pro-apoptotic peptides from neuronal mitochondria. J Biol Chem **276:**47524-9.

93. **Johannessen, M., M. P. Delghandi, and U. Moens.** 2004. What turns CREB on? Cell Signal **16:**1211-27.

94. **Johnson, G. L., H. R. Kaslow, Z. Farfel, and H. R. Bourne.** 1980. Genetic analysis of hormone-sensitive adenylate cyclase. Adv Cyclic Nucleotide Res **13:**1-37.

95. **Kalkhoven, E.** 2004. CBP and p300: HATs for different occasions. Biochem Pharmacol **68:**1145-55.

96. **Karin, M., and Y. Ben-Neriah.** 2000. Phosphorylation meets ubiquitination: the control of NF-[kappa]B activity. Annu Rev Immunol **18:**621-63.

97. **Kim, B. J., Y. H. Kim, S. Kim, J. W. Kim, J. Y. Koh, S. H. Oh, M. K. Lee, K. W. Kim, and M. S. Lee.** 2000. Zinc as a paracrine effector in pancreatic islet cell death. Diabetes **49:**367-72.

98. **Kim, C. H., J. H. Kim, J. Lee, and Y. S. Ahn.** 2003. Zinc-induced NF-kappaB inhibition can be modulated by changes in the intracellular metallothionein level. Toxicol Appl Pharmacol **190:**189-96.

99. **Kim, C. H., J. H. Kim, S. J. Moon, K. C. Chung, C. Y. Hsu, J. T. Seo, and Y. S. Ahn.** 1999. Pyrithione, a zinc ionophore, inhibits NF-kappaB activation. Biochem Biophys Res Commun **259:**505-9.

100. **Kim, J. Y., H. J. Ahn, J. H. Ryu, K. Suk, and J. H. Park.** 2004. BH3-only protein Noxa is a mediator of hypoxic cell death induced by hypoxia-inducible factor 1alpha. J Exp Med **199:**113-24.

101. **King JC, K. C.** 1999. Zinc, p. 223-239. *In* O. J. Shils M, Shike M, Ross AC, (ed.), Modern Nutrition in Health and Disease, 9th ed. Williams & Wilkins.

102. **Kizaki, H., H. Shimada, F. Ohsaka, and T. Sakurada.** 1988. Adenosine, deoxyadenosine, and deoxyguanosine induce DNA cleavage in mouse thymocytes. J Immunol **141:**1652-7.

103. **Knapp, L. T., and E. Klann.** 2000. Superoxide-induced stimulation of protein kinase C via thiol modification and modulation of zinc content. J Biol Chem **275:**24136-45.

104. **Koh, J. Y., S. W. Suh, B. J. Gwag, Y. Y. He, C. Y. Hsu, and D. W. Choi.** 1996. The role of zinc in selective neuronal death after transient global cerebral ischemia. Science **272:**1013-6.

105. **Kondoh, M., E. Tasaki, S. Araragi, M. Takiguchi, M. Higashimoto, Y. Watanabe, and M. Sato.** 2002. Requirement of caspase and p38MAPK activation in zinc-induced apoptosis in human leukemia HL-60 cells. Eur J Biochem **269:**6204-11.

106. **Kopperud, R., C. Krakstad, F. Selheim, and S. O. Doskeland.** 2003. cAMP effector mechanisms. Novel twists for an 'old' signaling system. FEBS Lett **546:**121-6.

107. **Korichneva, I., B. Hoyos, R. Chua, E. Levi, and U. Hammerling.** 2002. Zinc release from protein kinase C as the common event during activation by lipid second messenger or reactive oxygen. J Biol Chem **277:**44327-31.

108. **Kozin, S. A., S. Zirah, S. Rebuffat, G. H. Hoa, and P. Debey.** 2001. Zinc binding to Alzheimer's Aβ(1-16) peptide results in stable soluble complex. Biochem Biophys Res Commun **285:**959-64.

109. **Kuwana, T., L. Bouchier-Hayes, J. E. Chipuk, C. Bonzon, B. A. Sullivan, D. R. Green, and D. D. Newmeyer.** 2005. BH3 Domains of BH3-Only Proteins Differentially Regulate Bax-Mediated Mitochondrial Membrane Permeabilization Both Directly and Indirectly. Mol Cell **17:**525-35.

110. **Kuwana, T., M. R. Mackey, G. Perkins, M. H. Ellisman, M. Latterich, R. Schneiter, D. R. Green, and D. D. Newmeyer.** 2002. Bid, Bax, and lipids cooperate to form supramolecular openings in the outer mitochondrial membrane. Cell **111:**331-42.

111. **Lee, J. Y., T. B. Cole, R. D. Palmiter, and J. Y. Koh.** 2000. Accumulation of zinc in degenerating hippocampal neurons of ZnT3-null mice after seizures: evidence against synaptic vesicle origin. J Neurosci **20:**RC79.

112. **Lee, J. Y., T. B. Cole, R. D. Palmiter, S. W. Suh, and J. Y. Koh.** 2002. Contribution by synaptic zinc to the gender-disparate plaque formation in human Swedish mutant APP transgenic mice. Proc Natl Acad Sci U S A **99:**7705-10.

113. **Lee, S. L., and R. A. Steinberg.** 1996. Pathways for degradation of the catalytic subunit of cAMP-dependent protein kinase differ in wild-type and kinase-negative S49 mouse lymphoma cells. J Biol Chem **271:**16553-8.

114. **Lei, K., and R. J. Davis.** 2003. JNK phosphorylation of Bim-related members of the Bcl2 family induces Bax-dependent apoptosis. Proc Natl Acad Sci U S A **100:**2432-7.

115. **Letai, A., M. C. Bassik, L. D. Walensky, M. D. Sorcinelli, S. Weiler, and S. J. Korsmeyer.** 2002. Distinct BH3 domains either sensitize or activate mitochondrial apoptosis, serving as prototype cancer therapeutics. Cancer Cell **2:**183-92.

116. **Ley, R., K. Balmanno, K. Hadfield, C. Weston, and S. J. Cook.** 2003. Activation of the ERK1/2 signaling pathway promotes phosphorylation and proteasome-dependent degradation of the BH3-only protein, Bim. J Biol Chem **278:**18811-6.

117. **Ley, R., K. E. Ewings, K. Hadfield, E. Howes, K. Balmanno, and S. J. Cook.** 2004. Extracellular signal-regulated kinases 1/2 are serum-stimulated "Bim(EL) kinases" that bind to the BH3-only protein Bim(EL) causing its phosphorylation and turnover. J Biol Chem **279:**8837-47.

118. **Li, L. Y., X. Luo, and X. Wang.** 2001. Endonuclease G is an apoptotic DNase when released from mitochondria. Nature **412:**95-9.

119. **Li, P., D. Nijhawan, I. Budihardjo, S. M. Srinivasula, M. Ahmad, E. S. Alnemri, and X. Wang.** 1997. Cytochrome c and dATP-dependent formation of Apaf-1/caspase-9 complex initiates an apoptotic protease cascade. Cell **91:**479-89.

120. **Lindsten, T., A. J. Ross, A. King, W. X. Zong, J. C. Rathmell, H. A. Shiels, E. Ulrich, K. G. Waymire, P. Mahar, K. Frauwirth, Y. Chen, M. Wei, V. M. Eng, D. M. Adelman, M. C. Simon, A. Ma, J. A. Golden, G. Evan, S. J. Korsmeyer, G. R. MacGregor, and C. B. Thompson.** 2000. The combined functions of proapoptotic Bcl-2 family members bak and bax are essential for normal development of multiple tissues. Mol Cell **6:**1389-99.

121. **Link, T. A., and G. von Jagow.** 1995. Zinc ions inhibit the QP center of bovine heart mitochondrial bc1 complex by blocking a protonatable group. J Biol Chem **270:**25001-6.

122. **Liu, X., H. Zou, C. Slaughter, and X. Wang.** 1997. DFF, a heterodimeric protein that functions downstream of caspase-3 to trigger DNA fragmentation during apoptosis. Cell **89:**175-84.

123. **Liu, Y., G. Fiskum, and D. Schubert.** 2002. Generation of reactive oxygen species by the mitochondrial electron transport chain. J Neurochem **80:**780-7.

124. **Macho, A., T. Hirsch, I. Marzo, P. Marchetti, B. Dallaporta, S. A. Susin, N. Zamzami, and G. Kroemer.** 1997. Glutathione depletion is an early and calcium elevation is a late event of thymocyte apoptosis. J Immunol **158:**4612-9.

125. **Malewicz, M., N. Zeller, Z. B. Yilmaz, and F. Weih.** 2003. NF kappa B controls the balance between Fas and tumor necrosis factor cell death pathways during T cell receptor-induced apoptosis via the expression of its target gene A20. J Biol Chem **278:**32825-33.

126. **Mann, J. J., and P. J. Fraker.** 2005. Unpublished data- Thesis Chapter 2.

127. **Mann, J. J., and P. J. Fraker.** 2005. Unpublished data-Thesis Chapter 3.

128. **Mann, J. J., and P. J. Fraker.** 2005. Zinc pyrithione induces apoptosis and increases expression of Bim. Apoptosis **10:**369-379.

129. **Maret, W.** 2004. Zinc and sulfur: a critical biological partnership. Biochemistry **43:**3301-9.

130. **Marsden, V. S., L. O'Connor, L. A. O'Reilly, J. Silke, D. Metcalf, P. G. Ekert, D. C. Huang, F. Cecconi, K. Kuida, K. J. Tomaselli, S. Roy, D. W. Nicholson, D. L. Vaux, P. Bouillet, J. M. Adams, and A. Strasser.** 2002. Apoptosis initiated by Bcl-2-regulated caspase activation independently of the cytochrome c/Apaf-1/caspase-9 apoptosome. Nature **419:**634-7.

131. **Martinou, J. C.** 1999. Apoptosis. Key to the mitochondrial gate. Nature **399:**411-2.

132. **Masters, C. L., G. Simms, N. A. Weinman, G. Multhaup, B. L. McDonald, and K. Beyreuther.** 1985. Amyloid plaque core protein in Alzheimer disease and Down syndrome. Proc Natl Acad Sci U S A **82:**4245-9.

133. **McBride, K., B. Slotnick, and F. L. Margolis.** 2003. Does intranasal application of zinc sulfate produce anosmia in the mouse? An olfactometric and anatomical study. Chem Senses **28:**659-70.

134. **McConkey, D. J., S. Orrenius, and M. Jondal.** 1990. Agents that elevate cAMP stimulate DNA fragmentation in thymocytes. J Immunol **145:**1227-30.

135. **Meplan, C., K. Mann, and P. Hainaut.** 1999. Cadmium induces conformational modifications of wild-type p53 and suppresses p53 response to DNA damage in cultured cells. J Biol Chem **274:**31663-70.

136. **Meplan, C., M. J. Richard, and P. Hainaut.** 2000. Metalloregulation of the tumor suppressor protein p53: zinc mediates the renaturation of p53 after exposure to metal chelators in vitro and in intact cells. Oncogene **19:**5227-36.

137. **Montminy, M.** 1997. Transcriptional regulation by cyclic AMP. Annu Rev Biochem **66:**807-22.

138. **Montminy, M. R., K. A. Sevarino, J. A. Wagner, G. Mandel, and R. H. Goodman.** 1986. Identification of a cyclic-AMP-responsive element within the rat somatostatin gene. Proc Natl Acad Sci U S A **83:**6682-6.

139. **Moreau, C., P. F. Cartron, A. Hunt, K. Meflah, D. R. Green, G. Evan, F. M. Vallette, and P. Juin.** 2003. Minimal BH3 peptides promote cell death by antagonizing anti-apoptotic proteins. J Biol Chem **278:**19426-35.

140. **Muhl, H., D. Nitsch, K. Sandau, B. Brune, Z. Varga, and J. Pfeilschifter.** 1996. Apoptosis is triggered by the cyclic AMP signalling pathway in renal mesangial cells. FEBS Lett **382:**271-5.

141. **Myklebust, J. H., D. Josefsen, H. K. Blomhoff, F. O. Levy, S. Naderi, J. C. Reed, and E. B. Smeland.** 1999. Activation of the cAMP signaling pathway increases apoptosis in human B-precursor cells and is associated with downregulation of Mcl-1 expression. J Cell Physiol **180:**71-80.

142. **Newmeyer, D. D., and S. Ferguson-Miller.** 2003. Mitochondria. Releasing power for life and unleashing the machineries of death. Cell **112:**481-90.

143. **Nicholson, D. W.** 2000. From bench to clinic with apoptosis-based therapeutic agents. Nature **407:**810-6.

144. **Niquet, J., and C. G. Wasterlain.** 2004. Bim, Bad, and Bax: a deadly combination in epileptic seizures. J Clin Invest **113:**960-2.

145. **O'Connor, L., A. Strasser, L. A. O'Reilly, G. Hausmann, J. M. Adams, S. Cory, and D. C. Huang.** 1998. Bim: a novel member of the Bcl-2 family that promotes apoptosis. Embo J **17:**384-95.

146. **Opferman, J. T., and S. J. Korsmeyer.** 2003. Apoptosis in the development and maintenance of the immune system. Nat Immunol **4:**410-5.

147. **O'Reilly, L. A., L. Cullen, J. Visvader, G. J. Lindeman, C. Print, M. L. Bath, D. C. Huang, and A. Strasser.** 2000. The proapoptotic BH3-only protein bim is expressed in hematopoietic, epithelial, neuronal, and germ cells. Am J Pathol **157:**449-61.

148. **Paramanantham, R., K. H. Sit, and B. H. Bay.** 1997. Adding Zn^{2+} induces DNA fragmentation and cell condensation in cultured human Chang liver cells. Biol Trace Elem Res **58:**135-47.

149. **Perfettini, J. L., T. Roumier, M. Castedo, N. Larochette, P. Boya, B. Raynal, V. Lazar, F. Ciccosanti, R. Nardacci, J. Penninger, M. Piacentini, and G. Kroemer.** 2004. NF-kappaB and p53 are the dominant apoptosis-inducing transcription factors elicited by the HIV-1 envelope. J Exp Med **199:**629-40.

150. **Powis, G., and W. R. Montfort.** 2001. Properties and biological activities of thioredoxins. Annu Rev Biophys Biomol Struct **30:**421-55.

151. **Precht, T. A., R. A. Phelps, D. A. Linseman, B. D. Butts, S. S. Le, T. A. Laessig, R. J. Bouchard, and K. A. Heidenreich.** 2005. The permeability transition pore triggers Bax translocation to mitochondria during neuronal apoptosis. Cell Death Differ.

152. **Provinciali, M., A. Donnini, K. Argentati, G. Di Stasio, B. Bartozzi, and G. Bernardini.** 2002. Reactive oxygen species modulate Zn(2+)-induced apoptosis in cancer cells. Free Radic Biol Med **32:**431-45.

153. **Puthalakath, H., D. C. Huang, L. A. O'Reilly, S. M. King, and A. Strasser.** 1999. The proapoptotic activity of the Bcl-2 family member Bim is regulated by interaction with the dynein motor complex. Mol Cell **3:**287-96.

154. **Renatus, M., H. R. Stennicke, F. L. Scott, R. C. Liddington, and G. S. Salvesen.** 2001. Dimer formation drives the activation of the cell death protease caspase 9. Proc Natl Acad Sci U S A **98:**14250-5.

155. **Ricci, J. E., R. A. Gottlieb, and D. R. Green.** 2003. Caspase-mediated loss of mitochondrial function and generation of reactive oxygen species during apoptosis. J Cell Biol **160:**65-75.

156. **Rink, L., and P. Gabriel.** 2000. Zinc and the immune system. Proc Nutr Soc **59:**541-52.

157. **Ritchie, C. W., A. I. Bush, and C. L. Masters.** 2004. Metal-protein attenuating compounds and Alzheimer's disease. Expert Opin Investig Drugs **13:**1585-92.

158. **Rodriguez, J., and Y. Lazebnik.** 1999. Caspase-9 and APAF-1 form an active holoenzyme. Genes Dev **13:**3179-84.

159. **Romeo, G., W. H. Liu, V. Asnaghi, T. S. Kern, and M. Lorenzi.** 2002. Activation of nuclear factor-kappaB induced by diabetes and high glucose regulates a proapoptotic program in retinal pericytes. Diabetes **51:**2241-8.

160. **Rutty, C. J.** 1996. The middle-class plague: epidemic polio and the Canadian state, 1936-37. Can Bull Med Hist **13:**277-314.

161. **Ryu, R., Y. Shin, J. W. Choi, W. Min, H. Ryu, C. R. Choi, and H. Ko.** 2002. Depletion of intracellular glutathione mediates zinc-induced cell death in rat primary astrocytes. Exp Brain Res **143:**257-63.

162. **Sanchez, I., and J. Yuan.** 2001. A convoluted way to die. Neuron **29:**563-6.

163. **Sasson, R., V. Shinder, A. Dantes, A. Land, and A. Amsterdam.** 2003. Activation of multiple signal transduction pathways by glucocorticoids: protection of ovarian follicular cells against apoptosis. Biochem Biophys Res Commun **311:**1047-56.

164. **Savickiene, J., G. Treigyte, A. Pivoriunas, R. Navakauskiene, and K. E. Magnusson.** 2004. Sp1 and NF-{kappa}B Transcription Factor Activity in the Regulation of the p21 and FasL Promoters during Promyelocytic Leukemia Cell Monocytic Differentiation and Its Associated Apoptosis. Ann N Y Acad Sci **1030:**569-577.

165. **Schoots, A. F., W. E. Crusio, and J. H. Van Abeelen.** 1978. Zinc-induced peripheral anosmia and exploratory behavior in two inbred mouse strains. Physiol Behav **21:**779-84.

166. **Schrantz, N., M. T. Auffredou, M. F. Bourgeade, L. Besnault, G. Leca, and A. Vazquez.** 2001. Zinc-mediated regulation of caspases activity: dose-dependent inhibition or activation of caspase-3 in the human Burkitt lymphoma B cells (Ramos). Cell Death Differ **8:**152-61.

167. **Sensi, S. L., D. Ton-That, P. G. Sullivan, E. A. Jonas, K. R. Gee, L. K. Kaczmarek, and J. H. Weiss.** 2003. Modulation of mitochondrial function by endogenous Zn2+ pools. Proc Natl Acad Sci U S A **100:**6157-62.

168. **Sensi, S. L., H. Z. Yin, S. G. Carriedo, S. S. Rao, and J. H. Weiss.** 1999. Preferential Zn2+ influx through Ca2+-permeable AMPA/kainate channels triggers prolonged mitochondrial superoxide production. Proc Natl Acad Sci U S A **96:**2414-9.

169. **Sensi, S. L., H. Z. Yin, and J. H. Weiss.** 2000. AMPA/kainate receptor-triggered Zn2+ entry into cortical neurons induces mitochondrial Zn2+ uptake and persistent mitochondrial dysfunction. Eur J Neurosci **12:**3813-8.

170. **Seo, S. R., S. A. Chong, S. I. Lee, J. Y. Sung, Y. S. Ahn, K. C. Chung, and J. T. Seo.** 2001. Zn2+-induced ERK activation mediated by reactive oxygen species causes cell death in differentiated PC12 cells. J Neurochem **78:**600-10.

171. **Shaywitz, A. J., and M. E. Greenberg.** 1999. CREB: a stimulus-induced transcription factor activated by a diverse array of extracellular signals. Annu Rev Biochem **68:**821-61.

172. **Sheline, C. T., M. M. Behrens, and D. W. Choi.** 2000. Zinc-induced cortical neuronal death: contribution of energy failure attributable to loss of NAD(+) and inhibition of glycolysis. J Neurosci **20:**3139-46.

173. **Shi, Y.** 2002. Mechanisms of caspase activation and inhibition during apoptosis. Mol Cell **9:**459-70.

174. **Shimizu, S., M. Narita, and Y. Tsujimoto.** 1999. Bcl-2 family proteins regulate the release of apoptogenic cytochrome c by the mitochondrial channel VDAC. Nature **399:**483-7.

175. **Shinoda, S., C. K. Schindler, R. Meller, N. K. So, T. Araki, A. Yamamoto, J. Q. Lan, W. Taki, R. P. Simon, and D. C. Henshall.** 2004. Bim regulation may determine hippocampal vulnerability after injurious seizures and in temporal lobe epilepsy. J Clin Invest **113:**1059-68.

176. **Sies, H.** 1999. Glutathione and its role in cellular functions. Free Radic Biol Med **27:**916-21.

177. **Srinivasula, S. M., R. Hegde, A. Saleh, P. Datta, E. Shiozaki, J. Chai, R. A. Lee, P. D. Robbins, T. Fernandes-Alnemri, Y. Shi, and E. S. Alnemri.** 2001. A conserved XIAP-interaction motif in caspase-9 and Smac/DIABLO regulates caspase activity and apoptosis. Nature **410:**112-6.

178. **Srivastava, R. K., A. R. Srivastava, Y. S. Cho-Chung, and D. L. Longo.** 1999. Synergistic effects of retinoic acid and 8-Cl-cAMP on apoptosis require caspase-3 activation in human ovarian cancer cells. Oncogene **18:**1755-63.

179. **Steinberg, R. A.** 1991. A kinase-negative mutant of S49 mouse lymphoma cells is defective in posttranslational maturation of catalytic subunit of cyclic AMP-dependent protein kinase. Mol Cell Biol **11:**705-12.

180. **Steinberg, R. A., T. van Daalen Wetters, and P. Coffino.** 1978. Kinase-negative mutants of S49 mouse lymphoma cells carry a trans- dominant mutation affecting expression of cAMP-dependent protein kinase. Cell **15:**1351-61.

181. **Strasser, A., and M. Pellegrini.** 2004. T-lymphocyte death during shutdown of an immune response. Trends Immunol **25:**610-5.

182. **Suh, S. W., J. W. Chen, M. Motamedi, B. Bell, K. Listiak, N. F. Pons, G. Danscher, and C. J. Frederickson.** 2000. Evidence that synaptically-released zinc contributes to neuronal injury after traumatic brain injury. Brain Res **852:**268-73.

183. **Suh, S. W., R. B. Thompson, and C. J. Frederickson.** 2001. Loss of vesicular zinc and appearance of perikaryal zinc after seizures induced by pilocarpine. Neuroreport **12:**1523-5.

184. **Sunderman, F. W., Jr.** 2001. Nasal toxicity, carcinogenicity, and olfactory uptake of metals. Ann Clin Lab Sci **31:**3-24.

185. **Suzuki, M., R. J. Youle, and N. Tjandra.** 2000. Structure of Bax: coregulation of dimer formation and intracellular localization. Cell **103:**645-54.

186. **Suzuki, Y., Y. Imai, H. Nakayama, K. Takahashi, K. Takio, and R. Takahashi.** 2001. A serine protease, HtrA2, is released from the mitochondria and interacts with XIAP, inducing cell death. Mol Cell **8:**613-21.

187. **Suzuki, Y., Y. Nakabayashi, and R. Takahashi.** 2001. Ubiquitin-protein ligase activity of X-linked inhibitor of apoptosis protein promotes proteasomal degradation of caspase-3 and enhances its anti-apoptotic effect in Fas-induced cell death. Proc Natl Acad Sci U S A **98:**8662-7.

188. **Tandi, N. K., J. Nyamangara, and C. Bangira.** 2004. Environmental and potential health effects of growing leafy vegetables on soil irrigated using sewage sludge and effluent: a case of Zn and Cu. J Environ Sci Health B **39:**461-71.

189. **Tasken, K., and E. M. Aandahl.** 2004. Localized effects of cAMP mediated by distinct routes of protein kinase A. Physiol Rev **84:**137-67.

190. **Telford, W. G., and P. J. Fraker.** 1995. Preferential induction of apoptosis in mouse $CD4^{+}CD8^{+}\alpha\beta TCR^{lo}CD3\varepsilon^{lo}$ thymocytes by zinc. J Cell Physiol **164:**259-70.

191. **Telford, W. G., and P. J. Fraker.** 1998. Zinc induced apoptosis in bone marrow and splenic B-lineage lymphocytes of the mouse. Nutrition Research **18:**319-326.

192. **Thompson, C. B.** 1995. Apoptosis in the pathogenesis and treatment of disease. Science **267:**1456-62.

193. **Thompson, E. B., R. D. Medh, F. Zhou, S. Ayala-Torres, N. Ansari, W. Zhang, and B. H. Johnson.** 1999. Glucocorticoids, oxysterols, and cAMP with glucocorticoids each cause apoptosis of CEM cells and suppress c-myc. J Steroid Biochem Mol Biol **69:**453-61.

194. **Truong-Tran, A. Q., J. Carter, R. E. Ruffin, and P. D. Zalewski.** 2001. The role of zinc in caspase activation and apoptotic cell death. Biometals **14:**315-30.

195. **Tsujimoto, Y., J. Gorham, J. Cossman, E. Jaffe, and C. M. Croce.** 1985. The t(14;18) chromosome translocations involved in B-cell neoplasms result from mistakes in VDJ joining. Science **229:**1390-3.

196. **Untergasser, G., H. Rumpold, E. Plas, M. Witkowski, G. Pfister, and P. Berger.** 2000. High levels of zinc ions induce loss of mitochondrial potential and degradation of antiapoptotic Bcl-2 protein in in vitro cultivated human prostate epithelial cells. Biochem Biophys Res Commun **279:**607-14.

197. **Vallee, B. L., and K. H. Falchuk.** 1993. The biochemical basis of zinc physiology. Physiol Rev **73:**79-118.

198. **Vander Heiden, M. G., and C. B. Thompson.** 1999. Bcl-2 proteins: regulators of apoptosis or of mitochondrial homeostasis? Nat Cell Biol **1:**E209-16.

199. **Verhagen, A. M., P. G. Ekert, M. Pakusch, J. Silke, L. M. Connolly, G. E. Reid, R. L. Moritz, R. J. Simpson, and D. L. Vaux.** 2000. Identification of DIABLO, a mammalian protein that promotes apoptosis by binding to and antagonizing IAP proteins. Cell **102:**43-53.

200. **Viatour, P., M. P. Merville, V. Bours, and A. Chariot.** 2005. Phosphorylation of NF-kappaB and IkappaB proteins: implications in cancer and inflammation. Trends Biochem Sci **30:**43-52.

201. **Villunger, A., V. S. Marsden, Y. Zhan, M. Erlacher, A. M. Lew, P. Bouillet, S. Berzins, D. I. Godfrey, W. R. Heath, and A. Strasser.** 2004. Negative selection of semimature CD4+8-HSA+ thymocytes requires the BH3-only protein Bim but is independent of death receptor signaling. Proc Natl Acad Sci U S A **101:**7052-7.

202. **Villunger, A., E. M. Michalak, L. Coultas, F. Mullauer, G. Bock, M. J. Ausserlechner, J. M. Adams, and A. Strasser.** 2003. p53- and drug-induced apoptotic responses mediated by BH3-only proteins puma and noxa. Science **302:**1036-8.

203. **Wajant, H.** 2002. The Fas signaling pathway: more than a paradigm. Science **296:**1635-6.

204. **Walsh, C. T., H. H. Sandstead, A. S. Prasad, P. M. Newberne, and P. J. Fraker.** 1994. Zinc: health effects and research priorities for the 1990s. Environ Health Perspect **102 Suppl 2:**5-46.

205. **Walther, U. I., A. Czermak, H. Muckter, S. C. Walther, and B. Fichtl.** 2003. Decreased GSSG reductase activity enhances cellular zinc toxicity in three human lung cell lines. Arch Toxicol **77:**131-7.

206. **Walther, U. I., B. Wilhelm, S. Walther, H. Muckter, and B. Fichtl.** 2000. Zinc toxicity in various lung cell lines is mediated by glutathione and GSSG reductase activity. Biol Trace Elem Res **78:**163-77.

207. **Wang, P., A. P. Gilmore, and C. H. Streuli.** 2004. Bim is an apoptosis sensor that responds to loss of survival signals delivered by epidermal growth factor but not those provided by integrins. J Biol Chem **279:**41280-5.

208. **Waterhouse, N. J., J. C. Goldstein, O. von Ahsen, M. Schuler, D. D. Newmeyer, and D. R. Green.** 2001. Cytochrome c maintains mitochondrial transmembrane potential and ATP generation after outer mitochondrial membrane permeabilization during the apoptotic process. J Cell Biol **153:**319-28.

209. **Wei, M. C., T. Lindsten, V. K. Mootha, S. Weiler, A. Gross, M. Ashiya, C. B. Thompson, and S. J. Korsmeyer.** 2000. tBID, a membrane-targeted death ligand, oligomerizes BAK to release cytochrome c. Genes Dev **14:**2060-71.

210. **Wei, M. C., W. X. Zong, E. H. Cheng, T. Lindsten, V. Panoutsakopoulou, A. J. Ross, K. A. Roth, G. R. MacGregor, C. B. Thompson, and S. J. Korsmeyer.** 2001. Proapoptotic BAX and BAK: a requisite gateway to mitochondrial dysfunction and death. Science **292:**727-30.

211. **Whitfield, J., S. J. Neame, L. Paquet, O. Bernard, and J. Ham.** 2001. Dominant-negative c-Jun promotes neuronal survival by reducing BIM expression and inhibiting mitochondrial cytochrome c release. Neuron **29:**629-43.

212. **Widlak, P., L. Y. Li, X. Wang, and W. T. Garrard.** 2001. Action of recombinant human apoptotic endonuclease G on naked DNA and chromatin substrates: cooperation with exonuclease and DNase I. J Biol Chem **276:**48404-9.

213. **Wood, J. P., and N. N. Osborne.** 2001. The influence of zinc on caspase-3 and DNA breakdown in cultured human retinal pigment epithelial cells. Arch Ophthalmol **119:**81-8.

214. **Wu, G., J. Chai, T. L. Suber, J. W. Wu, C. Du, X. Wang, and Y. Shi.** 2000. Structural basis of IAP recognition by Smac/DIABLO. Nature **408:**1008-12.

215. **Yamamoto, Y., and R. B. Gaynor.** 2004. IkappaB kinases: key regulators of the NF-kappaB pathway. Trends Biochem Sci **29:**72-9.

216. **Yan, L., V. Herrmann, J. K. Hofer, and P. A. Insel.** 2000. beta-adrenergic receptor/cAMP-mediated signaling and apoptosis of S49 lymphoma cells. Am J Physiol Cell Physiol **279:**C1665-74.

217. **Yang, Q. H., R. Church-Hajduk, J. Ren, M. L. Newton, and C. Du.** 2003. Omi/HtrA2 catalytic cleavage of inhibitor of apoptosis (IAP) irreversibly inactivates IAPs and facilitates caspase activity in apoptosis. Genes Dev **17:**1487-96.

218. **Yang, Y., S. Fang, J. P. Jensen, A. M. Weissman, and J. D. Ashwell.** 2000. Ubiquitin protein ligase activity of IAPs and their degradation in proteasomes in response to apoptotic stimuli. Science **288:**874-7.

219. **Ye, B., W. Maret, and B. L. Vallee.** 2001. Zinc metallothionein imported into liver mitochondria modulates respiration. Proc Natl Acad Sci U S A **98:**2317-22.

220. **Yoon, S. O., C. H. Yun, and A. S. Chung.** 2002. Dose effect of oxidative stress on signal transduction in aging. Mech Ageing Dev **123:**1597-604.

221. **Zalewski, P. D., I. J. Forbes, R. F. Seamark, R. Borlinghaus, W. H. Betts, S. F. Lincoln, and A. D. Ward.** 1994. Flux of intracellular labile zinc during apoptosis (gene-directed cell death) revealed by a specific chemical probe, Zinquin. Chem Biol **1:**153-61.

222. **Zamzami, N., and G. Kroemer.** 2001. The mitochondrion in apoptosis: how Pandora's box opens. Nat Rev Mol Cell Biol **2:**67-71.

223. **Zhang, L., and P. A. Insel.** 2004. The Pro-apoptotic Protein Bim Is a Convergence Point for cAMP/Protein Kinase A- and Glucocorticoid-promoted Apoptosis of Lymphoid Cells. J Biol Chem **279:**20858-65.

224. **Zhu, Y., B. J. Swanson, M. Wang, D. A. Hildeman, B. C. Schaefer, X. Liu, H. Suzuki, K. Mihara, J. Kappler, and P. Marrack.** 2004. Constitutive association of the proapoptotic protein Bim with Bcl-2-related proteins on mitochondria in T cells. Proc Natl Acad Sci U S A.

Chapter 2

Zinc pyrithione induces apoptosis and increases expression of Bim[1].

Abstract

We demonstrate herein that zinc pyrithione can induce apoptosis at nanomolar concentrations. Zinc pyrithione was a potent inducer of cell death causing greater than 40-60% apoptosis among murine thymocytes, murine splenic lymphocytes and human Ramos B and human Jurkat T cells. Conversely, the addition of a zinc chelator protected thymocytes against zinc pyrithione induced apoptosis indicating these responses were specific for zinc. Zinc-induced apoptosis was dependent on transcription and translation which suggested possible regulation by a proapoptotic protein. Indeed, zinc induced a 1.9 and 3.4 fold increase respectively in expression of the BimEL and BimL isoforms and also stimulated production of the most potent isoform, BimS. This increase in Bim isoform expression was dependent on transcription being blocked by treatment with actinomycin D. Overexpression of Bcl-2 or Bcl-xL provided substantial protection of Ramos B and Jurkat T cells against zinc-induced apoptosis. Zinc also activated the caspase cascade demonstrated by cleavage of caspase 9. Addition of specific inhibitors for caspase 9 and caspase 3 also blocked zinc-induced apoptosis. The data herein adds to the growing evidence that free or unbound zinc could be harmful to cells of the immune system.

1 This work was published as the following manuscript: **Mann, J.J. and Fraker P.J.** (2005). Zinc pyrithione induces apoptosis and increases expression of Bim. Apoptosis 10, 369-379.

Introduction

Zinc is an essential biological trace metal vitally important for many cellular activities, therefore, the concentration of zinc is tightly regulated (7, 31). Zinc is critical as a cofactor for both catalytic and structural roles within the cell as well as numerous other processes including gene expression (7, 31). However exposure to excess unbound or extracellular zinc has been shown to have adverse effects at the cellular level through the induction of apoptosis in a number of cell types (8, 24, 28, 32). A variety of disease states are affected by the disruption of zinc homeostasis. During brain damage certain neurons which contain substantial amounts of zinc, up to 300μM of releasable free zinc within presynaptic boutons, as well as during seizures zinc is released with associated cell death observed in surrounding cells and tissues (10, 11, 26, 27). Addition of zinc chelators results in survival of these surrounding cells demonstrating a proapoptotic role for excess zinc. In the case of Alzheimer's disease, zinc has been shown to be associated with the β-amyloid proteins potentially enhancing aggregation and concomitant formation of plaques (6, 18). Chelation of zinc reduced the onset of Alzheimer's in a murine model making it of interest as a potential intervention in human trials (3, 5). Substantial amounts of zinc are also associated with the insulin stored in pancreatic islet β-cells which when released may act in a paracrine fashion to further accelerate the death of islet cells during the course of diabetes (16). Intracellular zinc exists as fixed pools of zinc, such as in transcription factors and as structural cofactors, or in labile pools of readily exchangeable zinc such as that bound by metallothionein (21) that are thought to be responsible for the regulation of apoptosis. Another example of this labile pool is the

release of zinc from protein kinase C (PKC) during activation in response to diacylglycerol or reactive oxygen species (17). Furthermore zinc has been demonstrated to be released within cells undergoing early events of apoptosis induced spontaneously or in response to various agents (34). Thus there are a number of situations where released zinc might have potentially adverse effects sometimes initiating apoptosis.

Zinc-induced apoptosis utilized the mitochondrial apoptotic pathway as will be demonstrated in this present study. The mitochondria are a central focusing point for many diverse signals initiating apoptosis in the intrinsic apoptotic pathway (22). Upon activation of this pathway cytochrome c is released from the mitochondria resulting in the assembly of the apoptosome which promotes cleavage and activation of caspase 9 and 3 (14, 15). Bcl-2 and Bcl-xL are the antiapoptotic proteins that sequester proapoptotic proteins such as Bax. These proteins prevent the multimerization of Bax and its interaction with the mitochondria thereby neutralizing its proapoptotic effects (2). Conversely proapoptotic BH3 only family members such as Bim (BimEL, BimL, BimS) antagonize the antiapoptotic functions of Bcl-2 and Bcl-xL through direct interaction (23). This interaction neutralizes these antiapoptotic proteins thus allowing Bax to multimerize resulting in the permeabilization of the mitochondrial outer membrane and release of molecules such as cytochrome c resulting in activation of the intrinsic apoptotic caspase cascade (23). As will be shown herein zinc-induced a substantial increase in Bim.

To further explore the capacity of zinc to induce apoptosis, we demonstrated several years ago that it could readily induce apoptosis in murine thymocytes causing all the classical changes in morphology to include cell shrinkage, chromatin condensation, and DNA fragmentation (28). Substantial concentrations of zinc sulfate (around 80-200 μM) were required to produce 40% thymic apoptosis probably because of the inefficient uptake of the zinc salts by cells (28). However addition of zinc pyrithione, an ionophore, induced substantial amounts of apoptosis (40-60%) at 400nM (normal plasma zinc is ~15-20 μM) (33) in both human and murine immune cells. These compounds caused a cellular increase in zinc of 1.2 and 19.5ng/1x10^7 cells for zinc pyrithione (400nM) and zinc sulfate (200μM) respectively for thymocytes after two hours of treatment. While zinc has been demonstrated to induce apoptosis in a variety of cell types a detailed analysis of the apoptotic death pathway utilized by zinc during apoptosis especially in cells of the immune system has not been fully established. The present study was therefore conducted to investigate the death pathway utilized by zinc in cells of the immune system. Such cells are an ideal model in which to determine the role of free zinc in apoptotic cell death since they are able to undergo zinc-induced apoptosis that is readily quantitated by FACS analysis and have well characterized death pathways (25). As will be demonstrated herein zinc-induced apoptosis utilized the caspase cascade and was blocked by overexpression of the antiapoptotic proteins Bcl-2 or Bcl-xL. To our knowledge it will also be shown for the first time that zinc induced the transcriptionally dependent BH3 only proapoptotic Bcl-2 family member Bim.

Materials and Methods

Materials. Roswell Park Memorial Institute (RPMI-1640) culture media, penicillin-streptomycin, HEPES buffer, sodium pyruvate, L-glutamine, G418 were obtained from Gibco BRL (Rockville, MD). Hanks balanced salt solution (HBSS), ultrapure zinc sulfate heptahydrate, 1-hydroxypyridine-2-thione zinc salt (zinc pyrithione), dexamethasone, bovine serum albumin (BSA) and the antibody for β-Actin were obtained from Sigma Chemical Co. (St. Louis, MO). N,N,N',N'-tetrakis (2-pyridinylmethyl) ethanediamine (TPEN), actinomycin D, cycloheximide, emetine, puromycin, caspase inhibitors, were obtained from Calbiochem (La Jolla, CA). Certified Australian fetal bovine serum (FBS) was obtained from Hyclone Laboratories, Inc. (Logan, UT). All antibodies used for phenotyping and antibodies to Bax, human Bcl-2, and Bcl-xL were obtained from Pharmingen (San Diego, CA). The antibody able to detect murine Bcl-2 was obtained from Santa Cruz Biotechnology, Inc. (Santa Cruz, CA). The antibodies directed against Bim and caspase 9 as well as the Chaps Cell Extract Buffer were from Cell Signaling Technology (Beverly, MA). Propidium iodide (PI), 4'-6-diaminido-2-phenylindole (DAPI) and merocyanine 540 (MC540) were obtained from Molecular Probes (Eugene, OR). Enhanced Chemiluminescence Plus (ECL^+) and Percoll were obtained from Amersham-Pharmacia (Piscataway, NJ). BCA Protein Concentration Assay was obtained from Pierce Chemical Company (Rockford, IL). The cell lines used Ramos (CRL-1596) and Jurkat (TIB-152) were obtained from American Type Culture Collection (Manassa, VA), murine S49 T cells were obtained from The Cell Culture

Facility University of California San Francisco (San Francisco, Ca.). Female A/J or CAF1/J mice were purchased from the Jackson Laboratory (Bar Harbor, ME).

Cell culture. Thymuses or spleens from young mice (8-12 weeks old) were passed through a 100 micron mesh stainless steel screen into harvest buffer (HBSS with 4% heat inactivated FBS). Single cell suspensions of spleens were then layered over a 70% percoll gradient to remove erythrocytes. The resuspended cell suspensions from the thymus or spleen were cultured in RPMI-1640 containing 10% heat inactivated FBS, 100 U/ml penicillin, 100 μg/ml streptomycin, 50 μM 2-mercaptoethanol, 2 mM L-glutamine in 24-well plates at 1-2x10^6 cells per ml for periods up to 8 hours at 37°C in 5% CO_2. Cell lines were cultured up to twelve hours in RPMI-1640 containing 10% heat inactivated FBS, 100 U/ml penicillin, 100 μg streptomycin, 2 mM L-glutamine, 10 mM HEPES buffer, 1 mM sodium pyruvate, D-glucose at 4.5 g/L. Media for transfected cell lines also contained 500 μg/ml G418. Where applicable, dexamethasone at 1 μM, zinc sulfate (180-200 μM), zinc pyrithione (ZnPy) (200-600 nM) were added at time zero. Inhibitors were added at the concentration indicated one hour prior to the addition of initiators of apoptosis. Viability and recovery were assessed at the beginning and end of culture periods using trypan blue dye exclusion. All use of mice was approved by the University Laboratory Animal Research Committee at MSU.

Immunophenotyping and DNA labeling of thymocytes and splenocytes. Following the designated incubation period, thymocytes and splenocytes were harvested, washed, and resuspended in label buffer (HBSS with 2% heat inactivated FBS and 0.1% sodium

azide) at 1-2x10^6 cells per ml per sample and immunophenotyped for T cell or B cell markers at 4°C. Antibodies used for T cell markers were Phycoerythrin (PE) conjugated anti-CD4 (GK1.5) and Fluorescein Isothiocyanate (FITC) conjugated anti-CD8a (53-6.7) while PE conjugated anti-B220 (RA3-6B2) was used for the B cell marker. Isotype/fluorochrome matched controls to all antibodies were used to determine background. Quantitation of cells in the hypodiploid region of the DNA cell cycle profile was as previously described.(29) Cells were resuspended in one part ice cold 50% FBS in phosphate buffered saline (PBS). Three parts ice cold 70% ethanol were added dropwise with gentle mixing and cells were incubated overnight at 4°C. After washing twice with label buffer the cells were resuspended in 1 ml of PBS with the addition of PI (50 μg/ml), RNaseA (100 units/ml), EDTA (0.1 mM) and 1% Triton X-100. In the case of three color analysis DAPI (1 μg/ml) was used to stain for DNA for 1 hour at room temperature in the dark. Between 10,000-20,000 cells per sample were analyzed.

Detection of Apoptosis. Initial gating of thymocytes through PI or DAPI width vs. area allowed for exclusion of debris and cell doublets without affecting the apoptotic region for cell cycle analysis. As previously described, quantitation of apoptosis was carried out by determination of the percentage of cells in the hypodiploid region of DNA cell cycle directly or after gating for phenotype (12).

Merocyanine 540 (MC540) labeling of cell lines for the detection of apoptosis. Since the hypodiploid peak or apoptotic region obtained with ethanol fixation is generally not well separated from the G_0/G_1 peak in cell lines undergoing apoptosis, it was necessary to

stain the cell lines (Jurkat, Ramos, S49) with MC540 for improved identification of apoptotic cells as per past publications (20). Briefly viable cells were removed from culture washed once in harvest buffer, resuspended in 100 µl MC540 staining solution (30 µM) and incubated 10 minutes in the dark at room temperature. After incubation, 900 µl harvest buffer was added and cells placed on ice in the dark. To differentiate between viable and dead cells, PI was added to a final concentration of 1 µg/ml two minutes prior to analysis. A 660 nm filter was used to detect MC540.

Data collection by FACS. All samples were analyzed on a Becton-Dickinson Vantage fluorescence activated cell sorter (FACS) (Becton-Dickinson, San Jose, CA) using CellQuest data acquisition and analysis software. Other software used to analyze data included WinList for Win32v4.0, ModFIT LT, and Microsoft Excel. Analysis of the immunophenotyped samples required use of an argon laser at 488 nm for excitation of FITC, PE, and PI with emission at 530 nm, 575 nm, and 630 nm, respectively. The UV lines of an argon/krypton mixed gas laser were used for simultaneous excitation of DAPI at 350 nm with emission at 470 nm where applicable. For MC540 analysis excitation was at 488 nm with emission at 575 nm and PI, used as a viability stain, was measured at 660 nm.

Inductively Coupled Plasma-Atomic Emission Spectrometry (ICP-AES) for the analysis of zinc content. Untreated or zinc pyrithione (400nM) or zinc sulfate (200µM) treated thymocytes (2 hours) were washed once with phosphate buffered saline. Samples were then resuspended in Milli-Q water and transferred to acid washed containers and

placed in an oven at 95°C to dry. Samples were digested overnight at 95°C with Ultrex II ultrapure nitric acid from JT Baker (Phillipsburg, NJ). The zinc content of each sample was measured at wavelength 213.857 nm using a Varian Vista Axial Inductively Coupled Plasma-Atomic Emission Spectrometer (Palo Alto, CA). Nitric acid digestion of standards containing reagents only (Milli-Q water or PBS) demonstrated no detectible zinc in these reagents while blank samples spiked with zinc pyrithione (400nM) or zinc sulfate (200μM) demonstrated the expected concentrations of zinc. The data shown was derived from quadruplicate samples ± standard error of the mean for each treatment group from one experiment representative of two independent experiments.

Western Blot analysis of protein levels. All cells, except for caspase 9 detection, were lysed in NP-40 lysis buffer which contained 50 mM Tris-Cl (pH 8.0), 150 mm NaCl, 0.02% sodium azide, 1% NP-40, phenylmethylsulfonyl fluoride (0.5 mM), sodium bisulfate (1 mM), benzamidine (1 mM), pepstatin A (1 μM), dithiothreitol (1 mM) and placed on ice for 30 minutes. Samples were then centrifuged to remove debris and the protein concentration was determined using the Pierce BCA assay. Cells used for caspase 9 detection were instead lysed in Chaps Cell Extract Buffer with dithiothreitol (5mM) and phenylmethylsulfonyl fluoride (0.5 mM). 25μg of protein were loaded per lane for the Western blots performed in extracts from murine thymocytes. For the Bcl-2 blot of human cell lines, 30 μg, 15 μg, 5 μg protein was used while 25 μg, 5 μg, 1 μg protein was used for the Bcl-xL blots. All samples were separated on a 12% resolving SDS-PAGE gel. The proteins were transferred to PVDF and blocked overnight at 4°C in 5% non-fat dry milk in Tris buffered saline with Tween 20 (TBST). The membranes were then

incubated with primary antibody diluted in 5% non-fat dry milk in TBST at room temperature on a rocker platform for 1 hour. As per manufacture protocol for the detection of Bim isoforms (BimEL, BimL, BimS), membranes were incubated with primary antibody diluted in 5% BSA in TBST at 4°C overnight. Blots were washed several times in TBST and incubated with secondary antibody horse radish peroxidase (HRP) conjugated in 5% non-fat dry milk in TBST for 1 hour at room temperature on a rocker platform. After multiple washes, the membranes were developed using ECL^+ detection agent following the manufacturers instructions and exposed to film for visualization. The relative levels of protein were evaluated by densitometry performed on scanned images using ImageJ by W. Rasband (developed at the U.S. National Institutes of Health and available on the Internet at http://rsb.info.nih.gov/ij/).

Statistical Methods. A representative experiment (mean $\pm$ SD) of at least two or more independent experiments is shown throughout. All samples were in triplicate unless otherwise noted. Immunophenotyping data was derived from triplicate samples generated from the assessment of three separate mice. Statistical calculations were made using SigmaStat 3.0 software (SPSS Inc., Chicago, IL). Samples were analyzed by One-way ANOVA with multiple comparison procedures using the Holm-Sidak Method. Data shown is the mean $\pm$ SD. An * indicates significant difference ($p \leq 0.05$) between treated and untreated samples within each group.

Results

Induction of apoptosis in murine thymocytes by zinc pyrithione (ZnPy). By utilizing ZnPy that has ionophore like qualities it was possible to increase the availability of exogenously added zinc to cells. As can be seen in figure 1A it was possible to induce up to 60% apoptosis in thymocytes using 400nM zinc pyrithione where FACS DNA analysis was used to quantitate apoptosis. The exogenously added ZnPy began to induce apoptosis at 250 nM with optimal induction observed at 400 nM for the 8 hr incubation period (Fig. 1B). At 600 nM apoptosis declined indicating a moderate range of efficacy for zinc. Thus zinc can induce apoptosis at extremely low concentrations (normal plasma zinc is ~15-20 μM) (33). In previous publications and subsequent figures it will be evident that substantial quantities of zinc salts were required to approach analogous levels of apoptosis (28). The reduction in apoptosis observed above 400nM zinc pyrithione was not due to cell loss or necrosis since viability and cell recovery were assessed using trypan blue exclusion. As previously shown, zinc sulfate (0-500μM) treatment of thymocytes resulted in a similar bell-shaped dose response curve (9). Prior studies illustrated that higher concentrations of zinc sulfate actually protect against apoptosis (temporarily) which may account for the bell-shape of the dose response curve (9). This temporary protection from apoptosis by zinc sulfate may also explain the similar dose response curve observed for zinc pyrithione (9). As also demonstrated in previous publications, zinc caused the standard morphological shrinkage of cells associated with apoptosis as demonstrated by phase contrast microscopy and by forward-side scatter analysis on the FACS (data not shown) (28). Extensive DNA fragmentation also occurred using ZnPy as demonstrated by the appearance of the apoptotic cells in the

Figure 2-1: Analysis of induction of apoptosis in thymocytes by zinc pyrithione using FACS to quantitate cells in the hypodiploid or apoptotic region.
A) Analysis of spontaneous levels of apoptosis and zinc pyrithione (400 nM) induced apoptosis after 8 hours in culture. Percent apoptosis is based on the number of cells within the hypodiploid region. **B)** Dose response curve for zinc pyrithione induced apoptosis. Thymocytes were incubated with indicated concentrations of zinc pyrithione and apoptosis measured after 8 hours in culture. Zinc pyrithione at 400 nM induced maximal apoptosis. **C)** TPEN (N,N,N',N'-tetrakis (2-pyridinylmethyl) ethanediamine) (5 μM), a cell permeable heavy metal chelator, abolished zinc pyrithione (400 nM) induced apoptosis while having no effect on dexamethasone induced apoptosis. Data shown is the mean $\pm$ SD. An * indicates significant difference ($p \leq 0.05$) between treated and untreated samples within each group.

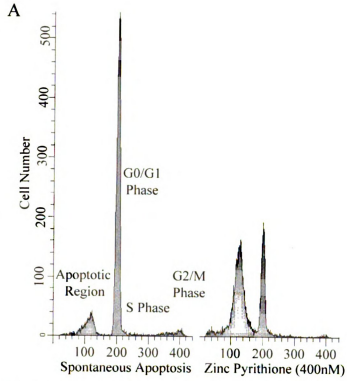
A
Cell Number
0
100
200
300
400
500
G0/G1
Phase
Apoptotic
Region
S Phase
G2/M
Phase
100 200 300 400
Spontaneous Apoptosis
100 200 300 400
Zinc Pyrithione (400nM)

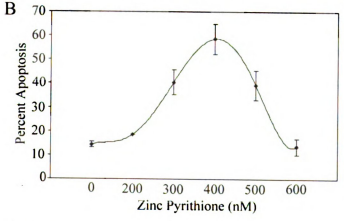
B
Percent Apoptosis
0
10
20
30
40
50
60
70
0 200 300 400 500 600
Zinc Pyrithione (nM)

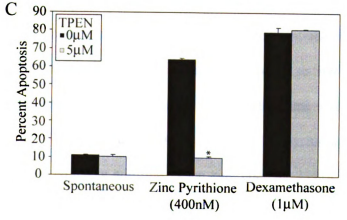
C
Percent Apoptosis
0
10
20
30
40
50
60
70
80
90
TPEN
0μM
5μM
*
Spontaneous
Zinc Pyrithione
(400nM)
Dexamethasone
(1μM)

hypodiploid region of the DNA histogram but at far lower concentrations (Fig. 1A). Observe the significant shift of thymocytes, which were predominantly in the G_0/G_1 region, to the low fluorescence or apoptotic region of the histogram subsequent to treatment with ZnPy (Fig. 1A). To make certain that the induction of apoptosis was, indeed, caused by zinc a highly specific chelator of zinc N,N,N',N'-tetrakis (2-pyridinylmethyl) ethanediamine (TPEN) was added to the cultures just prior to the addition of ZnPy. Additionally, the chelator completely blocked the ability of ZnPy to induce apoptosis while having no effect on dexamethasone induced apoptosis (Fig. 1C).

Time of induction of apoptosis by zinc. We next sought to determine the time required for maximal induction of apoptosis. The removal of media containing exogenously added ZnPy (400nM) or $ZnSO_4$ (180μM) and replacing it with regular media for the remainder of an 8 hour culture period resulted in no induction of apoptosis above spontaneous levels after removal of zinc by one hour and only 25% apoptosis after a two hour exposure (Fig. 2). The zinc content of thymocytes (19.5±0.2ng/1x10^7 cells) treated for two hours with zinc pyrithione (400nM) increased 1.2ng (20.7±0.2ng/1x10^7 cells) while zinc sulfate (200μM) treated thymocytes increased 19.5ng (38.9±3.4ng/1x10^7 cells) as measured by ICP-AES analysis. The difference observed between the zinc sulfate and zinc pyrithione treated thymocytes may potentially reflect intracellular as well as associated zinc since the zinc sulfate treated cells were exposed to 500 fold more zinc. However, as demonstrated by this data only a small amount of zinc was associated with treated thymocytes. As shown in figure 2 the sodium salt of pyrithione (400nM) also failed to induce apoptosis which in addition to the zinc chelator TPEN shown in figure

Figure 2-2. Time of induction of apoptosis by zinc in thymocytes.
Thymocytes were incubated in the presence of zinc pyrithione (400 nM), zinc sulfate (180 μM), or sodium pyrithione (400 nM) for indicated times (1, 2, 3, or 4 hours). At each time point the cells were washed to remove exogenously added zinc and replated in fresh media for the remainder of an eight hour total culture period at which time apoptosis was quantitated. Zinc must be present for approximately 3 hours to facilitate maximum apoptosis. Data shown is the mean $\pm$ SD.

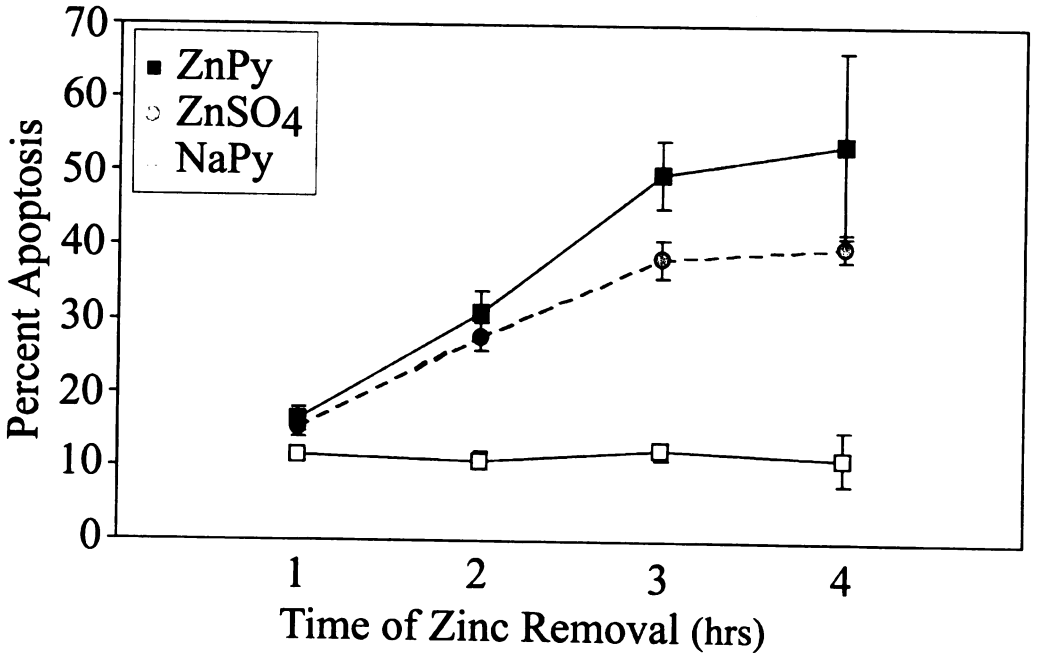
70
60
50
40
30
20
10
0
Percent Apoptosis
ZnPy
ZnSO4
NaPy
1
2
3
4
Time of Zinc Removal (hrs)

1C demonstrated that the response to zinc pyrithione was due to zinc (Fig. 2). Overall it was necessary to incubate cells at least 3 to 4 hours with either ZnPy or $ZnSO_4$ to optimize cell death. Now that the time frame for the initiation of apoptosis by zinc was established we next wanted to determine whether other cells of the immune system in addition to murine thymocytes were susceptible to zinc pyrithione induced apoptosis.

Various cells of the immune system are susceptible to zinc-induced apoptosis. Various cells of the immune system undergo apoptosis in response to zinc pyrithione treatment (400nM) shown in Table I. These cells include primary murine splenic T and B cells and the murine S49 T cell line as well as both human Jurkat T cell and human Ramos B cell lines all of which readily undergo apoptosis in response to zinc pyrithione. The experiments shown in figures 1 and 2 utilized thymocytes that, in fact, consist of four distinct cell subsets that include the earliest of T cells or the pro-T cells, pre-T cells that are involved in the gene arrangement of the TCR, mature helper T cells, and mature cytolytic T cells (28). It is known that pre-T cells are very vulnerable to apoptosis, possible due to the lower expression of Bcl-2, and succumb more readily to treatment with glucocorticoids, irradiation, etc., when compared to the pro-T, mature Helper T or Cytolytic T cells (4, 25, 28). Thus, the pattern of sensitivity of thymocytes to ZnPy treatment, of which the pre-T cells undergo 60% apoptosis shown in Table I, partially paralleled the previously reported expression of the antiapoptotic protein Bcl-2 raising the possibility that zinc-induced apoptosis might utilize the Bcl-2 regulated pathway (13, 25, 28).

Table I. Susceptibility of various cells of the immune system to zinc pyrithione (400nM) induced apoptosis

	Origin	Untreated	Zinc Pyrithione	Time of Incubation
Primary cells:				
Thymocytes:				
Pro T-cells	murine	17%	24%	8 hrs
Pre T-cells	murine	13%	60%	8 hrs
Helper T-cells	murine	4%	39%	8 hrs
Cytolytic T-cells	murine	7%	39%	8 hrs
Spleen:				
Helper T-cells	murine	7%	48%	8 hrs
Cytolytic T-cells	murine	3%	66%	8 hrs
B-cells	murine	15%	33%	8 hrs
Cell Lines:				
S49 T-cell	murine	11%	51%	12 hrs
Jurkat T-cell	human	6%	43%	12 hrs
Ramos B-cell	human	5%	44%	8 hrs

Dependence of ZnPy induced apoptosis on transcription and translation. Many of the classical apoptotic pathways are dependent on transcription and translation (25). Using dexamethasone induced apoptosis as a standard, it was evident in figure 3A that both ZnPy and zinc sulfate induced apoptosis require transcription. Actinomycin D at 5 μg/ml completely inhibited both zinc and dexamethasone induced apoptosis. Conversely in figure 3B, 50 to 100 μg cycloheximide which completely blocked dexamethasone induced cell death, indicating the inhibitor was functioning, only partially blocked zinc-induced death for either ZnPy or the zinc salt. Higher concentrations of cycloheximide were toxic to thymocytes but other inhibitors of translation such as emitine and puromycin also failed to completely block zinc-induced apoptosis for either form of zinc (data not shown). Since the inhibitor of transcription completely blocked zinc pyrithione induced apoptosis and the translation inhibitor at least partially blocked apoptosis this indicated that the apoptotic signaling pathway required for zinc-induced apoptosis were dependent upon an increase in the production of both mRNA and protein.

Treatment with ZnPy up-regulates the BH3 only proapoptotic protein Bim. Since transcription and translation are required for zinc-induced apoptosis in murine thymocytes the identity of possible candidate proteins responsible for apoptosis was investigated. We were especially interested in possible roles for Bcl-2 family members, as shown in figure 4 the BH3 only proapoptotic protein Bim was up-regulated in response to zinc treatment. To our knowledge this is the first time that the transcriptionally dependent up-regulation of Bim has been shown in response to zinc treatment.

Figure 2-3. Zinc-induced apoptosis is dependent upon transcription and translation in thymocytes.
A) The addition of actinomycin D, an inhibitor of transcription, completely abolished zinc-induced apoptosis. **B)** Cycloheximide, an inhibitor of translation, partially blocked zinc-induced apoptosis. Data shown is the mean $\pm$ SD. An * indicates significant difference ($p \leq 0.05$) between treated and untreated samples within each group.

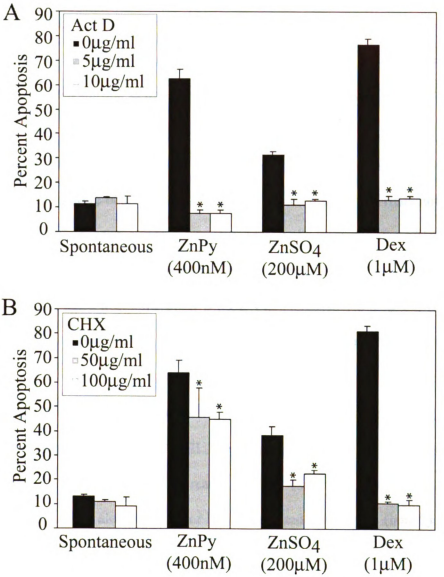
A
Act D
0μg/ml
5μg/ml
10μg/ml
Percent Apoptosis
90
80
70
60
50
40
30
20
10
0
Spontaneous
ZnPy
(400nM)
ZnSO4
(200μM)
Dex
(1μM)
B
CHX
0μg/ml
50μg/ml
100μg/ml
Percent Apoptosis
Spontaneous
ZnPy
(400nM)
ZnSO4
(200μM)
Dex
(1μM)

Thymocytes were dosed with 400nM ZnPy and placed into culture which at the times indicated 0, 2, 4, or 8 hours samples were removed and processed for FACS analysis or Western blot analysis (Fig. 4A). Densitometry was performed on the scanned Western blot images and the protein levels at time 0 hour (lane 1) for each protein (BimEL, BimL, Bax, Bcl-2, β-actin) were set to one for comparison purposes across the time course as shown in figure 4B. Three isoforms of Bim exist of which BimEL and BimL are present in murine thymocytes starting at time 0 hour (Fig. 4A lane 1). Within 2 hours (lane 2) of exposure to ZnPy BimEL and BimL were strongly up-regulated 1.7 and 2.4 fold respectively. By 4 hours (lane 3) BimEL increased 1.9 fold while BimL increased 2.6 fold. Similar results were observed for zinc sulfate treated thymocytes (data not shown). Additionally detection of the strongest proapoptotic isoform BimS, which wasn't observed at 0 hour, appeared by 4 hours while the strongest levels occurred by 8 hours (lane 3 and 4). At the 8 hour time point BimEL was increased 1.8 fold and BimL was increased 3.4 fold. The overall up-regulation of Bim in response to zinc treatment corresponded to the induction of apoptosis as measured by FACS analysis. Addition of actinomycin D (5μg/ml) which was shown to block zinc-induced apoptosis (Fig. 3A) blocked the strong up-regulation of BimEL, BimL and BimS as well as apoptosis induced by zinc (lane 5). However, no increase in Bim expression was observed with actinomycin D treatment alone (lane 6) or in the untreated thymocytes (lane 7) analyzed for spontaneous apoptosis after 8 hours in culture. β-actin was used as a control to demonstrate equal loading of protein for each sample. As demonstrated in figure 4B Bim levels increased in response to zinc treatment while Bax and Bcl-2 levels did not change. Since Bim functions by neutralizing antiapoptotic proteins such as Bcl-2 or Bcl-xL the

Figure 2-4. The BH3 only proapoptotic protein Bim is up-regulated in response to zinc pyrithione treatment in contrast to Bax or Bcl-2.
A) Murine thymocytes were untreated (lanes 1 and 7) or treated with 400nM zinc pyrithione (lanes 2-5) and/or 5μg/ml actinomycin D (lanes 5 and 6) for indicated times (0-8 hours) at which point samples were processed for FACS or Western blot analysis. FACS analysis demonstrated the percentage of cells undergoing apoptosis for each sample at the indicated times. Western blot analysis was performed to determine the protein levels of the Bcl-2 family members: Bim (three isoforms: BimEL, BimL, BimS), Bax and Bcl-2. β-actin was used as a loading control. The arrow shown in lane 3 denotes the most potent proapoptotic Bim isoform BimS detected as a faint band within 4 hours of zinc pyrithione treatment. **B)** Densitometry was preformed on lanes 1-4 from part A and the relative fold increase in protein levels compared to the 0 hr sample (lane 1) is shown for each protein. Data shown for FACS analysis is the mean ± SD. Overall data shown is one biological replicate representative of two independent experiments.

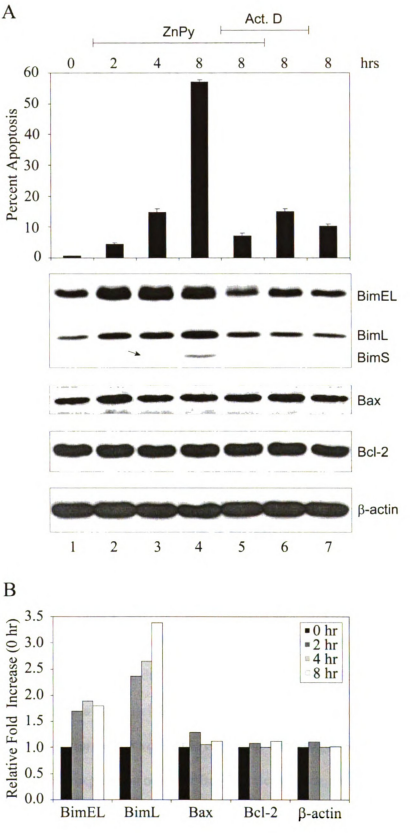
A
ZnPy
Act. D
0 2 4 8 8 8 8 hrs
Percent Apoptosis
60
50
40
30
20
10
0
BimEL
BimL
BimS
Bax
Bcl-2
β-actin
1 2 3 4 5 6 7
B
Relative Fold Increase (0 hr)
3.5
3.0
2.5
2.0
1.5
1.0
0.5
0.0
0 hr
2 hr
4 hr
8 hr
BimEL
BimL
Bax
Bcl-2
β-actin

increase in Bim levels would be expected to shift the cells fate in favor of promoting apoptosis, which was observed in lanes 1-4 of figure 4A. It was also anticipated that overexpression of Bcl-2 or Bcl-xL would result in the protection of cells from apoptosis induced by ZnPy treatment.

Modulation of ZnPy induced apoptosis by Bcl-2. In order to test whether zinc-induced apoptosis could be suppressed by overexpression of Bcl-2 or Bcl-xL two cell lines, Ramos B cells and Jurkat T cell lines, were acquired that overexpressed these antiapoptotic proteins. As demonstrated earlier (Table I) both wild type Ramos B cells and Jurkat T cells were susceptible to zinc pyrithione induced apoptosis. As observed in Fig. 5A and B it was evident that the wild type Ramos B cell and Jurkat T cells were very sensitive to ZnPy which resulted in 50-60% apoptosis as measured by changes in membrane order using MC540 fluorescence (20). MC540 analysis for the identification of apoptosis was undertaken since the analysis of the hypodiploid peak used for thymocytes can sometimes be difficult to cleanly separate from the G_0/G_1 peak in human cell lines. Our lab has previously shown that MC540 detects equivalent amounts of apoptosis as compared to hypodiploid analysis and Annexin V staining in murine thymocytes (20). Therefore results obtained utilizing MC540 analysis in these cell lines was comparable. In the case of both Ramos B cells and Jurkat T cells, Bcl-xL provided complete protection against zinc-induced death (Fig. 5A and B). Partial protection was provided in Ramos B cells since Bcl-2 was more moderately expressed (Fig 5A and C). A Western blot was performed to verify the degree of expression of these antiapoptotic proteins (Fig. 5C). Overexpression of either Bcl-2 or Bcl-xL was able to suppress

Figure 2-5. The antiapoptotic Bcl-2 family of proto-oncogenes regulate zinc-induced apoptosis. A) The human Ramos B cell line overexpressing Bcl-2 or Bcl-xL, and **B)** the human Jurkat T cell line overexpressing Bcl-xL were analyzed for their sensitivity to zinc-induced apoptosis. Apoptosis was measured using MC540 fluorescence at eight and twelve hours, respectively. Error bars are shown for every sample being not apparent in some cases where variation was very small. **C)** A Western blot was performed to verify expression levels of the antiapoptotic proteins in the transfected cell lines. Data shown is the mean $\pm$ SD.

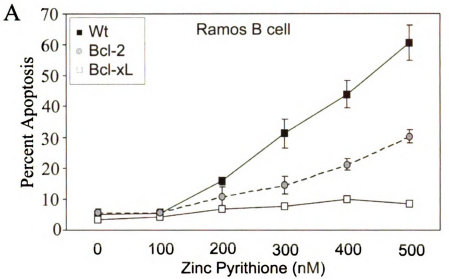
A
Ramos B cell
Wt
Bcl-2
Bcl-xL
Percent Apoptosis
0
10
20
30
40
50
60
70
0
100
200
300
400
500
Zinc Pyrithione (nM)

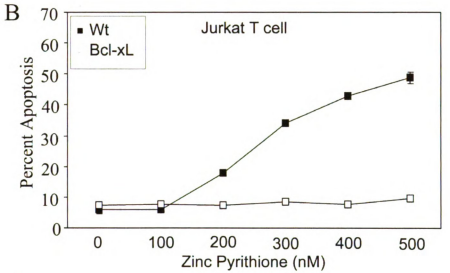
B
Jurkat T cell
Wt
Bcl-xL
Percent Apoptosis
0
10
20
30
40
50
60
70
0
100
200
300
400
500
Zinc Pyrithione (nM)

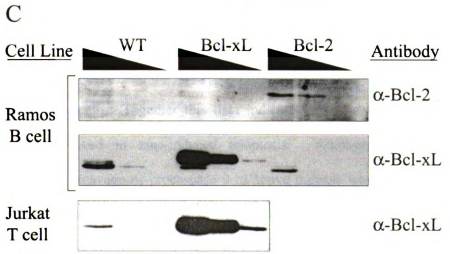
C
Cell Line
WT
Bcl-xL
Bcl-2
Antibody
Ramos
B cell
α-Bcl-2
α-Bcl-xL
Jurkat
T cell
α-Bcl-xL

apoptosis induced by zinc further indicating that a Bcl-2 proapoptotic family member such as Bim was involved in activation of the intrinsic mitochondrial apoptotic pathway.

Caspase activation by ZnPy. In this paper we have thus far demonstrated that the BH3 only proapoptotic protein Bim (Fig. 4) was up-regulated in response to zinc which was blocked by the transcriptional inhibitor actinomycin D (Fig. 4). Overexpression of Bcl-2 or Bcl-xL that can block the effects of Bim blocked zinc-induced apoptosis (Fig. 5). This data clearly indicated that the mitochondrial apoptotic pathway was utilized during zinc-induced apoptosis. Proapoptotic activation of the mitochondria results in the release of various molecules including cytochrome c which activates the apoptosome with further activation of caspase 9 and 3. To further investigate this pathway the caspase family of cysteine proteases which play key roles as executioners during mitochondrial induced apoptosis(25) were examined in response to zinc treatment. As shown in figure 6A murine thymocytes were treated with the broad spectrum caspase inhibitor Z-VAD-FMK (2 μM and 10 μM) which was able to completely block ZnPy induced apoptosis in thymocytes. The more specific caspase 9 inhibitor Z-LEHD-FMK (10 μM and 80 μM) was tested and reduced the degree of zinc-induced cell death to 35% and 12%, respectively (Fig. 6A). Z-DEVD-FMK (10 μM and 80 μM), a specific inhibitor of caspase 3 the executioner caspase downstream of initiator caspases, was able to block zinc-induced cell death. Together this data indicated that the mitochondrial caspase cascade was involved in zinc-induced apoptosis. Additionally further analysis demonstrated that cleavage of procaspase 9 to active caspase was observed within two hours in response to zinc pyrithione (400nM) treatment in thymocytes with stronger

Figure 2-6. The dependency of zinc-induced apoptosis on the caspase cascade.
A) The broad spectrum caspase inhibitor (Z-VAD-FMK), the caspase 9 inhibitor (Z-LEHD-FMK), and the caspase 3 inhibitor (Z-DEVD-FMK) were evaluated for their impact on zinc pyrithione induced apoptosis. Zinc pyrithione (400 nM) induced apoptosis in thymocytes was reduced in the presence of increasing concentrations of these caspase inhibitors: Z-VAD (2 μM, 10 μM), Z-LEHD (10 μM, 80 μM), Z-DEVD (10 μM, 80 μM). **B)** Procaspase 9 cleavage resulting in active caspase 9 occurs in response to zinc pyrithione treatment in thymocytes. β-actin was used as a loading control. Data shown is the mean $\pm$ SD. An * indicates significant difference ($p \leq 0.05$) between treated and untreated samples within each group.

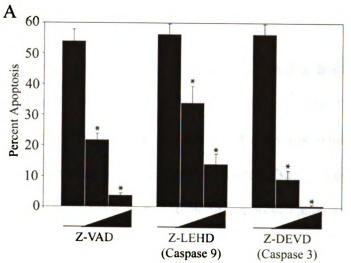
A
60
50
40
30
20
10
0
Percent Apoptosis
Z-VAD
Z-LEHD
(Caspase 9)
Z-DEVD
(Caspase 3)

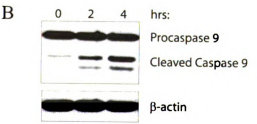
B
0
2
4
hrs:
Procaspase 9
Cleaved Caspase 9
β-actin

cleavage occurring by four hours (Fig. 6B). These results provide additional evidence that the intrinsic mitochondrial apoptotic pathway was active and utilized in response to zinc treatment.

Discussion

Modulation of cellular zinc, either resulting in deficiency or excess, has been shown to be involved in the regulation of cell death in various types of cells (30). During deficiency cells become more susceptible to numerous inducers of apoptosis, while the addition of exogenous zinc may reverse these apoptotic effects (30). Supra-physiological concentrations of zinc (mM) have been shown to suppress apoptosis in response to various inducers of apoptosis (30); however as demonstrated in murine thymocytes the protection afforded by zinc was only temporary as cell death still resulted several hours later (9). Furthermore lower concentrations of zinc were shown to induce apoptosis in murine thymocytes (28). Other labs have established that zinc can induce cell death in the case of cells of the lung, liver, prostate, etc. (8, 24, 32). Thus, a wide array of cell types can enter an apoptotic death phase upon exposure to exogenous or free zinc. Moreover among trace elements, this phenomenon appears to be somewhat peculiar to zinc since nickel, copper, cadmium and gold, did not initiate apoptosis in thymocytes in our hands (9).

Using zinc pyrithione it was possible to show that 400nM exogenously added zinc could induce apoptosis in various cells of the immune system from primary thymocytes and

splenic B and T cells to the human Ramos B and Jurkat T cell lines. As shown in Table I, a variety of cell types can undergo apoptosis in response to zinc pyrithione (400nM) treatment. ICP-AES analysis of thymocytes treated with zinc pyrithione (400nM) or zinc sulfate (200μM) demonstrated that a relatively small amount of zinc (1.2 and 19.5ng/1x10^7 cells) was associated with the treated cells. Zinc pyrithione induced apoptosis was demonstrated herein to be a zinc specific event through the inhibition of apoptosis by the zinc chelator TPEN and the lack of induction of apoptosis by sodium pyrithione. We further determined that zinc must be present for approximately three hours to maximize activation of the death pathway in thymocytes. Activation of this death pathway required transcription and translation. The inhibitor of transcription, actinomycin D, provided extensive blockage of apoptosis. However, cycloheximide and other translation inhibitors gave only partial inhibition in contrast to earlier studies in our lab with zinc salts where substantial inhibition was noted (28). It is not uncommon for these inhibitors to not only give moderate inhibition, but actually become inducers dependent on the cell lines and culture conditions (4). Overall though, the inhibition of zinc-induced apoptosis by the transcription and translation inhibitors suggested regulation by induction or increased expression of potentially proapoptotic genes.

In thymocytes zinc pyrithione had a preferential effect on pre-T cells that have been shown to contain little Bcl-2 (13) which potentially indicated regulation by the mitochondrial based Bcl-2 pathway. We therefore investigated possible Bcl-2 family members in the regulation of zinc-induced apoptosis. Indeed, all three isoforms of the BH3 only proapoptotic family member Bim were increased. Zinc-induced a 1.9 and 3.4

fold increase in expression of the BimEL and BimL isoforms respectively and also stimulated production of the most potent isoform, BimS. In contrast the levels of the proapoptotic protein Bax and the antiapoptotic protein Bcl-2 were unaffected. As others have previously shown Bim functions through neutralization of Bcl-2 or Bcl-xL thereby allowing Bax or other proapoptotic proteins already present to initiate mitochondrial apoptosis (23). Since Bim functions by neutralizing antiapoptotic proteins an increase in Bim levels with no increase in Bcl-2 levels would be expected to shift the cells fate in favor of promoting apoptosis which was observed herein. Moreover, as would be expected overexpression of the antiapoptotic Bcl-2 or Bcl-xL proteins, which have been shown to block Bim dependent apoptosis(23), prevented zinc initiated apoptosis. The difference in the ectopic expression of these antiapoptotic proteins may also explain the variation observed between the complete suppression of apoptosis in the Bcl-xL overexpressing cells and the protection provided by the Bcl-2 overexpressing cells. It has been shown that in response to cytokine withdrawal or treatment with taxol *bim*$^{-/-}$ pre-T cells survived 10-30 times better than wild type cells while heterozygous cells responded in between wild type and *bim*$^{-/-}$ cells (1). The amount of the proapoptotic protein Bim or the level of overexpression of the antiapoptotic proteins such as Bcl-2 or Bcl-xL might therefore have profound effects on the induction of apoptosis. Overall, suppression of zinc-induced apoptosis by overexpression of Bcl-2 or Bcl-xL provides further evidence of the mitochondrial apoptotic pathway in apoptosis.

Initiation of the mitochondrial pathway results in the release of cytochrome c and the assembly of the apoptosome which promotes cleavage and activation of caspase 9 and

3.(14, 15) This caspase cascade was shown herein to be required for zinc-induced apoptosis where inhibition of caspase 9, the initiator caspase of the mitochondrial pathway (19), and the executioner caspase 3 provided effective blockage of zinc-induced apoptosis. Cleavage of procaspase 9 to active caspase 9 also occurred in response to zinc treatment by two hours further demonstrating activation of the Bcl-2 family regulated mitochondrial apoptotic death pathway.

Conclusion

Excess free zinc has been implicated in various disease states having roles from neuronal damage (10, 26, 27) to Alzheimer's disease (6, 18) and diabetes (16). While zinc has been shown to induce apoptosis in a variety of cell types (8, 24, 32) a detailed analysis of the apoptotic death pathway utilized by zinc during apoptosis especially in cells of the immune system was not fully established. This is the first study to demonstrate the transcriptionally dependent up-regulation of Bim leading to the caspase dependent mitochondrial pathway in the induction of apoptosis by a very low concentration of zinc.

References

1. **Bouillet, P., D. Metcalf, D. C. Huang, D. M. Tarlinton, T. W. Kay, F. Kontgen, J. M. Adams, and A. Strasser.** 1999. Proapoptotic Bcl-2 relative Bim required for certain apoptotic responses, leukocyte homeostasis, and to preclude autoimmunity. Science **286:**1735-8.

2. **Chao, D. T., and S. J. Korsmeyer.** 1998. BCL-2 family: regulators of cell death. Annu Rev Immunol **16:**395-419.

3. **Cherny, R. A., C. S. Atwood, M. E. Xilinas, D. N. Gray, W. D. Jones, C. A. McLean, K. J. Barnham, I. Volitakis, F. W. Fraser, Y. Kim, X. Huang, L. E. Goldstein, R. D. Moir, J. T. Lim, K. Beyreuther, H. Zheng, R. E. Tanzi, C. L. Masters, and A. I. Bush.** 2001. Treatment with a copper-zinc chelator markedly and rapidly inhibits β-amyloid accumulation in Alzheimer's disease transgenic mice. Neuron **30:**665-76.

4. **Cohen, J. J., R. C. Duke, V. A. Fadok, and K. S. Sellins.** 1992. Apoptosis and programmed cell death in immunity. Annu Rev Immunol **10:**267-93.

5. **Cuajungco, M. P., K. Y. Faget, X. Huang, R. E. Tanzi, and A. I. Bush.** 2000. Metal chelation as a potential therapy for Alzheimer's disease. Ann N Y Acad Sci **920:**292-304.

6. **Curtain, C. C., F. Ali, I. Volitakis, R. A. Cherny, R. S. Norton, K. Beyreuther, C. J. Barrow, C. L. Masters, A. I. Bush, and K. J. Barnham.** 2001. Alzheimer's disease amyloid-β binds copper and zinc to generate an allosterically ordered membrane-penetrating structure containing superoxide dismutase-like subunits. J Biol Chem **276:**20466-73.

7. **Dardenne, M.** 2002. Zinc and immune function. Eur J Clin Nutr **56 Suppl 3:**S20-3.

8. **Feng, P., J. Y. Liang, T. L. Li, Z. X. Guan, J. Zou, R. Franklin, and L. C. Costello.** 2000. Zinc induces mitochondria apoptogenesis in prostate cells. Mol Urol **4:**31-6.

9. **Fraker, P. J., and W. G. Telford.** 1997. A reappraisal of the role of zinc in life and death decisions of cells. Proc Soc Exp Biol Med **215:**229-36.

10. **Frederickson, C. J., and A. I. Bush.** 2001. Synaptically released zinc: physiological functions and pathological effects. Biometals **14:**353-66.

11. **Frederickson, C. J., W. Maret, and M. P. Cuajungco.** 2004. Zinc and excitotoxic brain injury: a new model. Neuroscientist **10:**18-25.

12. **Garvy, B. A., W. G. Telford, L. E. King, and P. J. Fraker.** 1993. Glucocorticoids and irradiation-induced apoptosis in normal murine bone marrow B-lineage lymphocytes as determined by flow cytometry. Immunology **79:**270-7.

13. **Gratiot-Deans, J., L. Ding, L. A. Turka, and G. Nunez.** 1993. Bcl-2 proto-oncogene expression during human T cell development. Evidence for biphasic regulation. J Immunol **151:**83-91.

14. **Green, D. R., and J. C. Reed.** 1998. Mitochondria and apoptosis. Science **281:**1309-12.

15. **Hengartner, M. O.** 2000. The biochemistry of apoptosis. Nature **407:**770-6.

16. **Kim, B. J., Y. H. Kim, S. Kim, J. W. Kim, J. Y. Koh, S. H. Oh, M. K. Lee, K. W. Kim, and M. S. Lee.** 2000. Zinc as a paracrine effector in pancreatic islet cell death. Diabetes **49:**367-72.

17. **Korichneva, I., B. Hoyos, R. Chua, E. Levi, and U. Hammerling.** 2002. Zinc release from protein kinase C as the common event during activation by lipid second messenger or reactive oxygen. J Biol Chem **277:**44327-31.

18. **Kozin, S. A., S. Zirah, S. Rebuffat, G. H. Hoa, and P. Debey.** 2001. Zinc binding to Alzheimer's Aβ(1-16) peptide results in stable soluble complex. Biochem Biophys Res Commun **285:**959-64.

19. **Kumar, S., and D. L. Vaux.** 2002. Apoptosis. A cinderella caspase takes center stage. Science **297:**1290-1.

20. **Laakko, T., L. King, and P. Fraker.** 2002. Versatility of merocyanine 540 for the flow cytometric detection of apoptosis in human and murine cells. J Immunol Methods **261:**129-39.

21. **Maret, W.** 2003. Cellular zinc and redox states converge in the metallothionein/thionein pair. J Nutr **133:**1460S-2S.

22. **Newmeyer, D. D., and S. Ferguson-Miller.** 2003. Mitochondria. Releasing power for life and unleashing the machineries of death. Cell **112:**481-90.

23. **Opferman, J. T., and S. J. Korsmeyer.** 2003. Apoptosis in the development and maintenance of the immune system. Nat Immunol **4:**410-5.

24. **Paramanantham, R., K. H. Sit, and B. H. Bay.** 1997. Adding Zn^{2+} induces DNA fragmentation and cell condensation in cultured human Chang liver cells. Biol Trace Elem Res **58:**135-47.

25. **Rathmell, J. C., and C. B. Thompson.** 1999. The central effectors of cell death in the immune system. Annu Rev Immunol **17:**781-828.

26. **Suh, S. W., J. W. Chen, M. Motamedi, B. Bell, K. Listiak, N. F. Pons, G. Danscher, and C. J. Frederickson.** 2000. Evidence that synaptically-released zinc contributes to neuronal injury after traumatic brain injury. Brain Res **852:**268-73.

27. **Suh, S. W., R. B. Thompson, and C. J. Frederickson.** 2001. Loss of vesicular zinc and appearance of perikaryal zinc after seizures induced by pilocarpine. Neuroreport **12:**1523-5.

28. **Telford, W. G., and P. J. Fraker.** 1995. Preferential induction of apoptosis in mouse $CD4^{+}CD8^{+}\alpha\beta TCR^{lo}CD3\varepsilon^{lo}$ thymocytes by zinc. J Cell Physiol **164:**259-70.

29. **Telford, W. G., L. E. King, and P. J. Fraker.** 1994. Rapid quantitation of apoptosis in pure and heterogeneous cell populations using flow cytometry. J Immunol Methods **172:**1-16.

30. **Truong-Tran, A. Q., J. Carter, R. E. Ruffin, and P. D. Zalewski.** 2001. The role of zinc in caspase activation and apoptotic cell death. Biometals **14:**315-30.

31. **Walsh, C. T., H. H. Sandstead, A. S. Prasad, P. M. Newberne, and P. J. Fraker.** 1994. Zinc: health effects and research priorities for the 1990s. Environ Health Perspect **102 Suppl 2:**5-46.

32. **Walther, U. I., B. Wilhelm, S. Walther, H. Muckter, and B. Fichtl.** 2000. Zinc toxicity in various lung cell lines is mediated by glutathione and GSSG reductase activity. Biol Trace Elem Res **78:**163-77.

33. **Whitehouse, R. C., A. S. Prasad, P. I. Rabbani, and Z. T. Cossack.** 1982. Zinc in plasma, neutrophils, lymphocytes, and erythrocytes as determined by flameless atomic absorption spectrophotometry. Clin Chem **28:**475-80.

34. **Zalewski, P. D., I. J. Forbes, R. F. Seamark, R. Borlinghaus, W. H. Betts, S. F. Lincoln, and A. D. Ward.** 1994. Flux of intracellular labile zinc during apoptosis (gene-directed cell death) revealed by a specific chemical probe, Zinquin. Chem Biol **1:**153-61.

Chapter 3

The cAMP-PKA signal transduction pathway is a mediator of zinc-induced apoptosis via activation of Bim

Abstract

Although zinc is an essential trace metal exogenous cellular zinc can have deleterious effects. A proapoptotic role for exogenous zinc has emerged although the signaling pathways used during zinc-induced apoptosis were not known. SQ22536, an inhibitor of adenylate cyclase the enzyme responsible for cAMP production, reduced zinc mediated apoptosis from 52% to 29% in thymocytes. To explore the role of the cAMP-PKA signaling pathway the wild type S49 T-cell line was used along with two variants that were deficient in protein kinase A activity (S49 Kin^-) and ability to activate adenylate cyclase (S49 Cyc^-). Zinc pyrithione (400nM) induced 51% apoptosis in wild type S49 cells that included a prolonged 2 fold increase in cAMP over 8 hours. Production of cAMP results in the activation of PKA. One well documented target of PKA is the cAMP response element binding protein (CREB). Strong and sustained phosphorylation of the transcription factor CREB was observed in response to zinc treatment. In turn binding of a ^{32}P-labled DNA probe containing a cAMP response element (CRE) was increased. Conversely, the variant cell lines underwent only ~20% apoptosis and no phosphorylation of CREB was observed. In the S49 wild type cells there was also a five fold increase in mRNA levels and a corresponding eight fold increase in protein for the

proapoptotic Bcl-2 family member Bim. Increased occupancy of the Bim promoter by CREB was also observed in response to zinc treatment as assessed by chromatin immunoprecipitation (ChIP) analysis. Since no change in protein expression levels were observed for Bax, Bcl-2, or Bcl-xL, the increase in Bim appears instrumental in shifting the cells towards death. Overall, the data are consistent with a proapoptotic role for zinc and provides further delineation of the mechanisms utilized by zinc to induce apoptosis.

Introduction

Zinc is well known as an essential trace element, being key to the function of many metalloenzymes and transcription factors (5, 8, 9, 30, 43). However, there is very little unbound zinc in cells or body fluid thus the free metal was thought to have deleterious effects on cell function (43). Indeed, exposure to excess exogenous zinc causes apoptosis in a variety of cell types (11, 29, 41, 45). For example certain neurons contain as much as 300μM zinc which when released during seizures, ischemia or brain damage caused extensive cell death in surrounding cells (12, 13, 38, 39). Over supplementation with zinc can lead to gastric distress while its presence in the air can cause lung damage (43). Exogenous addition of zinc to cells has also been shown to induce apoptosis in neuronal (4, 31, 34), lung (44), prostate (10) and thyroid cells (15). More recently our lab has shown that zinc pyrithione (ZnPy) is a potent inducer of apoptosis causing 40-60% apoptosis in a variety of cells of the immune system to include thymocytes, splenic T and B cells and human Ramos B and Jurkat T-cells at nanomolar concentration (22). Use of zinc chelators prevented apoptosis indicating a clear role for zinc-induced cell death (6,

22). From the collective data a proapoptotic role for zinc has emerged (4, 6, 10-13, 15, 22, 29, 31, 34, 38, 39, 41, 44, 45).

Recent research has identified some of the molecular components involved in zinc-induced death (22). In the case of thymocytes, 400nM of zinc pyrithione was capable of inducing 60% apoptosis when added exogenously. The zinc chelator TPEN blocked zinc-induced apoptosis as did inhibitors of transcription and translation (22). Overexpression of Bcl-2 or Bcl-xL in Ramos or Jurkat cells provided substantial protection against zinc-induced apoptosis. The addition of caspase inhibitors including an inhibitor of caspase 9 also blocked zinc initiated apoptosis (22). Collectively the data indicate zinc employed the intrinsic mitochondrial mediated apoptotic pathway being regulated by Bcl-2 family members (22).

However, the signaling events utilized during zinc-induced apoptosis remained to be identified being the subject of this paper. To identify which signaling pathways might be involved we tested a number of inhibitors of a variety of pathways which included the adenylate cyclase pathway. cAMP is a well known and important secondary messenger that has been shown to induce apoptosis in a variety of cell types including cells of the immune system (20, 23, 25, 27, 32, 35, 42). As will be demonstrated the adenylate cyclase inhibitor SQ22536 blocked zinc-induced apoptosis. To better define the role of the cAMP signal transduction pathway in zinc-induced apoptosis we used the mouse S49 T-cell line. It was originally isolated from a Balb/c mouse derived immature pre-T cell ($CD4^+/CD8^+$) tumor, being particularly useful since there are also two well characterized

variants deficient in the cAMP signaling pathway (3, 7, 36, 37). The S49 Cyc$^-$ cell line is deficient in the Gαs subunit of the heterotrimeric G-protein coupled receptors that activate adenylate cyclase, the enzyme responsible for the *de novo* synthesis of cAMP (14, 19). The S49 *Kin*$^-$ cell line is deficient in protein kinase A (PKA) activity (36, 37). cAMP binds to the regulatory subunits of PKA which in turn releases the active catalytic subunits that phosphorylate a variety of substrates including the cAMP response element binding protein (CREB). The data will show that zinc induced substantially less apoptosis in these two variants which were defective in the cAMP-PKA signaling pathways. As will also be shown, there was substantial activation of the cAMP response element binding protein (CREB) via phosphorylation of Ser^{133} in the wild type S49 cells upon exposure to zinc. Phosphorylation of CREB increased both the transactivation potential and DNA binding of CREB (33) thus leading to increased transcription of target genes. One proapoptotic target gene activated in S49 WT cells in response to zinc was the novel BH3 only Bcl-2 family member Bim (22). Indeed, the induction of Bim was specific for zinc-induced apoptosis and was not a general effect of apoptosis since neither the extrinsic Fas mediated apoptotic pathway nor etoposide treatment of S49 WT cells induced Bim. Additionally, we show that transcriptional activator CREB is targeted to the Bim promoter as a result of zinc treatment via chromatin immunoprecipitation assays. The results provided herein will demonstrate that zinc-induced apoptosis utilizes a cAMP-PKA mediated signaling pathway that ultimately results in induction of Bim.

Materials and Methods

Materials. Roswell Park Memorial Institute (RPMI-1640) culture media, Dulbecco's Modified Eagle's Medium (DMEM), penicillin-streptomycin-amphotericin B, HEPES buffer, L-glutamine, were obtained from Gibco BRL (Rockville, MD). Hanks balanced salt solution (HBSS), 1-hydroxypyridine-2-thione zinc salt (zinc pyrithione), dexamethasone and the antibody directed against β-actin were obtained from Sigma Chemical Co. (St. Louis, MO). SQ22536, etoposide were obtained from Calbiochem (La Jolla, CA). Certified Australian fetal bovine serum (FBS) or horse serum (HS) was obtained from Hyclone Laboratories, Inc. (Logan, UT) Propidium iodide (PI) and merocyanin 540 (MC540) were obtained from Molecular Probes (Eugene, OR). Enhanced Chemiluminescence Plus (ECL^+) was obtained from Amersham-Pharmacia (Piscataway, NJ). The Bicinchoninic acid (BCA) protein concentration assay and the NE-PER (Nuclear and Cytoplasmic Extraction Reagents) were obtained from Pierce Chemical Company (Rockford, IL). QIAquick PCR purification columns were obtained from Qiagen (Valencia, Ca.). All oligonucleotides were synthesized at the Macromolecular Structure, Sequencing and Synthesis Facility at Michigan State University (East Lansing, MI). Syber Green Core Reagents were from Applied Biosystems (Foster City, CA). Trizol and Superscript II Reverse Transcriptase were obtained from Invitrogen (Carlsbad, California). Female A/J or CAF1/J mice were purchased from the Jackson Laboratory (Bar Harbor, ME). Antibodies directed against CREB and phosphorylated CREB on Ser^{133} were from Cell Signaling Technologies (Beverly, MA). Antibodies to Bax, and Bcl-xL as well as the anti-Fas antibody, which

results in the activation of Fas pathway, were obtained from Pharmingen (San Diego, CA). The antibodies directed against CREB used for the supershift analysis in the Electrophoretic mobility shift assay (EMSA) were from Santa Cruz Biotech (Santa Cruz, Ca). Female A/J or CAF1/J mice were purchased from the Jackson Laboratory (Bar Harbor, ME).

Cell culture. Thymuses from young mice (8-12 weeks old) were passed through a 100 micron mesh stainless steel screen into harvest buffer (HBSS with 4% heat inactivated FBS). Cell suspensions from the thymus were cultured in RPMI-1640 containing 10% heat inactivated FBS, 100 U/ml penicillin, 100 μg/ml streptomycin, 50 μM 2-mercaptoethanol, 2 mM L-glutamine in 24-well plates at $1\text{-}2x10^6$ cells per ml for periods up to 8 hours at 37°C in 5% CO_2. All cell lines were cultured in DMEM containing 10% heat inactivated horse serum, 100 U/ml penicillin, 100 μg/ml streptomycin, 0.25 μg/ml amphotericin B, 2 mM L-glutamine, 10 mM HEPES buffer at 37°C in 10% CO_2. Viability and recovery were assessed at the beginning and end of culture periods using trypan blue dye exclusion. All use of mice was approved by the University Laboratory Animal Research Committee at MSU.

Detection of apoptosis in mouse thymocytes. Thymocytes were gated to exclude debris and cell doublets. As previously described, quantitation of apoptosis was carried out by determination of the percentage of cells in the hypodiploid region of the DNA cell cycle using propidium iodide staining (22).

Merocyanine 540 (MC540) labeling of cell lines for the detection of apoptosis. Since the hypodiploid peak or apoptotic region obtained with ethanol fixation is generally not well separated from the G_0/G_1 peak in some cell lines undergoing apoptosis, it was necessary to stain the cell lines with MC540 for improved identification of apoptotic cells as per past publications (21, 22). Apoptotic cells with disregulated membranes stain MC540 bright, being well separated from the healthy cells that stain MC540 dim. Briefly viable cells were removed from culture washed once in harvest buffer, resuspended in 100 µl MC540 staining solution (30 µM) and incubated 10 minutes in the dark at room temperature. After incubation, 900 µl harvest buffer was added and cells placed on ice in the dark. To differentiate between viable and dead cells, PI was added to a final concentration of 1 µg/ml two minutes prior to analysis. A 660 nm filter was used to detect MC540.

Data collection by FACS. All samples were analyzed on a Becton-Dickinson DIVA fluorescence activated cell sorter (FACS) (Becton-Dickinson, San Jose, CA) using CellQuest data acquisition and analysis software. Other software used to analyze data included WinList for Win32v4.0, ModFIT LT, and Microsoft Excel. Analysis of the samples required use of an argon laser at 488 nm for excitation of MC540, PI with emission at 575 nm and 660 nm, respectively.

Scintillation Proximity Assay for the determination of cAMP. cAMP concentrations were detected using the cAMP [^{125}I] Direct Biotrak Scintillation Proximity Assay (RPA538, Amersham Biosciences). Briefly, cells were plated at a density of $1x10^6$

cells/ml in a plastic 24-well cell-culture plate, pretreated with the phosphodiesterase inhibitor 100μM IBMX (3-isobutyl-1-methylxanthine) for 1 hour then treated with 400nM ZnPy for indicated times, and cAMP subsequently isolated. Experimental cAMP levels were quantified through use of a standard curve using known amounts of cAMP.

Western Blot analysis of protein levels. Western blot analysis was performed using the method previously described in *Mann and Fraker* (22). Briefly all cells were lysed in 1% NP-40 lysis buffer. Protein concentrations were determined using the Pierce BCA assay. Western blots were performed with extracts, 25μg of protein per lane from murine thymocytes and 50μg of protein extracts from S49 cells were loaded per lane. All samples were separated on a 12% or 17% resolving SDS-PAGE gel. The proteins were transferred to PVDF and blocked overnight at 4°C in 5% non-fat dry milk in Tris buffered saline with Tween 20 (TBST). The membranes were then incubated with primary antibody diluted in 5% non-fat dry milk in TBST at room temperature. The manufacture protocol was followed for the detection of Bim. After multiple washes, the membranes were developed using ECL^+ detection agent and exposed to film for visualization.

Electrophoretic mobility shift assay:

Complementary oligonucleotides containing either a specific CRE (CTAGAAGAGATTGCCTGACGTCAGAGAGCTAGG-forward, GATCCCTAGCTCTCTGACGTCAGGCAATCTCTT-reverse) or a *mutant* CRE

(CTAGAAGAGATTGCCTG***TG***GTCAGAGAGCTAGG-forward, GATCCCTAGCTCTCTGACCACAGGCAATCTCTT-reverse) were annealed and inserted into the pUC119 plasmid using XbaI and BamHI sites. The inserted sequence of the plasmid was then verified. Probes were generated by PCR amplification of these constructs using the universal sequencing primer (GCCAGGGTTTTCCCAGTCACG) end-labeled with [γ-^{32}P]ATP and T4 polynucleotide kinase and the reverse sequencing primer (AGCGGATAACAATTTCACAGA) for pUC119. All probes were gel purified. All of the probes were generated with the same radiolabeled primer and therefore had the same specific activity. All DNA binding reactions were performed in a 20-µl total volume in buffer containing 60 mM KCl, 20 mM HEPES pH 7.9, 5 mM $MgCl_2$, 0.2 mM EDTA, 10% glycerol, 0.5 µg of poly(dI-dC), and 0.5 µg of pUC119 plasmid. Nuclear extract was prepared as per manufacturer instructions for the NE-PER kit. Reactions containing 7µg nuclear extract were incubated for 30 min at room temperature after which 10,000 cpm of probe (CRE) was added, and reactions were incubated an additional 30 min. For supershift analysis 2µg of antibody was incubated in the reaction mixture for 30 min at room temperature after which probe was added, and reactions were incubated an additional 30 min. Samples were fractionated on a 5% non-denaturing polyacrylamide gel (39:1) in TGE running buffer (50 mM Tris, 380 mM glycine, 2 mM EDTA). Gels were dried and exposed to film in the presence of an intensifying screen at -80°C for visualization.

RNA isolation and Real Time PCR analysis. RNA was isolated from 5x10^6 cells by the Trizol extraction method using the manufacturer protocol. First strand synthesis of

cDNA was performed using Superscript II reverse transcriptase and oligo-dT. Real Time PCR analysis was performed in triplicate on cDNA samples using Applied Biosystems Syber Green Core Reagents with the mouse specific Bim primers (TGTGACAGAGAAGGTGGACAA -forward, TTCAGGTTCCTCCTGAGACTG-reverse) or the mouse specific β-actin primers (TGCTGACAGGATGCAGAAG-forward, GCTGGAAGGTGGACAGTGA-reverse) on the ABI Prism 7000 Sequence Detection System (SDS). Results were normalized to β-actin at indicated times. Results were then normalized to the untreated sample (0 hr). Results shown are the average of three independent experiments.

Formaldehyde Crosslinking and Soluble Chromatin Preparation. S49 WT cells were treated with zinc for indicated times. Cells were crosslinked using 1% final concentration formaldehyde for 10 minutes at room temperature with gentle swirling. The formaldehyde was quenched with using 18 mls of 2.5 M glycine at room temperature for 5 minutes. Cells were then pelleted at 500xg for 7 minutes, washed twice with ice cold PBS, and washed three times in Run-on lysis buffer (10 mM Tris pH 7.5, 10 mM NaCl, 3 mM $MgCl_2$, and 0.5% NP40). Recovered nuclei were aliquoted, flash frozen in liquid nitrogen and stored at –80°C until use. Micrococcal nuclease (MNase) digestions were then performed such that there were the equivalent of approximately $2x10^8$ cells per digestion. Frozen pellets were resuspended to a volume of 1.5 ml MNase reaction buffer (10 mM Tris pH 7.5, 10 mM NaCl, 3 mM $MgCl_2$, 1 mM $CaCl_2$, 4% NP40, 1 mM PMSF). Thirty units of MNase (USB) were added to each reaction, samples were incubated at 37°C for 10 minutes, and the digestion halted by the addition of 30 μl 200 mM EGTA.

Forty μl of 100 mM PMSF, 3μl of Aprotinin (2mg/ml), 3μl of Leupeptin (2mg/ml), 3μl of Pepstatin (2mg/ml) and 141 μl MNase reaction buffer, 200 μl 10% sodium dodecyl sulfate, and 80 μl 5 M NaCl were subsequently added to each reaction. Next, samples were sonicated four times for 1 minute at a power level setting of 2 and 60% duty. The cellular debris were then cleared by centrifugation on high speed for 10 minutes at 4°C. The supernatant was then removed to a new tube, aliquoted to volumes equivalent to $2x10^7$ cells per tube, flash frozen on liquid nitrogen, and stored at -80°C until use. For each sample, a small aliquot was treated with Proteinase K, the crosslinks reversed, and run on a 1% TAE-agarose gel to monitor MNase digestion. The average size fragments for each chromatin preparation were 500-1000 base pairs.

Chromatin Immunoprecipitation. Chromatin immunoprecipitations were performed using a volume of soluble chromatin equivalent to $2x10^7$ cells. Chromatin was diluted 1:5 using immunoprecipitation (IP) dilution buffer (20mM Tris pH 8.0, 2mM EDTA, 1% TritonX-100, 150mM NaCl, and 1μl of Aprotinin (2mg/ml), 1μl of Leupeptin (2mg/ml), 1μl of Pepstatin (2mg/ml) and pre-cleared with Protein G (Amersham) sepharose beads for 15 minutes at 4°C on a rotator. The pre-cleared diluted chromatin was then incubated with 10μl of CREB antibody (Santa Cruz Biotech) overnight at 4°C. Fifty μl of protein G sepharose was then added to each IP and incubated for 3 hours at 4°C. IPs were washed in 1 ml Dilution Buffer, centrifuged, and the beads were resuspended in 0.7 ml IP dilution buffer. Samples were washed for 5 minutes at room temperature on a rotator using the following buffers respectively: ChIP Wash Buffer 1 (20mM Tris pH 8.0, 2mM EDTA, 1% TritonX-100, 0.1% SDS, 150mM NaCl, 1mM PMSF), ChIP Wash Buffer 2

(20mM Tris pH 8.0, 2mM EDTA, 1% TritonX-100, 0.1% SDS, 500mM NaCl, 1mM PMSF), ChIP Wash Buffer 3 (10mM Tris pH 8.0, 1mM EDTA, 0.25 M LiCl, 0.5% NP-40, 0.5% deoxycholate), and three times in TE buffer (10mM Tris-Cl pH 8.0, 1mM EDTA). Samples were eluted in 200 µl Elution buffer (25mM Tris pH 7.5, 5mM EDTA, 0.5% SDS) at 65°C for 30 minutes and transferred to new tubes. Pronteinase K was added to each sample and to pre-cleared input chromatin samples to a final concentration of 1.5 µg/µl. Samples were incubated at 42°C for 2 hours and at 65°C overnight to reverse the crosslinks. Precipitated DNA was then recovered using QIAquick PCR purification columns as per manufacturer specifications and eluted in 100 µl 10 mM Tris pH 8.5. Real Time PCR analysis was performed using primers directed at the promoter of Bim (GAAGCTGTGCAAAGCAAGG –forward, GCAGAGCGGAACTTAGGG – reverse) or as a negative control primers directed against Exon 3 of Actin (ACAGCTGAGAGGGAAATCGT –forward, GCAGCTCATAGCTCTTCTCCA – reverse). IP samples were normalized to the actin negative control.

Statistical Analysis. A representative experiment of duplicate or triplicate sets of data are provided where each sample was done in triplicate unless otherwise noted. Data shown are standard deviations (SD) of the mean. Statistical calculations were made using SigmaStat 3.0 software (SPSS Inc., Chicago, IL).

Results

Adenylate Cyclase involvement in zinc-induced apoptosis.

A variety of different signal transduction pathways could be utilized during zinc-induced apoptosis. To identify candidate pathways inhibitors of various pathways were used which ultimately identified the adenylate cyclase signaling pathway as a potential signaling pathway. Mouse thymocytes were preincubated for one hour with or without the adenylate cyclase inhibitor SQ22536 (200μM) at which point zinc pyrithione (400nM) or zinc sulfate (200μM) were added. Dexamethasone (0.1μM), served as a control for the induction of apoptosis. After eight hours in culture the cells were processed and assayed for apoptosis by flow cytometry. As shown in **Figure 3-1A**, zinc pyrithione induced apoptosis was reduced from 52% to 29% by the adenylate cyclase inhibitor whereas zinc sulfate induced apoptosis was reduced from 36% to 18%. Spontaneous apoptosis was 10%. Since the inhibitor itself caused 19% apoptosis, it precluded the use of higher concentrations and may explain the partial inhibition observed. The inhibitor had no effect on dexamethasone-induced apoptosis as would be expected. These results suggested that adenylate cyclase and its product cAMP were involved in the induction of apoptosis by zinc but further investigation was needed to verify its role.

Figure 3-1: Requirement for the adenylate cyclase-PKA signaling pathway for zinc-induced apoptosis.

A) SQ22536 an adenylate cyclase inhibitor reduced zinc-induced apoptosis in mouse thymocytes. Mouse thymocytes were preincubated with SQ22536 (200μM) for one hour prior to the addition of zinc pyrithione (400nM) or dexamethasone (0.1μM). Apoptosis was measured after eight hours in culture. This inhibitor had no effect upon dexamethasone induced apoptosis, which was used as a positive control for the induction of apoptosis in thymocytes. **B)** In order to investigate the cAMP-PKA signal transduction pathway further a genetic approach utilizing the well characterized S49 lymphoma cell lines S49 wild type and S49 cell lines deficient either in the activation of adenylate cyclase activity (S49 Cyc^-) or deficient in PKA activity (S49 Kin^-) was undertaken. Cells were treated with increasing concentrations of zinc pyrithione (0-500nM) and analyzed for apoptosis after twelve hours in culture. **C)** To verify that the low response of the Cyc^- and Kin^- cells to zinc was due to the loss of the cAMP-PKA signal transduction pathway the cell lines were either treated with Etoposide (100 μM) or α-Fas (500ng/ml) antibody plus actinomycin D (25ng/ml) or untreated for twelve hours and apoptosis was measured. **D)** To determine whether cAMP was produced in response to zinc. S49 WT cells were preincubated with the phosphodiesterase inhibitor IBMX (100μM) for one hour. Cells were then incubated with zinc pyrithione (400nM) for the indicated times and the cAMP produced was determined by scintillation proximity assay of quadruplicate samples.

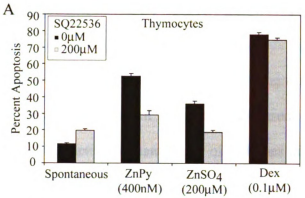
A
SQ22536
0μM
200μM
Thymocytes
Percent Apoptosis
Spontaneous
ZnPy (400nM)
ZnSO4 (200μM)
Dex (0.1μM)

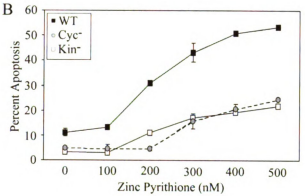
B
WT
Cyc-
Kin-
Percent Apoptosis
Zinc Pyrithione (nM)

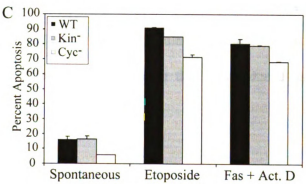
C
WT
Kin-
Cyc-
Percent Apoptosis
Spontaneous
Etoposide
Fas + Act. D

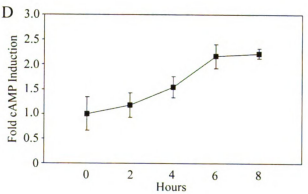
D
Fold cAMP Induction
Hours

Confirmation of zinc utilization of the cAMP-PKA pathway using S49 variant cell lines.

In order to better define the function of adenylate cyclase during zinc-induced apoptosis, genetic variants of a T-cell lymphoma cell line (S49) were used. This approach took advantage of a previously characterized matched set of cell lines in which the wild type (WT) cells could be directly compared to cells deficient for either the activation of adenylate cyclase (S49 *Cyc*$^-$) or protein kinase A activity (S49 *Kin*$^-$) which allowed the exploration of several steps in the adenylate cyclase signaling pathway. The S49 *Cyc*$^-$ (19%) and S49 *Kin*$^-$ (21%) cell lines were clearly less susceptible than the S49 WT cells (51%) to zinc pyrithione (400nM) induced apoptosis as shown in **Figure 3-1B**. Nevertheless, the mutant cell lines responded to etoposide (100μM) and anti-Fas (500ng/ml) antibody plus actinomycin D (25ng/ml) induced apoptosis as shown in **Figure 3-1C** exhibiting over 70% apoptosis. This indicated that although they are less susceptible to zinc-induced apoptosis, they could in fact undergo apoptosis when treated with other inducers. These results indicated that zinc-induced apoptosis utilized the cAMP-PKA signaling pathway.

Prolonged production of cAMP in response to zinc.

To further characterize the role of cAMP during zinc mediated apoptosis, the increase in cAMP in the S49 WT cells was measured by scintillation proximity assay after zinc treatment as shown in **Figure 3-1D.** Initially, S49 WT cells were preincubated for one hour with 100μM IBMX (3-isobutyl-1-methylxanthine), a phosphodiesterase inhibitor that preserves any cAMP produced. Cells were then incubated with 400nM zinc

pyrithione for indicated times, quadruplicate samples were processed and assayed for the presence of cAMP. As shown in **Figure 3-1D**, a 1.5 fold increase in cAMP was observed by 4 hours with a 2-fold increase noted for another 2 hours. The prolonged production of cAMP after zinc treatment was further suggestive of a role for cAMP during zinc-induced apoptosis was in keeping with our earlier observation that the maximum induction of zinc-induced apoptosis requires a period of exposure of 4-6 hours (22).

CREB phosphorylation on Ser^{133} by PKA.

CREB phosphorylation on Ser^{133} is an indicator of PKA activity being followed by changes in gene expression (24). Therefore CREB phosphorylation was monitored by Western blot analysis in S49 WT cells treated with 400nM zinc pyrithione over an eight hour time course. As shown in **Figure 3-2A,** some phosphorylation of CREB was already apparent within 15 minutes upon exposure of S49 WT cells to exogenous zinc. Significant phosphorylation was noted between 1 and 2 hours (lanes 4 and 5 compared to lane 1) being sustained out to 8 hours. This correlated with the kinetics of production of cAMP observed in **Figure 3-1D**. The Western blots were then stripped and reprobed for non-phosphorylated CREB to verify equal protein loading of all lanes.

A similar time course was performed in *Cyc*$^-$ and *Kin*$^-$ cells exposed to zinc in order to verify that the phosphorylation in WT cells was due to PKA activity and not other possible kinases, such as the MAPK pathway (26). The eight hour WT sample treated with zinc was added as a positive control for the phosphorylation of CREB with the *Cyc*$^-$ and *Kin*$^-$ blots. No strong phosphorylation of CREB was observed in the variant cell lines

Figure 3-2: Zinc treatment induced CREB phosphorylation at Ser^{133}.
Phosphorylation of CREB at Ser^{133} is an indicator of PKA activity. S49 lymphoma cells were incubated with zinc pyrithione (400nM) for indicated times. **A)** A Western blot directed against CREB or CREB phosphorylated on Ser^{133} was preformed. In S49 WT cells CREB phosphorylation was observed starting at one hour being very strong from two to eight hours. The variant S49 cell lines that are less sensitive to zinc-induced apoptosis showed no CREB phosphorylation in response to zinc treatment. As a positive control the 8 hour WT sample was analyzed along side the Cyc^- and Kin^- samples for comparison purposes which demonstrated that this signal transduction pathway was not functional in these variant cell lines in response to zinc treatment. **B)** Activation of the cAMP-PKA signaling pathway and increased phosphorylation of CREB on Ser^{133} in response to zinc treatment (400nM) was also noted in mouse thymocytes. Equal loading of all lanes was verified with β-actin.

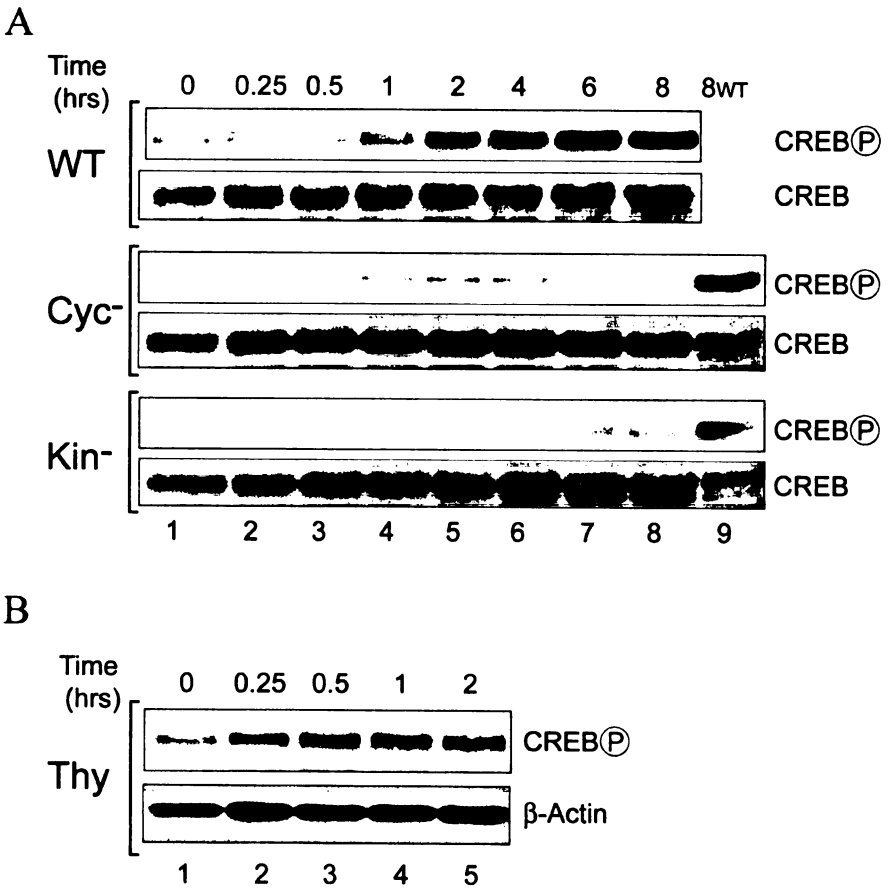
A
Time (hrs)
0 0.25 0.5 1 2 4 6 8 8WT
WT
CREB(P)
CREB
Cyc-
CREB(P)
CREB
Kin-
CREB(P)
CREB
1 2 3 4 5 6 7 8 9
B
Time (hrs)
0 0.25 0.5 1 2
Thy
CREB(P)
β-Actin
1 2 3 4 5

in response to zinc treatment as shown in **Figure 3-1D**. This result clearly indicated that the CREB phosphorylation observed in the WT cells was in fact due to PKA activity and not other signaling pathways.

As an additional verification of the importance of the PKA pathway, CREB phosphorylation was also analyzed in mouse thymocytes. Zinc pyrithione (400nM) induced strong CREB phosphorylation in mouse thymocytes (**Figure 3-2B**) from 15 minutes to 2 hours indicating activation of the PKA signaling pathway in thymocytes as well. Thus zinc pyrithione treatment resulted in the induction of cAMP and activation of PKA that produced prolonged and intense phosphorylation of CREB in both the S49 WT T-cell line as well as primary thymocytes.

Zinc treatment increases DNA binding specifically at CRE elements.

Phosphorylation at Ser^{133} has been shown to increase both the transactivation and DNA binding potential of CREB (33). Given that zinc robustly stimulated a sustained phosphorylation event in the CREB protein in S49 WT cells (**Figure 3-2A**), we wanted to determine whether the DNA binding activity of CREB increased concurrently and by extension its ability to regulate gene expression. To this end, electrophoretic mobility shift assays (EMSA) were performed to analyze DNA binding activity resulting from zinc treatment.

As shown in **Figure 3-3,** nuclear extracts were prepared from untreated S49 WT cells (0 hour) or zinc pyrithione (400nM) treated cells (2 hours) and were tested for their ability

to bind to consensus cAMP response elements (CRE), a known target sequence for CREB. These extracts were incubated with ^{32}P-labeled DNA probes containing either a wild type cAMP response element (CRE) or a mutated CRE as a negative control for sequence specificity. The resulting stable protein-DNA complexes were fractionated by electrophoresis and visualized by autoradiography. The probe containing a mutated CRE was used in lanes 1-3 of **Figure 3-3** with the mobility of the free probe shown in lane 1. Lanes 2 and 3 show a lack of transcription factor binding to the mutant probe in zinc treated and non-treated cells suggesting that any complex detected using the wild type CRE probe is specific.

The DNA binding reactions in lanes 4-8 were performed using the wild type CRE DNA probe. Lane 4 shows the mobility of the free probe since no extract was added. In lanes 5 and 6, DNA binding reactions containing nuclear extracts from 0 or 2 hours, resulted in the formation of two complexes, a higher mobility complex (C) and a lower mobility complex (B). These complexes are specific to the CRE sequence as they are not observed when using the mutated CRE probe. Addition of zinc (compare lane 5 to lane 6) results in an increase in DNA binding as well as the formation of higher order complexes seen as a modest shift in mobility in complexes B and C. This change in mobility is suggestive of additional factor recruitment or post-translation modification such as phosphorylation at this complex which resulted in a shift.

In order to determine whether CREB was included in the DNA-protein complexes B and C as observed in lane 6, an antibody directed against CREB was tested in the DNA

Figure 3-3: Zinc treatment increased DNA binding specifically at CRE elements. Since zinc-induced CREB phosphorylation on Ser^{133}, an electrophoretic mobility shift assay (EMSA) was performed to determine whether cAMP response element (CRE) DNA binding activity also increased in response to zinc treatment. Nuclear extracts were prepared from an untreated sample (0 hr) or zinc pyrithione (400nM) treated sample (2 hr). A mutant CRE ^{32}P-labeled probe was used in lanes 1-3 which demonstrated the specificity of the wild type probe used in lanes 4-8. An antibody-supershift assay was preformed using antibodies directed against CREB (lane 7) or an isotype control IgG (lane 8). A shifted band (A) was observed in lane 7 indicating CREB was responsible for band C. Free probe is present at the bottom of each lane.

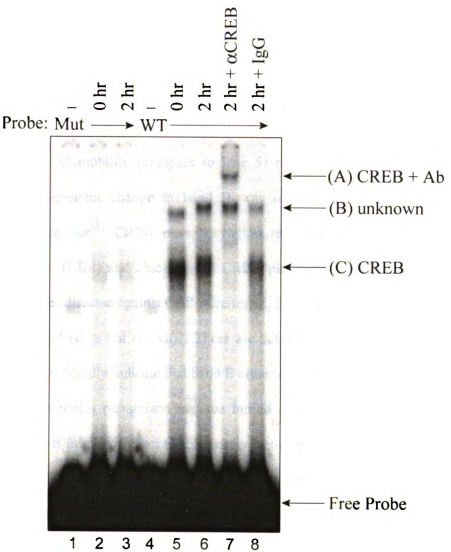
–
0 hr
2 hr
–
0 hr
2 hr
2 hr + αCREB
2 hr + IgG
Probe: Mut → WT →
(A) CREB + Ab
(B) unknown
(C) CREB
Free Probe
1 2 3 4 5 6 7 8

binding reactions (lane 7). Lane 7 shows a supershifted band (A) resulting from addition of the antibody with the concurrent loss of band C indicating that band C definitively contained CREB. An isotype control antibody (IgG) was also tested (lane 8) to demonstrate the result observed with the CREB antibody was specific and not a general effect of antibody addition.

Interestingly, complex B (lane 6) clearly showed an increase in DNA binding and a modest change in mobility (compare to lane 5) resulting from the addition of zinc. However, no apparent change in band B was observed upon anti-CREB antibody addition. Since Ser^{133} CREB phosphorylation results in the recruitment of CREB Binding Protein (CBP) and zinc-induced CREB phosphorylation occurs strongly by 2 hours, antibodies directed against CBP were tested, however no differences in bands B or C were observed (data not shown). There are several possible explanations for these results. They potentially indicate that band B either did not contain CREB or CBP, or the epitope the antibodies recognized may be buried or masked by the binding of other proteins. Band B might also be a CREB family member since this band resulted from the binding of a CRE specific probe but not the mutant probe suggesting specificity for the CRE. Additionally, the results of the antibody supershift did not rule out the possibility that the lowest mobility band was not complex B supershifted and that complex A has moved up to an overlapping position with the addition of the antibody. Overall there was a clear increase in the CRE specific DNA binding of band B and a reduction in mobility of both band B and CREB containing band C consistent with Ser^{133} phosphorylation of CREB by 2 hours which indicated CREB or a CRE specific binding protein may be

active in these cells in response to zinc treatment. Together, the results (**Figure 3-2**) suggest that addition of zinc to S49 cells and thymocytes vigorously transactivate the CREB protein, as determined by phosphorylation status, while the EMSA experiments (**Figure 3-3**) illustrate increased capacity for DNA binding by CREB family members concurrent with zinc treatment and potential changes in gene expression.

Zinc pyrithione treatment of S49 WT cells induced the proapoptotic BH3 only Bcl-2 family member Bim.

At this point we have demonstrated that zinc activated the cAMP-PKA signal transduction pathway with resultant the strong phosphorylation of CREB (**Figure 3-2A**). We have previously demonstrated in mouse thymocytes that zinc-induced apoptosis required transcription and translation which indicated potential regulation by the increase or induction in the expression of genes which might include proapoptotic proteins (22). We identified the proapoptotic BH3 only Bcl-2 family member Bim as one gene that was up-regulated during zinc-induced apoptosis in mouse thymocytes (22). To verify Bim was also up-regulated in S49 WT cells in response to zinc treatment, cells as shown in **Figure 3-4A and 3-4B** were treated with zinc pyrithione (400nM) for indicated times 0, 2, 4, or 8 hours and concurrent samples were assessed by Real Time PCR analysis or Western blot analysis. Real Time PCR analysis demonstrated a 2.6 fold increase in Bim mRNA by 2 hours with a 3.4 fold increase by 4 hours and a 5 fold increase by 8 hours in response to zinc treatment. The increase in Bim mRNA correlated well with the protein expression of BimEL as demonstrated by Western blot analysis of concurrent samples shown in **Figure 3-4B** where a 3.8 fold increase was observed by 2 hours and an 8.3 fold

increase in Bim was observed by 8 hours. Additionally, the induction of Bim was preceded by the activation of the cAMP-PKA signal transduction pathway and CREB phosphorylation. In contrast to the increase observed in BimEL protein levels over an 8 hour time course no increase in Bax, Bcl-2 or Bcl-xL was observed thus demonstrating the specificity of Bim induction during apoptosis. Equal loading of all lanes was verified by β-actin.

The above data correlates well with the known function of Bim as a major physiological antagonist of prosurvival proteins like Bcl-2 or Bcl-xL in hematopoietic cells (1). In order to determine whether the induction of Bim was a general event involved with apoptosis or induced specifically during zinc mediated apoptosis S49 WT cells, as shown in **Figure 3-4C,** were treated with zinc pyrithione (400nM), anti-Fas (500ng/ml) antibody plus actinomycin D (25ng/ml), etoposide (100μM) or were untreated for four hours. A Western blot was performed for the detection of Bim while equal loading was verified with β-actin. The induction of Bim was only observed in the zinc pyrithione (400nM) treated cells in contrast to the anti-Fas or etoposide treated cells which confirmed that Bim was specifically induced by zinc treatment. Overall the data presented herein demonstrated that zinc activated the cAMP-PKA signal transduction pathway and induced apoptosis in these cells in part through the up-regulation of the proapoptotic protein Bim.

Figure 3-4: Zinc-induced proapoptotic Bim expression.
S49 WT cells were incubated with zinc pyrithione (400nM) for indicated times (0-8 hours) and concurrent treated samples were prepared either for Real Time PCR analysis for mRNA expression or for Western blot analysis of the BH3 only Bcl-2 proapoptotic family member Bim. **A**) A 5 fold increase in Bim mRNA levels (normalized to β-actin) was observed by 8 hours. A vehicle control demonstrated no increase in Bim mRNA levels. **B**) Western blot analysis demonstrated an increase in Bim protein levels in response to zinc treatment in S49 WT cells correlating with the observed increase in Bim mRNA levels. Bax, Bcl-2 and Bcl-xL levels were unchanged which demonstrated that Bim was specifically induced in response to zinc. Equal loading of all lanes was verified with β-actin. **C**) In order to demonstrate the specific induction of Bim in response to zinc treatment but not other inducers of apoptosis S49 WT cells were treated with zinc pyrithione (400nM), α-Fas (500ng/ml) antibody plus actinomycin D (25ng/ml), or Etoposide (100μM) or untreated for 4 hours and samples processed for Western blot analysis for Bim expression.

A

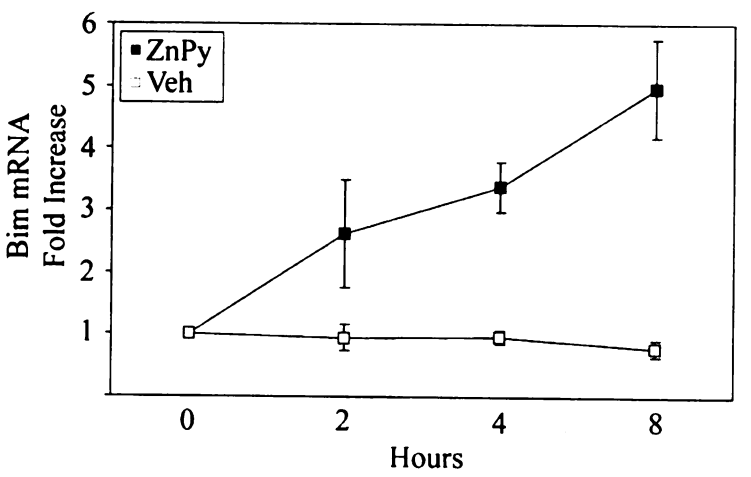
ZnPy
Veh
Bim mRNA
Fold Increase
6
5
4
3
2
1
0
2
4
8
Hours

B

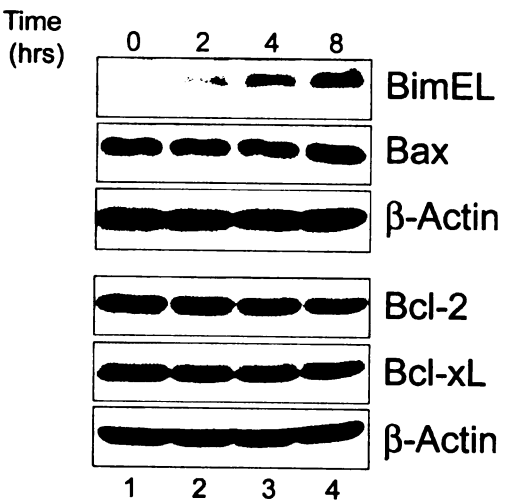
Time
(hrs)
0
2
4
8
BimEL
Bax
β-Actin
Bcl-2
Bcl-xL
β-Actin
1
2
3
4

C

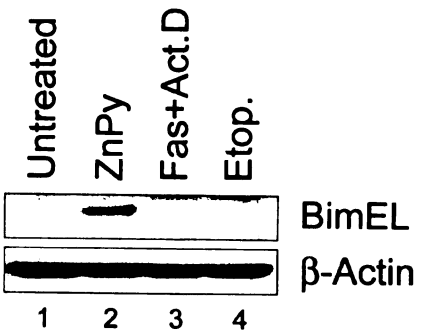
Untreated
ZnPy
Fas+Act.D
Etop.
BimEL
β-Actin
1
2
3
4

CREB is recruited to the Bim promoter *in vivo* in response to zinc treatment.

Thus far, evidence for both the activation of the cAMP signaling pathway resulting in CREB activation and evidence for up-regulation of a potential transcriptional target, Bim have been provided. The next obvious step was to study the convergence of these two results by determining whether CREB directly targets Bim, modifying its gene expression during zinc induced apoptosis. One powerful tool for analyzing *in vivo* targets of transcription factors is chromatin immunoprecipitation (ChIP). These assays directly assess whether a factor is associated with the DNA and chromatin structure at the promoter of a gene of interest. Briefly, S49 WT cells are treated with 400 nM zinc pyrithione for the indicated time and then treated with formaldehyde to covalently crosslink proteins to proteins and proteins to DNA. The cells are then treated with a combination of microccocal nuclease digestion and sonication to fragment and solubilize the genomic DNA resulting in fragments approximately 500-1000 bp in length. This soluble chromatin was then immunoprecipitated with antibodies specific to CREB. These immunoprecipitations isolated both the CREB protein and any associated DNA fragments to which CREB is bound. These isolated DNA fragments were then purified and analyzed by Real Time PCR using primers specific to the Bim promoter as well as primers to β-actin as a measure of non-specific background binding. The data obtained was then used to calculate Bim promoter occupancy as a measure of fold over background (Bim/β-actin). As shown in **Figure 3-5**, CREB occupancy increased approximately 2-fold at the Bim promoter over time after zinc treatment which also closely correlated with the observed increase in cAMP levels shown in **Figure 3-1D**. Overall, the increase in CREB occupancy at the Bim promoter demonstrated a direct link

Figure 3-5: CREB directly targets the Bim promoter *in vivo* during zinc apoptosis. In order to determine whether CREB binds to the Bim promoter, chromatin immunoprecipitations were preformed. S49 WT cells were treated with 400 nM zinc pyrithione for the indicated time before crosslinking with formaldehyde. Genomic DNA was fragmented, solubilized and immunoprecipitated with α-CREB antibodies. Recovered DNA was analyzed by Real Time PCR using primers specific to the CREB promoter as well as primers to β-actin exon three. The data in this graph represents CREB binding as a function of fold over background (β-actin) binding.

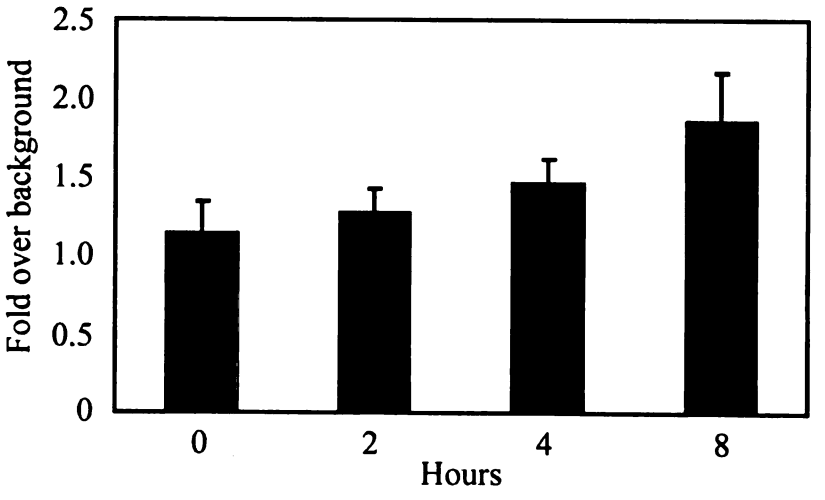
2.5
2.0
1.5
1.0
0.5
0
Fold over background
0
2
4
8
Hours

between the cAMP signaling pathway and the up-regulation of the proapoptotic pathway via Bim.

Discussion

Although zinc has been shown to induce apoptosis, the signaling events had not been established, therefore the present study was undertaken. The adenylate cyclase inhibitor SQ22536 reduced zinc-mediated apoptosis in mouse thymocytes which indicated potential regulation by the cAMP-PKA signaling pathway. It seemed a probable player since cAMP had been shown to induce apoptosis in a variety of cell types from mouse thymocytes and human $CD10^+$ B-precursor cells as well as renal mesangial cells and ovarian cancer cells (20, 23, 25, 27, 32, 35, 42). Therefore additional analysis of this signaling pathway was initiated. As discussed, we took advantage of a genetic model available using S49 WT cells underwent 51% apoptosis in response to zinc pyrithione treatment. It has variant cell lines S49 Cyc^- (19%) and S49 Kin^- (21%) that were less susceptible due to the deficiencies in the cAMP-PKA signaling pathway. However, the variant cell lines could still undergo apoptosis in response to other inducers therefore demonstrating that it was in fact the cAMP-PKA signaling pathway involved in zinc-induced apoptosis. While PKA is the primary and most well-known effector of cAMP other effectors have been identified (40). If another cAMP effector was indeed involved in zinc-induced apoptosis then the S49 Kin^- cells, which are deficient in PKA activity (37), should have been as susceptible as the S49 WT cells to zinc-induced apoptosis. Since they were not, it was further evidence of key involvement of the cAMP-PKA pathway during zinc-induced apoptosis.

While the increase in cAMP herein was sustained it was moderate in concentration. Nevertheless other studies have also shown that small changes in cAMP levels were able to affect biological processes (16, 18). For example during membrane depolarization in PC12 cells a Ca^{2+} influx stimulated a modest increase (40-80%) in cAMP levels which led to PKA activation that enhanced or synergized with other signaling events (16, 18). The moderate increase in cAMP, up to 2 fold by 6 hours, observed in S49 WT cells was enough to activate the PKA signaling pathway that contributed to the induction of apoptosis as demonstrated in **Figure 3-1B** where cells that lacked the fully functional cAMP-PKA signaling pathway were less susceptible to zinc-induced apoptosis. Activation of PKA was confirmed by the prolonged and intense phosphorylation of CREB on Ser^{133}. However, the phosphorylation of CREB on Ser^{133} could also result from other signaling pathways (33). If a PKA independent signaling pathway was responsible for the phosphorylation of CREB then phosphorylation should have occurred in response to zinc treatment in the variant cell lines, which was not observed confirming that the phosphorylation in the WT cells was due to PKA activity. Thus, the data presented in this paper clearly demonstrated that the cAMP signal transduction pathway was important and actively involved in zinc-induced apoptosis in these cells.

Activation of the cAMP-PKA signal transduction pathway was further exemplified in the results of the EMSA which demonstrated an increased capacity for DNA binding by CREB or a CRE specific binding protein in response to zinc treatment. This corresponded with increased transactivation potential of CREB, as determined by

phosphorylation status, which would lead to the increased transcription of target genes (33). One target gene we identified in mouse thymocytes as being transcriptionally regulated in response to zinc treatment was the BH3 only Bcl-2 family member Bim (22). Bim has been shown to function through the neutralization of prosurvival proteins such as Bcl-2 or Bcl-xL thereby allowing other proapoptotic proteins such as Bax to initiate the intrinsic mitochondrial apoptotic caspase cascade (2, 28). In the zinc treated S49 WT cell line we observed an ~5 fold increase in Bim mRNA levels by 8 hours and an ~8 fold increase in BimEL isoform was observed. This data was consistent with our previous findings that this proapoptotic BH3 only Bcl-2 family member was induced in response to zinc.

The induction of Bim and apoptosis occurred relatively quickly in response to zinc in S49 WT cells (12 hours). This is in contrast to the data presented by *Zhang and Insel* (46) where the induction of apoptosis in response to glucocorticoids and cAMP treatment was slower (24-48 hours) in S49 WT cells. Additionally they showed that cAMP treatment failed to induce any apoptosis in the S49 Kin^- cell line (46) which demonstrated that only the PKA pathway was involved in cAMP mediated apoptosis in this cell line. However, as shown herein, zinc treatment (400nM) induced ~20% apoptosis in the variant cell lines after 12 hours while spontaneous apoptosis was ~5%. Additionally, the differences in the timeframe and the susceptibility of the variant cell lines between zinc treatment and direct cAMP treatment (46) could indicate the additional utilization of other unidentified signaling pathways. *Zhang and Insel* also demonstrated a close correlation between Bim expression and apoptosis that was consistent with the idea that Bim mediated cAMP

induced apoptosis in S49 WT cells (46). Consistent with this concept our results demonstrated that zinc utilized the cAMP-PKA signaling pathway and strongly induced Bim in S49 WT cells during apoptosis. Furthermore, our chromatin immunoprecipitation data demonstrated a direct link between the cAMP signal transduction pathway CREB phosphorylation and expression of Bim. Finally, our data was also consistent with a recent large scale genome-wide analysis of CREB targets that identified a number of novel CREB targets including Bim (17).

Activation of the signaling pathways in response to zinc treatment resulted in a strong increase in BimEL levels in S49 WT cells and since Bim functions by neutralizing prosurvival proteins an increase in Bim with no change in Bcl-2 or Bcl-xL levels would shift the cells fate from survival towards apoptotic cell death as was observed herein. As previously demonstrated overexpression of Bcl-2 or Bcl-xL protected cells from zinc induced apoptosis (22). This data taken together further implicates the involvement of Bim during zinc-induced apoptosis and may be part of the reason zinc is such a potent cell death inducer. A unique role for Bim has been demonstrated in lymphocytes where in response to cytokine withdrawal or treatment with taxol *bim*$^{-/-}$ pre-T cells survived 10-30 times better than wild type cells (1). We demonstrated that Bim was specifically induced in response to zinc treatment during apoptosis in S49 WT cells. Collectively the data also illustrated that the signaling pathways (cAMP-PKA) activated by zinc were distinctive from the pathways utilized by etoposide or activation of the Fas pathway since Bim was not induced in response to these apoptotic cues.

Whether it is a result of industrial exposure, over-supplementation, or released from damaged cells, exposure to excess zinc had detrimental effects on a range of cell types from neuronal and lung to prostate as well as cells of the immune system. However, identification of the signal transduction pathways activated in response to zinc prior to our studies had been insufficient. We demonstrated the intrinsic mitochondrial apoptotic signaling pathway was utilized during zinc-induced apoptosis in cells of the immune system (22) though the signaling pathway leading to activation of this death pathway still remained unknown. This report demonstrated that zinc was utilizing the cAMP-PKA signaling pathway in cells of the immune system resulting in the induction of Bim. Overall, the data presented herein significantly enhances the current knowledge of the signaling pathways and target genes involved in zinc-induced apoptosis in cells of the immune system.

While we have clearly demonstrated utilization of the cAMP signaling pathway by zinc other unknown pathways may also contribute to apoptosis. In addition to cAMP signaling we have identified another pathway that is activated in response to zinc treatment in mouse thymocytes and S49 WT cells. This other signaling pathway is the NF-κB signaling pathway. Data demonstrating activation of the NF-κB signaling pathway in response to zinc stimulation will be discussed in the following chapter.

References

1. **Bouillet, P., D. Metcalf, D. C. Huang, D. M. Tarlinton, T. W. Kay, F. Kontgen, J. M. Adams, and A. Strasser.** 1999. Proapoptotic Bcl-2 relative Bim required for certain apoptotic responses, leukocyte homeostasis, and to preclude autoimmunity. Science **286:**1735-8.

2. **Bouillet, P., and A. Strasser.** 2002. BH3-only proteins - evolutionarily conserved proapoptotic Bcl-2 family members essential for initiating programmed cell death. J Cell Sci **115:**1567-74.

3. **Bourne, H. R., P. Coffino, and G. M. Tomkins.** 1975. Somatic genetic analysis of cyclic AMP action: characterization of unresponsive mutants. J Cell Physiol **85:**611-20.

4. **Chen, C. J., and S. L. Liao.** 2003. Zinc toxicity on neonatal cortical neurons: involvement of glutathione chelation. J Neurochem **85:**443-53.

5. **Chesters, J. K.** 1997. Zinc, p. 185-230. *In* B. L. S. O'Dell, Roger Allan (ed.), Handbook of nutritionally essential mineral elements. Marcel Dekker, New York.

6. **Choi, D. W., and J. Y. Koh.** 1998. Zinc and brain injury. Annu Rev Neurosci **21:**347-75.

7. **Coffino, P., H. R. Bourne, and G. M. Tomkins.** 1975. Somatic genetic analysis of cyclic AMP action: selection of unresponsive mutants. J Cell Physiol **85:**603-10.

8. **Dardenne, M.** 2002. Zinc and immune function. Eur J Clin Nutr **56 Suppl 3:**S20-3.

9. **Dreosti, I. E.** 2001. Zinc and the gene. Mutat Res **475:**161-7.

10. **Feng, P., T. L. Li, Z. X. Guan, R. B. Franklin, and L. C. Costello.** 2002. Direct effect of zinc on mitochondrial apoptogenesis in prostate cells. Prostate **52:**311-8.

11. **Feng, P., J. Y. Liang, T. L. Li, Z. X. Guan, J. Zou, R. Franklin, and L. C. Costello.** 2000. Zinc induces mitochondria apoptogenesis in prostate cells. Mol Urol **4:**31-6.

12. **Frederickson, C. J., and A. I. Bush.** 2001. Synaptically released zinc: physiological functions and pathological effects. Biometals **14:**353-66.

13. **Frederickson, C. J., W. Maret, and M. P. Cuajungco.** 2004. Zinc and excitotoxic brain injury: a new model. Neuroscientist **10:**18-25.

14. **Hurley, J. H.** 1999. Structure, mechanism, and regulation of mammalian adenylyl cyclase. J Biol Chem **274:**7599-602.

15. **Iitaka, M., S. Kakinuma, S. Fujimaki, I. Oosuga, T. Fujita, K. Yamanaka, S. Wada, and S. Katayama.** 2001. Induction of apoptosis and necrosis by zinc in human thyroid cancer cell lines. J Endocrinol **169:**417-24.

16. **Impey, S., and R. H. Goodman.** 2001. CREB signaling--timing is everything. Sci STKE **2001:**PE1.

17. **Impey, S., S. R. McCorkle, H. Cha-Molstad, J. M. Dwyer, G. S. Yochum, J. M. Boss, S. McWeeney, J. J. Dunn, G. Mandel, and R. H. Goodman.** 2004. Defining the CREB regulon: a genome-wide analysis of transcription factor regulatory regions. Cell **119:**1041-54.

18. **Impey, S., K. Obrietan, S. T. Wong, S. Poser, S. Yano, G. Wayman, J. C. Deloulme, G. Chan, and D. R. Storm.** 1998. Cross talk between ERK and PKA is required for Ca2+ stimulation of CREB-dependent transcription and ERK nuclear translocation. Neuron **21:**869-83.

19. **Johnson, G. L., H. R. Kaslow, Z. Farfel, and H. R. Bourne.** 1980. Genetic analysis of hormone-sensitive adenylate cyclase. Adv Cyclic Nucleotide Res **13:**1-37.

20. **Kizaki, H., H. Shimada, F. Ohsaka, and T. Sakurada.** 1988. Adenosine, deoxyadenosine, and deoxyguanosine induce DNA cleavage in mouse thymocytes. J Immunol **141:**1652-7.

21. **Laakko, T., L. King, and P. Fraker.** 2002. Versatility of merocyanine 540 for the flow cytometric detection of apoptosis in human and murine cells. J Immunol Methods **261:**129-39.

22. **Mann, J. J., and P. J. Fraker.** 2005. Zinc pyrithione induces apoptosis and increases expression of Bim. Apoptosis **10:**369-379.

23. **McConkey, D. J., S. Orrenius, and M. Jondal.** 1990. Agents that elevate cAMP stimulate DNA fragmentation in thymocytes. J Immunol **145:**1227-30.

24. **Montminy, M.** 1997. Transcriptional regulation by cyclic AMP. Annu Rev Biochem **66:**807-22.

25. **Muhl, H., D. Nitsch, K. Sandau, B. Brune, Z. Varga, and J. Pfeilschifter.** 1996. Apoptosis is triggered by the cyclic AMP signalling pathway in renal mesangial cells. FEBS Lett **382:**271-5.

26. **Muthusamy, N., and J. M. Leiden.** 1998. A protein kinase C-, Ras-, and RSK2-dependent signal transduction pathway activates the cAMP-responsive element-binding protein transcription factor following T cell receptor engagement. J Biol Chem **273:**22841-7.

27. **Myklebust, J. H., D. Josefsen, H. K. Blomhoff, F. O. Levy, S. Naderi, J. C. Reed, and E. B. Smeland.** 1999. Activation of the cAMP signaling pathway increases apoptosis in human B-precursor cells and is associated with downregulation of Mcl-1 expression. J Cell Physiol **180:**71-80.

28. **Opferman, J. T., and S. J. Korsmeyer.** 2003. Apoptosis in the development and maintenance of the immune system. Nat Immunol **4:**410-5.

29. **Paramanantham, R., K. H. Sit, and B. H. Bay.** 1997. Adding Zn^{2+} induces DNA fragmentation and cell condensation in cultured human Chang liver cells. Biol Trace Elem Res **58:**135-47.

30. **Prasad, A.** 2002. Zinc, Infection and Immune Function, Frontiers in Nutritional Science, No. 1 ed. CAB International 2002, University of Southampton, UK, University of Alberta, Canada, Massey University, New Zealand.

31. **Ryu, R., Y. Shin, J. W. Choi, W. Min, H. Ryu, C. R. Choi, and H. Ko.** 2002. Depletion of intracellular glutathione mediates zinc-induced cell death in rat primary astrocytes. Exp Brain Res **143:**257-63.

32. **Sasson, R., V. Shinder, A. Dantes, A. Land, and A. Amsterdam.** 2003. Activation of multiple signal transduction pathways by glucocorticoids: protection of ovarian follicular cells against apoptosis. Biochem Biophys Res Commun **311:**1047-56.

33. **Shaywitz, A. J., and M. E. Greenberg.** 1999. CREB: a stimulus-induced transcription factor activated by a diverse array of extracellular signals. Annu Rev Biochem **68:**821-61.

34. **Sheline, C. T., M. M. Behrens, and D. W. Choi.** 2000. Zinc-induced cortical neuronal death: contribution of energy failure attributable to loss of NAD(+) and inhibition of glycolysis. J Neurosci **20:**3139-46.

35. **Srivastava, R. K., A. R. Srivastava, Y. S. Cho-Chung, and D. L. Longo.** 1999. Synergistic effects of retinoic acid and 8-Cl-cAMP on apoptosis require caspase-3 activation in human ovarian cancer cells. Oncogene **18:**1755-63.

36. **Steinberg, R. A.** 1991. A kinase-negative mutant of S49 mouse lymphoma cells is defective in posttranslational maturation of catalytic subunit of cyclic AMP-dependent protein kinase. Mol Cell Biol **11:**705-12.

37. **Steinberg, R. A., T. van Daalen Wetters, and P. Coffino.** 1978. Kinase-negative mutants of S49 mouse lymphoma cells carry a trans- dominant mutation affecting expression of cAMP-dependent protein kinase. Cell **15:**1351-61.

38. **Suh, S. W., J. W. Chen, M. Motamedi, B. Bell, K. Listiak, N. F. Pons, G. Danscher, and C. J. Frederickson.** 2000. Evidence that synaptically-released zinc contributes to neuronal injury after traumatic brain injury. Brain Res **852:**268-73.

39. **Suh, S. W., R. B. Thompson, and C. J. Frederickson.** 2001. Loss of vesicular zinc and appearance of perikaryal zinc after seizures induced by pilocarpine. Neuroreport **12:**1523-5.

40. **Tasken, K., and E. M. Aandahl.** 2004. Localized effects of cAMP mediated by distinct routes of protein kinase A. Physiol Rev **84:**137-67.

41. **Telford, W. G., and P. J. Fraker.** 1995. Preferential induction of apoptosis in mouse $CD4^{+}CD8^{+}\alpha\beta TCR^{lo}CD3\varepsilon^{lo}$ thymocytes by zinc. J Cell Physiol **164:**259-70.

42. **Thompson, E. B., R. D. Medh, F. Zhou, S. Ayala-Torres, N. Ansari, W. Zhang, and B. H. Johnson.** 1999. Glucocorticoids, oxysterols, and cAMP with glucocorticoids each cause apoptosis of CEM cells and suppress c-myc. J Steroid Biochem Mol Biol **69:**453-61.

43. **Walsh, C. T., H. H. Sandstead, A. S. Prasad, P. M. Newberne, and P. J. Fraker.** 1994. Zinc: health effects and research priorities for the 1990s. Environ Health Perspect **102 Suppl 2:**5-46.

44. **Walther, U. I., A. Czermak, H. Muckter, S. C. Walther, and B. Fichtl.** 2003. Decreased GSSG reductase activity enhances cellular zinc toxicity in three human lung cell lines. Arch Toxicol **77:**131-7.

45. **Walther, U. I., B. Wilhelm, S. Walther, H. Muckter, and B. Fichtl.** 2000. Zinc toxicity in various lung cell lines is mediated by glutathione and GSSG reductase activity. Biol Trace Elem Res **78:**163-77.

46. **Zhang, L., and P. A. Insel.** 2004. The Pro-apoptotic Protein Bim Is a Convergence Point for cAMP/Protein Kinase A- and Glucocorticoid-promoted Apoptosis of Lymphoid Cells. J Biol Chem **279:**20858-65.

Chapter 4

The NF-κB signal transduction pathway is activated during zinc-induced apoptosis

Abstract

As discussed in Chapter 2 and Chapter 3, zinc-induced apoptosis utilized the cAMP-PKA signal transduction pathway leading to the induction of the proapoptotic protein Bim and activation of the mitochondrial caspase cascade. However, additional signaling pathways could contribute to the induction of apoptosis. As will be shown herein, the NF-κB signaling pathway was activated in response to zinc treatment. Treatment of mouse thymocytes with curcumin, an anti-inflammatory agent that inhibits NF-κB signaling, blocked zinc-induced apoptosis. Additionally, IκBα degradation occurred in response to zinc treatment in mouse thymocytes as well as in S49 WT cells. Activation of the NF-κB signaling pathway was further verified and demonstrated by an increase in DNA binding of a ^{32}P-labeled NF-κB specific DNA probe in response to zinc treatment. Overall, zinc induced the activation of this additional signaling pathway which could contribute to the induction of apoptosis.

Introduction

As shown in Chapter 2, zinc-induced apoptosis in various cells of the immune system and resulted in the induction of the proapoptotic protein Bim in mouse thymocytes. As further demonstrated in Chapter 3 zinc-induced apoptosis clearly utilized the cAMP-PKA signal transduction pathway resulting in the induction of the proapoptotic protein Bim. S49 WT cells underwent 51% apoptosis in response to zinc pyrithione (400nM) treatment as shown in the Figure 3-1B. The variant cell lines S49 Cyc^- (19%) and S49 Kin^- (21%) were less susceptible due to their deficiencies in the cAMP-PKA signaling pathway. However, since these variant cell lines underwent ~20% apoptosis in response to zinc treatment, the potential involvement of other signaling pathways in addition to the cAMP-PKA pathway could not be ruled out.

As will be demonstrated herein, the NF-κB signaling pathway was activated in response to zinc treatment. The NF-κB signal transduction pathway has important roles in normal immune and inflammatory responses as well as in cell proliferation, differentiation and apoptosis (5). Depending upon cellular context, NF-κB can act as either a prosurvival or proapoptotic factor (5, 6). NF-κB is sequestered in the cytoplasm of the cell bound by its inhibitor IκBα in an inactive complex. Activation of this pathway, as illustrated in Figure 1-6, occurs when IκBα is phosphorylated by the IKK complex and marked for ubiquitin-mediated degradation. Degradation of IκBα releases the inactive NF-κB heterodimer which translocate to the nucleus and activates transcription of target genes (5). Additionally, phosphorylation of NF-κB p65 on Ser^{276} by the catalytic subunit of

PKA results in its increased transactivation potential (15). Therefore, this may be a potential site of cross talk between these two signaling pathways.

A proapoptotic role for NF-κB was demonstrated in one study where a transgenic mouse model was used that expressed a super-inhibitory mutant form of IκBα that cannot be phosphorylated at Ser^{32} and Ser^{36} that mark it for degradation (4). Thus NF-κB was kept inactively sequestered in the cytoplasm. This study demonstrated that NF-κB proteins were necessary for $CD4^+/CD8^+$ thymocyte apoptosis in response to α-CD3 treatment *in vivo* (4). Moreover, a proapoptotic role for the activation of NF-κB was also demonstrated in retinal pericytes in response to diabetes or high glucose (8). Additionally, the proapoptotic proteins Fas and FasL have been shown to be direct targets of NF-κB (2, 3, 7, 9). Depending upon the cellular context, NF-κB can function as a proapoptotic factor that includes cells of the immune system.

As will be shown herein, treatment of mouse thymocytes with curcumin blocked zinc-induced apoptosis. Curcumin is an agent with anti-inflammatory and antioxidant properties that has been shown to block TNF-α as well as hydrogen peroxide induced activation of NF-κB (1, 11, 12). Since curcumin inhibited zinc-induced apoptosis in thymocytes and has been shown to block NF-κB activation in response to other inducers, a potential role for NF-κB signaling in response to zinc was investigated. As will be shown, zinc treatment resulted in IκBα degradation in both thymocytes as well as S49 WT cells. Additionally, increased NF-κB DNA binding activity was observed in response to zinc treatment in S49 WT cells as assessed by an electrophoretic mobility

shift assay. The results provided herein will demonstrate that zinc activated the NF-κB signaling pathway during apoptosis, which in addition to the cAMP-PKA signaling pathway may be utilized by zinc during the induction of the proapoptotic protein Bim. However, a direct link between NF-κB and Bim has not been established being a subject of future investigation by our laboratory.

Materials and Methods

The methods and materials utilized herein were essentially the same as those described in Chapter 2 and Chapter 3. Differences and additions are noted below.

Materials

Curcumin was obtained from Calbiochem (La Jolla, Ca.). Antibodies directed against NF-κB and Oct1 were obtained from Santa Cruz Biotech (Santa Cruz, Ca.), and antibodies directed against Oct-1 were obtained from Stressgen (San Diego, Ca.). The remaining materials used are already described in Chapter 2 and Chapter 3.

Electrophoretic mobility shift assay:

Complementary oligonucleotides containing either a specific NF-κB site (CTAGAAGTTGAGGGGACTTTCCCAGGCG-forward, GATCCGCCTGGGAAAGTCCCCTCAACTT-reverse) or ***mutant*** NF-κB site (CTAGAAGTTGAGG***C***GACTTTCCCAGGCG-forward, GATCCGCCTGGGAAAGTCGCCTCAACTT-reverse) were annealed and inserted into

the pUC119 plasmid using XbaI and BamHI sites. The same methods as discussed in Chapter 3 were used for the generation of the probe containing the NF-κB site. Nuclear extract was prepared as per manufacturer instructions for the NE-PER kit (Pierce). The same nuclear extracts utilized in these experiments were also used in the CRE EMSA experiments in Chapter 3. Reactions containing 10μg nuclear extract were incubated for 30 min at room temperature after which 20,000 cpm of probe (NF-κB) was added, and reactions were incubated an additional 30 min. For supershift analysis 2μg of antibody directed against NF-κB p65, p50, or a non-specific control antibody was incubated in the reaction mixture for 30 min at room temperature after which probe was added, and reactions were incubated an additional 30 min. Samples were fractionated on a 5% non-denaturing polyacrylamide gel (39:1) in TGE running buffer (50 mM Tris, 380 mM glycine, 2 mM EDTA). Gels were dried and exposed to film in the presence of an intensifying screen at -80°C for visualization.

Results

Treatment of mouse thymocytes with curcumin blocks zinc-induced apoptosis.

Other potential signaling pathways may be involved in zinc-induced apoptosis besides the cAMP-PKA pathway. Therefore, curcumin, which has anti-inflammatory and antioxidant properties that have been shown to block the NF-κB signaling pathway, was tested. As shown in Figure 4-1, treatment of mouse thymocytes with indicated concentrations of curcumin blocked zinc pyrithione (400nM) induced apoptosis. Dexamethasone was additionally used as a positive control for the induction of apoptosis

Figure 4-1: Curcumin blocks zinc-induced apoptosis in mouse thymocytes.
Curcumin, an anti-inflammatory agent that inhibits activation of the NF-κB signaling pathway, blocked zinc-induced apoptosis in mouse thymocytes. Mouse thymocytes were preincubated with curcumin (10 or 30 μM) for one hour prior to the addition of zinc pyrithione (400nM) or dexamethasone (1 μM). Apoptosis was measured after eight hours in culture.

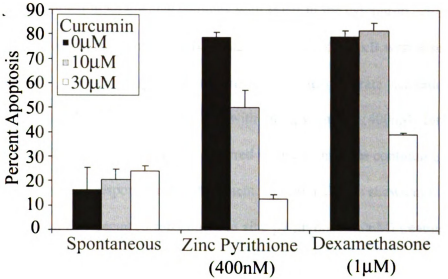
Curcumin
0μM
10μM
30μM
Percent Apoptosis
90
80
70
60
50
40
30
20
10
0
Spontaneous
Zinc Pyrithione
(400nM)
Dexamethasone
(1μM)

in thymocytes. Since curcumin has been shown to block NF-κB signaling this result potentially indicated that the NF-κB signaling pathway was utilized during zinc-induced apoptosis. However, further evidence of the utilization of this pathway was needed. Therefore, Western blot analysis of IκBα was undertaken.

IκBα was degraded in response to zinc treatment.

NF-κB is sequestered in an inactive complex with IκBα in the cytoplasm. Activation of this pathway results in the degradation of IκBα and release of NF-κB with translocates to the nucleus and activates target genes. In order to demonstrate activation of this signaling pathway thymocytes were treated with zinc pyrithione (400nM) for indicated times (Figure 4-2A). IκBα degradation occurred within 15 minutes continuing through 2 hours in thymocytes in response to zinc treatment. Additionally, as shown in Figure 4-2B IκBα degradation also occurred subsequent to zinc pyrithione (400nM) treatment in S49 WT cells. However, in the cell line degradation began between 2 and 4 hours extending to 8 hours. Overall this data demonstrated activation of the NF-κB signaling pathway in response to zinc treatment in both thymocytes and S49 WT cells. To further investigate activation of this pathway an EMSA was performed.

An increase in the binding of a ^{32}P-labeled NF-κB specific DNA probe occurred upon treatment with zinc.

An EMSA, shown in Figure 4-3, demonstrated an increase in DNA binding of a ^{32}P-labeled NF-κB specific DNA probe in response to zinc (400nM) treatment. A strong increase in the top band (p65) was observed within 15 minutes which diminished slightly

Figure 4-2: IκBα degradation was observed in response to zinc treatment.
Degradation of IκBα results in the release and activation of NF-κB. **A)** Mouse thymocytes were treated with zinc pyrithione (400nM) for indicated times (0-2 hours) and samples were processed for Western blot analysis. **B)** S49 WT cells were treated with 400nM zinc pyrithione over the indicated times (0-8 hours) and samples were processed for Western blot analysis.

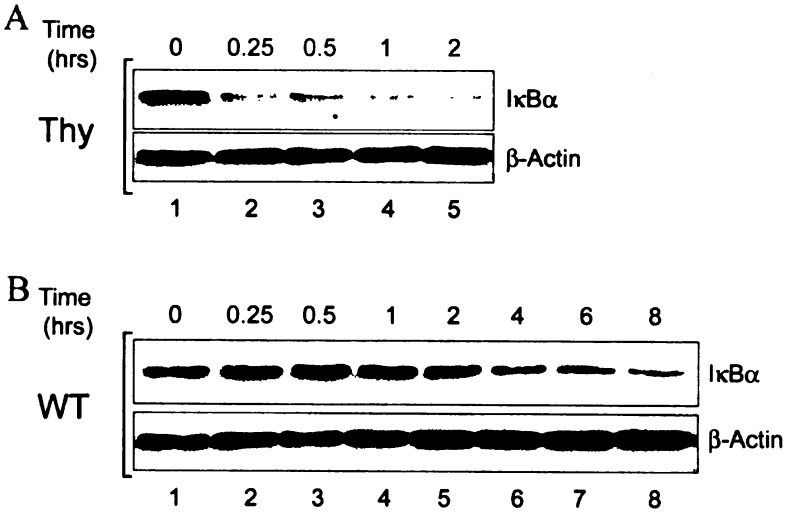
A
Time (hrs)
0 0.25 0.5 1 2
Thy
IκBα
β-Actin
1 2 3 4 5
B
Time (hrs)
0 0.25 0.5 1 2 4 6 8
WT
IκBα
β-Actin
1 2 3 4 5 6 7 8

by 30 minutes while increasing strongly again between 2 and 4 hours. In order to verify that NF-κB was responsible for the increased DNA binding activity observed upon zinc addition a mutant NF-κB DNA probe was tested. In Figure 4-4, Lanes 1-3 show the NF-κB WT probe alone or incubated with nuclear extracts untreated or zinc pyrithione (400nM) treated for four hours. A strong increase in the band labeled p65 was demonstrated in Figure 4-4. Utilization of a mutant NF-κB probe indicated that the bands labeled p50 and p65 were specific for the NF-κB binding site since no bands in this area appear in lanes 5-7. However a band does appear in both the NF-κB and mutant NF-κB probe indicating this band was due to a non-specific (ns) DNA binding event. In order to determine whether NF-κB was part of the two DNA complexes that occurred after 4 hours of zinc treatment antibodies directed against NF-κB were added as shown in **Figure 4-4**. Antibodies directed against the p65 subunit supershifted the upper band shown in lane 7, while antibodies directed against the p50 subunit of NF-κB supershifted the lower band in lane 8. This definitively indicated that these NF-κB proteins (p65/p50) were part of the DNA binding complexes. An isotype control antibody (IgG) was also tested (lane 9) to demonstrate the result observed with the NF-κB antibodies were specific and not a general effect of antibody addition. Overall these experiments indicated that NF-κB was active in response to zinc treatment.

The purity of the nuclear extracts used in the EMSA was verified by Western blot.

In order to verify that the results observed in the EMSA was due to nuclear NF-κB activity a Western blot was performed as shown in **Figure 4-5**. Hsp90, a cytoplasmic protein, and Oct1, a nuclear protein, were used to verify the purity of the samples used in

Figure 4-3: The NF-κB signaling pathway was activated in response to zinc pyrithione treatment as demonstrated by EMSA. An EMSA of a NF-κB specific ^{32}P-labeled probed was performed using nuclear extracts derived from zinc pyrithione (400nM) treated S49 WT cells over the indicated times (0-8 hours). Lane 1 demonstrated free probe without incubation with nuclear extract. Lane 2-8 demonstrated the DNA binding activity of nuclear extract from zinc treated S49 WT cells. Two bands labeled ns (non specific) or p50 were observed in the untreated 0 hour sample (lane 2). Upon addition of zinc (lanes 3-9) a third band labeled p65 was observed with maximal binding at 4 hours (lane 7).

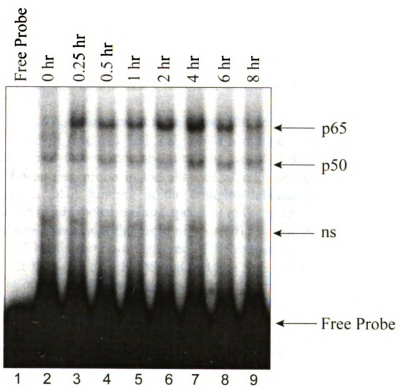
Free Probe
0 hr
0.25 hr
0.5 hr
1 hr
2 hr
4 hr
6 hr
8 hr
p65
p50
ns
Free Probe
1 2 3 4 5 6 7 8 9

Figure 4-4: Identification of the components involved in the NF-κB DNA binding complex analyzed by EMSA.

Samples from the 0 hour and 4 hour time point were chosen for analysis. NF-κB specific ^{32}P-labeled probed was used in lane 1-3 and 7-9, while a mutant ^{32}P-labeled NF-κB probed was used in lanes 4-6 to demonstrate specificity of the DNA binding complex to the NF-κB site. Lane 1 was free probe in the absence of nuclear extract. Lane 2-3 demonstrated an increase in DNA binding of the complex labeled p65. Lanes 5-6 demonstrated binding of the band labeled ns (non specific) to the mutant ^{32}P-labeled NF-κB probed indicating that this band was therefore non specific for the NF-κB site. The binding of the p50 and p65 bands were not observed in the mutant probe demonstrating the required specificity for the wild type NF-κB site. Lane 7 demonstrated the 4 hour sample incubated with an antibody directed against p65 which resulted in a supershift (noted by an *) in the top band indicating that this band contained p65. Lane 8 demonstrated the 4 hour sample incubated with an antibody directed against p50 which produced a supershift (noted by an *) of the band labeled p50. Lane 9 demonstrated a non specific antibody (IgG) failed to shift either band indicating the specificity of the other antibodies used.

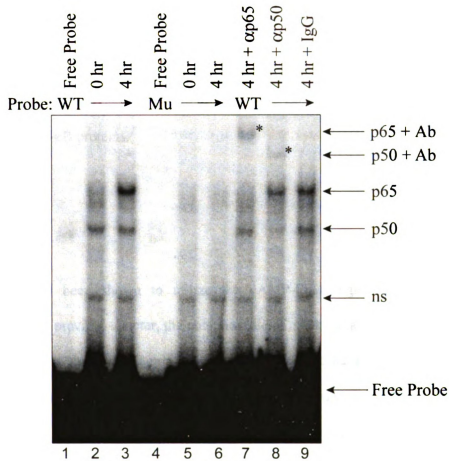
Free Probe
0 hr
4 hr
Free Probe
0 hr
4 hr
4 hr + αp65
4 hr + αp50
4 hr + IgG
Probe: WT
Mu
WT
p65 + Ab
p50 + Ab
p65
p50
ns
Free Probe
1 2 3 4 5 6 7 8 9

the EMSA. Nuclear extracts were prepared using the manufacturer's protocol for the NE-PER extraction kit from Pierce Biotechnology. S49 WT cells were either untreated (0 hr) or treated with zinc pyrithione (400nM) for two hours and samples were prepared. As demonstrated in **Figure 4-5**, the cytoplasmic protein Hsp90 was found in the cytosolic fraction as expected, while the nuclear protein Oct1 was found specifically in the nuclear extract as expected. Overall, these results verify the purity of the nuclear extracts utilized in the EMSA. Thus, the results observed in the NF-κB EMSA were due to nuclear and not cytoplasmic NF-κB proteins.

Discussion

Although zinc has been shown to utilize the cAMP-PKA signaling pathway, as demonstrated in the previous chapter, the potential role of other signaling pathways could not be ruled out. As shown in Figure 4-1, curcumin blocked zinc-induced apoptosis in mouse thymocytes and has been shown to block NF-κB activation normally involved in many inflammatory responses. Therefore, inhibition of apoptosis by curcumin potentially indicated a role for the NF-κB signaling pathway in response to zinc treatment. As demonstrated herein, IκBα was degraded in both mouse thymocytes and S49 WT cells. IκBα degradation in turn results in the release of active NF-κB which translocates to the nucleus resulting in DNA binding and activation of target genes. As shown in Figure 4-3, an increase in the binding of a ^{32}P-labeled NF-κB specific DNA probe occurred in nuclear extracts of S49 WT cells in response to treatment with zinc.

Figure 4-5: Western blot analysis of the purity of nuclear extracts used in the electrophoretic mobility shift assays. Samples shown were prepared from either untreated (0 hr) S49 WT cells or cells treated with zinc pyrithione (400nM) for two hours. Cytoplasmic and nuclear extracts from these cells were prepared and analyzed by Western blot. As expected the nuclear protein Oct1 was observed in the nuclear extract, while the cytosolic protein Hsp90 was located in the cytoplasmic extract thus verifying the purity of the extracts utilized in the EMSA.

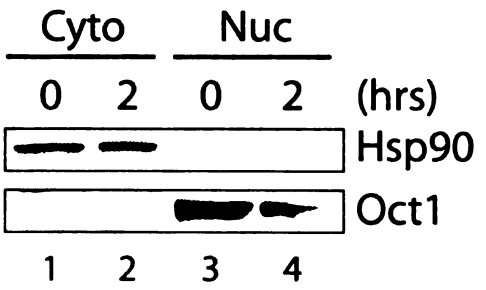
Cyto
Nuc
0
2
0
2
(hrs)
Hsp90
Oct1
1
2
3
4

Overall, this data demonstrated that the NF-κB signaling pathway was activated in response to zinc.

Activation of the NF-κB signaling pathway coincides with the activation of the cAMP signaling pathway in response to zinc. A direct link between activation of the cAMP signaling pathway and the proapoptotic protein Bim has been established, as shown in Chapter 3. Additionally, the Bim promoter potentially contains NF-κB sites. Currently it is a matter of speculation that Bim may function as a point of convergence for both the cAMP and NF-κB signaling pathways in response to zinc treatment. Future work will need to be undertaken to further explore whether Bim is also a direct target of the NF-κB signaling pathway in response to zinc.

Interestingly, another point of convergence for these pathways may include PKA and NF-κB p65 (13, 14). *In vitro* analysis demonstrated that NF-κB could be activated in cytosolic fractions treated with the active catalytic PKA subunit (10). Additionally, when nuclei from unstimulated cells were incubated with PKA treated cytosolic fractions nuclear translocation of NF-κB was observed (10). It has since been demonstrated that the catalytic subunit of PKA phosphorylates NF-κB p65 on Serine 276 (14). Phosphorylation at this site results in increased interaction with CBP/p300 resulting in the increased transactivational potential of p65 (15). Further investigation identified a novel cytoplasmic complex that contained IκBα/NF-κB and the inactive catalytic subunit of PKA (14). Activation of PKA was independent of cAMP in this complex and resulted when degradation of IκBα occurred (14). However, identification of this complex does

not exclude the possibility that NF-κB p65 is a target of PKA activated in response to cAMP.

Exposure to increased levels of zinc has been shown to be detrimental in various situations and in a number of different cell types including neuronal and immune. Until recently the identification of the signaling mechanisms utilized during zinc-induced apoptosis has remained inadequate. As demonstrated in Chapter 2 and Chapter 3, zinc utilized the cAMP-PKA signal transduction pathway leading to the induction of the proapoptotic protein Bim and activation of the caspase cascade resulting in apoptosis. However, the utilization of additional signaling pathways could not be ruled out. As such, activation of the NF-κB signaling pathway was demonstrated herein. Overall, the presented data enhances our understanding of the signaling pathways utilized during zinc-induced apoptosis in cells of the immune system.

References

1. **Bharti, A. C., Y. Takada, and B. B. Aggarwal.** 2004. Curcumin (diferuloylmethane) inhibits receptor activator of NF-kappaB ligand-induced NF-kappaB activation in osteoclast precursors and suppresses osteoclastogenesis. J Immunol **172:**5940-7.

2. **Chan, H., D. P. Bartos, and L. B. Owen-Schaub.** 1999. Activation-dependent transcriptional regulation of the human Fas promoter requires NF-kappaB p50-p65 recruitment. Mol Cell Biol **19:**2098-108.

3. **Chen, X., V. Zachar, M. Zdravkovic, M. Guo, P. Ebbesen, and X. Liu.** 1997. Role of the Fas/Fas ligand pathway in apoptotic cell death induced by the human T cell lymphotropic virus type I Tax transactivator. J Gen Virol **78 (Pt 12):**3277-85.

4. **Hettmann, T., J. DiDonato, M. Karin, and J. M. Leiden.** 1999. An essential role for nuclear factor kappaB in promoting double positive thymocyte apoptosis. J Exp Med **189:**145-58.

5. **Kucharczak, J., M. J. Simmons, Y. Fan, and C. Gelinas.** 2003. To be, or not to be: NF-kappaB is the answer--role of Rel/NF-kappaB in the regulation of apoptosis. Oncogene **22:**8961-82.

6. **Lin, B., C. Williams-Skipp, Y. Tao, M. S. Schleicher, L. L. Cano, R. C. Duke, and R. I. Scheinman.** 1999. NF-kappaB functions as both a proapoptotic and antiapoptotic regulatory factor within a single cell type. Cell Death Differ **6:**570-82.

7. **Malewicz, M., N. Zeller, Z. B. Yilmaz, and F. Weih.** 2003. NF kappa B controls the balance between Fas and tumor necrosis factor cell death pathways during T cell receptor-induced apoptosis via the expression of its target gene A20. J Biol Chem **278:**32825-33.

8. **Romeo, G., W. H. Liu, V. Asnaghi, T. S. Kern, and M. Lorenzi.** 2002. Activation of nuclear factor-kappaB induced by diabetes and high glucose regulates a proapoptotic program in retinal pericytes. Diabetes **51:**2241-8.

9. **Savickiene, J., G. Treigyte, A. Pivoriunas, R. Navakauskiene, and K. E. Magnusson.** 2004. Sp1 and NF-{kappa}B Transcription Factor Activity in the Regulation of the p21 and FasL Promoters during Promyelocytic Leukemia Cell Monocytic Differentiation and Its Associated Apoptosis. Ann N Y Acad Sci **1030:**569-577.

10. **Shirakawa, F., and S. B. Mizel.** 1989. In vitro activation and nuclear translocation of NF-kappa B catalyzed by cyclic AMP-dependent protein kinase and protein kinase C. Mol Cell Biol **9:**2424-30.

11. **Shishodia, S., P. Potdar, C. G. Gairola, and B. B. Aggarwal.** 2003. Curcumin (diferuloylmethane) down-regulates cigarette smoke-induced NF-kappaB activation through inhibition of IkappaBalpha kinase in human lung epithelial cells: correlation with suppression of COX-2, MMP-9 and cyclin D1. Carcinogenesis **24:**1269-79.

12. **Singh, S., and B. B. Aggarwal.** 1995. Activation of transcription factor NF-kappa B is suppressed by curcumin (diferuloylmethane). J Biol Chem **270:**24995-5000.

13. **Viatour, P., M. P. Merville, V. Bours, and A. Chariot.** 2005. Phosphorylation of NF-kappaB and IkappaB proteins: implications in cancer and inflammation. Trends Biochem Sci **30:**43-52.

14. **Zhong, H., H. SuYang, H. Erdjument-Bromage, P. Tempst, and S. Ghosh.** 1997. The transcriptional activity of NF-kappaB is regulated by the IkappaB-associated PKAc subunit through a cyclic AMP-independent mechanism. Cell **89:**413-24.

15. **Zhong, H., R. E. Voll, and S. Ghosh.** 1998. Phosphorylation of NF-kappa B p65 by PKA stimulates transcriptional activity by promoting a novel bivalent interaction with the coactivator CBP/p300. Mol Cell **1:**661-71.

Chapter 5

Summary

Zinc can function as an inducer of apoptosis in addition to its traditional role as an essential biological trace metal. Exposure to increased levels of free zinc can trigger apoptosis in a number of cell types including neuronal and cells of the immune system. Whether these increases in zinc result from potential environmental factors, released from metalloproteins within cells, or released from the cells themselves, an understanding of zinc's regulation of apoptosis is essential to combating potential zinc toxicity. Until recently the mechanisms whereby zinc induces apoptosis have remained elusive. However, as shown herein, significant progress has been made toward identifying the components of the signaling pathways involved thus considerably increasing our current knowledge of the regulation of apoptosis by zinc. In addition, it provided molecular targets that can be used to inhibit zinc-induced apoptosis.

As demonstrated in Chapter 2, very low concentrations (400nM) of zinc pyrithione induces apoptosis in a number of cells including mouse thymocytes, splenic lymphocytes, S49 T cells and human Ramos B and Jurkat T cells. The use of a highly specific chelator of zinc, TPEN, verified that the induction of apoptosis in response to zinc pyrithione was indeed to due to zinc. In addition, zinc-induced apoptosis was dependent upon transcription and translation which indicated potential regulation of apoptosis by some proapoptotic protein. However, the identity of this protein and the signaling pathways

utilized remained unknown at this point but now have been identified via these studies as illustrated in Figure 5-1.

Inhibitors to a variety of different signaling pathways were tested in order to identify candidate signaling pathways that might be utilized during zinc-induced apoptosis. An inhibitor of adenylate cyclase, SQ22536, reduced zinc-pyrithione mediated apoptosis in mouse thymocytes. This result indicated that one candidate pathway involved during zinc-induced apoptosis was the cAMP-PKA signal transduction pathway. In order to further investigate this signaling pathway the mouse S49 T cell line was utilized. The S49 T cell line has historically been used in the study of the cAMP-PKA signaling pathway since two variants deficient in this pathway exist. The S49 Cyc^- variant is deficient in the $G\alpha s$ subunit of the heterotrimeric G-proteins and thus deficient in the ability to activate adenylate cyclase, while the S49 Kin^- variant is deficient in PKA activity. Zinc pyrithione (400nM) induced 51% apoptosis in S49 WT cells and a prolonged 2 fold increase in cAMP. Additionally, strong and sustained phosphorylation of CREB on Ser^{133}, a well documented PKA target, was observed in response to zinc treatment in S49 WT cells as well as in mouse thymocytes. However, no CREB phosphorylation was observed in the variant cell lines which were less susceptible to zinc and underwent only ~20% apoptosis. However, the variant cell lines were still susceptible to other inducers of apoptosis. Overall, this data verified that zinc was utilizing the cAMP-PKA signal transduction pathway.

Figure 5-1: Summary of the cAMP and NF-κB signal transduction pathways involved in zinc-induced apoptosis.

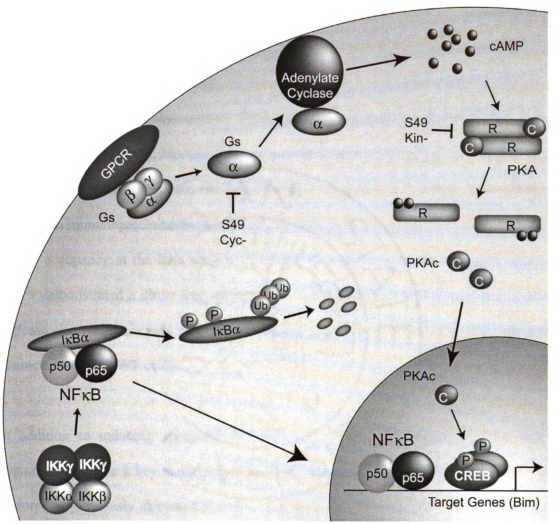
cAMP
Adenylate Cyclase
α
S49 Kin-
R
C
C
R
PKA
R
R
GPCR
β
γ
α
Gs
Gs
α
S49 Cyc-
PKAc
C
C
Ub
Ub
Ub
P
P
IκBα
IκBα
p50
p65
NFκB
PKAc
C
NFκB
P
P
p50
p65
CREB
Target Genes (Bim)
IKKγ
IKKγ
IKKα
IKKβ

As demonstrated in Chapter 3, in addition to the strong and sustained CREB phosphorylation, an increase in the binding of a ^{32}P-labled DNA probe containing a cAMP response element (CRE) was observed in S49 WT cells. Furthermore, in response to zinc treatment there was also a five fold increase in mRNA levels and a corresponding eight fold increase in protein expression for the BH3-only proapoptotic protein Bim in S49 WT cells. A robust increase in the protein expression level of Bim was also observed in zinc treated thymocytes. Treatment of thymocytes with actinomycin D, an inhibitor of transcription, blocked Bim up-regulation and apoptosis in response to zinc. This is the first time that zinc has been shown to promote the up-regulation of Bim. Chromatin immunoprecipitation (ChIP) analysis further demonstrated a 2 fold increase in CREB occupancy at the Bim promoter in S49 WT cells in response to zinc treatment which demonstrated a direct link between the cAMP signaling pathway and Bim. This increase also correlates well with the prolonged 2 fold increase in cAMP levels observed in zinc treated S49 WT cells.

In addition to inducing apoptosis in cells of the immune system, zinc has been demonstrated to be a key modulator of neuronal cell death in response to ischemia and seizures as previously discussed (1-3, 7). Interestingly, Bim may also regulate neuronal cell death in response to seizures and in temporal lobe epilepsy (4-6). Bim is a regulator of zinc-induced apoptosis in cells of the immune system as demonstrated herein, whether it is a regulator of zinc-induced cell death in neuronal cells currently remains unknown and will require further study.

Bim is known to function at the level of the mitochondria through interactions with both multidomain proapoptotic proteins such as Bax and antiapoptotic proteins such as Bcl-2 or Bcl-xL. The antiapoptotic proteins can sequester and neutralize Bim. However, if increased expression levels of Bim arise, such as in response to zinc treatment, Bim can overcome the antiapoptotic neutralization and interact with and activate the multidomain proapoptotic proteins thus shifting the cell towards death. Consistent with the involvement of Bim in zinc-induced apoptosis overexpression of either Bcl-2 or Bcl-xL in Ramos B or Jurkat T cells provided substantial protection. Additionally, activation of the intrinsic mitochondrial caspase cascade in response to zinc was demonstrated in thymocytes by cleavage of caspase 9 as well as with caspase inhibitors.

The evidence presented herein clearly demonstrated that the cAMP-PKA signaling pathway was utilized during zinc-induced apoptosis. However, since the variant cell lines deficient in the cAMP-PKA signaling pathway were not completely resistant to zinc-induced apoptosis and still underwent ~20% apoptosis the potential for activation of additional signaling pathways was investigated. Another transcription factor cascade, the NF-κB pathway, was activated in response to zinc. IκBα was degraded in response to zinc treatment in both thymocytes and S49 WT cells. IκBα degradation results in the release and activation of NF-κB. Interestingly, potential cross-talk might also occur between the cAMP and NF-κB pathways. PKA has been shown to phosphorylate NF-κB p65 on Ser^{276} which increases its transactivational potential. Furthermore, increased binding of a ^{32}P-labled DNA probe containing a NF-κB site was observed presenting a potential second link to the transcriptional regulation of Bim. However, a direct link

between NF-κB and Bim remains to be established being the subject of future investigations.

The data presented herein is consistent with a proapoptotic role for zinc and adds to the increasing evidence that free zinc can be harmful to cells. As demonstrated herein, considerable advances have been made in identifying the signaling components and pathways involved during zinc-induced apoptosis. These advancements increase our current knowledge of the regulation of apoptosis by zinc and provide a solid foundation for which future studies.

Reference:

1. **Choi, D. W., and J. Y. Koh.** 1998. Zinc and brain injury. Annu Rev Neurosci **21:**347-75.

2. **Frederickson, C. J., W. Maret, and M. P. Cuajungco.** 2004. Zinc and excitotoxic brain injury: a new model. Neuroscientist **10:**18-25.

3. **Frederickson, C. J., S. W. Suh, D. Silva, and R. B. Thompson.** 2000. Importance of zinc in the central nervous system: the zinc-containing neuron. J Nutr **130:**1471S-83S.

4. **Niquet, J., and C. G. Wasterlain.** 2004. Bim, Bad, and Bax: a deadly combination in epileptic seizures. J Clin Invest **113:**960-2.

5. **Sanchez, I., and J. Yuan.** 2001. A convoluted way to die. Neuron **29:**563-6.

6. **Shinoda, S., C. K. Schindler, R. Meller, N. K. So, T. Araki, A. Yamamoto, J. Q. Lan, W. Taki, R. P. Simon, and D. C. Henshall.** 2004. Bim regulation may determine hippocampal vulnerability after injurious seizures and in temporal lobe epilepsy. J Clin Invest **113:**1059-68.

7. **Suh, S. W., R. B. Thompson, and C. J. Frederickson.** 2001. Loss of vesicular zinc and appearance of perikaryal zinc after seizures induced by pilocarpine. Neuroreport **12:**1523-5.